

การบรรยายเชิงฮอโลกราฟีของดาวมัลติควาร์ก



นายสิทธิชัย ปิ่นกาญจนโรจน์

# ศูนย์วิทยพัทยากร จุฬาลงกรณ์มหาวิทยาลัย

วิทยานิพนธ์นี้เป็นส่วนหนึ่งของการศึกษาตามหลักสูตรปริญญาวิทยาศาสตรมหาบัณฑิต

สาขาวิชาฟิสิกส์ ภาควิชาฟิสิกส์

คณะวิทยาศาสตร์ จุฬาลงกรณ์มหาวิทยาลัย

ปีการศึกษา 2553

ลิขสิทธิ์ของจุฬาลงกรณ์มหาวิทยาลัย

HOLOGRAPHIC DESCRIPTION OF A MULTIQUARK STAR

Mr. Sittichai Pinkanjanarod



ศูนย์วิทยทรัพยากร  
จุฬาลงกรณ์มหาวิทยาลัย

A Thesis Submitted in Partial Fulfillment of the Requirements

for the Degree of Master of Science Program in Physics

Department of Physics

Faculty of Science

Chulalongkorn University

Academic Year 2010

Copyright of Chulalongkorn University

Thesis Title HOLOGRAPHIC DESCRIPTION OF A MULTIQUARK  
STAR  
By Mr. Sitthichai Pinkanjanarod  
Field of Study Physics  
Thesis Advisor Piyabut Burikham, Ph.D.

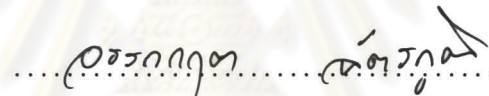
---

Accepted by the Faculty of Science, Chulalongkorn University in Partial  
Fulfillment of the Requirements for the Master's Degree

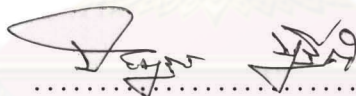


..... Dean of the Faculty of Science  
(Professor Supot Hannongbua, Dr.rer.nat.)

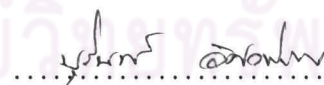
THESIS COMMITTEE



..... Chairman  
(Auttakit Chatrabhuti, Ph.D.)



..... Thesis Advisor  
(Piyabut Burikham, Ph.D.)



..... Examiner  
(Burin Asavapibhop, Ph.D.)



..... External Examiner  
(Khampee Karwan, Ph.D.)

สิทธิชัย ปิ่นกาญจนโรจน์: การบรรยายเชิงฮอโลกราฟีของดาวมัลติควาร์ก.  
(HOLOGRAPHIC DESCRIPTION OF A MULTIQUARK STAR)  
อ. ที่ปรึกษาวิทยานิพนธ์หลัก: อ. ดร. ปิยะบุตร บุรีคำ, 75 หน้า.

งานวิจัยนี้มีการทบทวนทวิภาคระหว่างทฤษฎีเกจและทฤษฎีความโน้มถ่วงหรือหลักการฮอโลกราฟี โดยเริ่มจาก AdS/CFT จนถึง แบบจำลองซาไก-ซูกิโมโตะ รวมถึงมีการทบทวนแบบจำลองเชิงฮอโลกราฟีของเมซอนและแบรีออนตามแบบจำลองซาไก-ซูกิโมโตะ นอกจากนี้ยังมีการทบทวนสมบัติทางฟิสิกส์ โดยเฉพาะความสัมพันธ์ทางอุณหพลศาสตร์ของทฤษฎีเกจในกรณีที่มีการกักขังและกรณีที่ไม่มีการกักขัง จากการทบทวนพบว่าทฤษฎีเกจในกรณีที่ไม่มีการกักขังนั้นมีความน่าสนใจมาก เนื่องจากกลูออนสามารถเคลื่อนที่ได้อย่างอิสระแต่ควาร์กสามารถรวมตัวกันเป็นสถานะใหม่ได้โดยไม่มีเงื่อนไขที่ว่า เลขควอนตัมเชิงรังสีต้องรวม กันแล้วไม่มีสี่ซึ่งเรียกว่าสถานะมัลติควาร์ก งานวิจัยนี้ศึกษาอุณหพลศาสตร์ของสถานะมัลติ-ควาร์กโดยการวิเคราะห์เชิงทฤษฎีและโดยวิธีเชิงเลข พบว่ามีความเป็นไปได้ที่ภายในแก่นของดาวที่มีความหนาแน่นมากพอและอุณหภูมิไม่สูงมากนัก สสารนิวเคลียร์จะอยู่ในสถานะมัลติ-ควาร์กมากกว่าสถานะนิวเคลียร์อื่นๆ งานวิจัยนี้สมมติให้ดาวขนาดใหญ่นี้มีสมมาตรแบบทรงกลมและอยู่ในสภาวะไม่กักขังตลอดทั้งดาว เนื่องจากความหนาแน่นที่มีค่าสูงและอุณหภูมিরะหว่างสภาพไม่กักขังและการเสียสมมาตรไครอด ดังนั้นดาวที่ศึกษาจึงมีชื่อว่าดาวมัลติควาร์ก เมื่อใช้สมการโทลมัน-โอเพนไฮม์เมอร์-วอลคอฟ ร่วมกับสมการสถานะมัลติควาร์กจากแบบจำลองซาไก-ซูกิโมโตะแล้วทำให้ประมาณค่าจำกัดมวลของดาวมัลติควาร์กได้สำหรับค่าความหนาแน่นพลังงานประมาณ  $10 \text{ GeV}/\text{fm}^3$  มวลของดาวมีค่าประมาณ 2.6-3.9 เท่าของดาวอาทิตย์และรัศมีของดาวมีค่าประมาณ 15-27 km. นอกจากนี้ยังได้วิเคราะห์ถึงดัชนีอะเดียบัติกและการแจกแจงความเร็วเสียงภายในดาว พบว่าความเร็วเสียงภายในดาวมีค่าไม่เกินความเร็วแสงซึ่งยืนยันถึงความเป็นไปได้ที่ดาวจะที่มีความหนาแน่นและมีความดันสูง

จุฬาลงกรณ์มหาวิทยาลัย

ภาควิชา.....ฟิสิกส์..... ลายมือชื่อนิสิต.....  
สาขาวิชา.....ฟิสิกส์..... ลายมือชื่อ อ.ที่ปรึกษาวิทยานิพนธ์หลัก.....  
ปีการศึกษา.....2553.....

## 5172493023 : MAJOR PHYSICS

KEYWORDS: MULTIQUARK/ MULTIQUARK STAR/ SAKAI-SUGIMOTOMODEL

SITTHICHAJ PINKANJANAROD : HOLOGRAPHIC DESCRIPTION  
OF A MULTIQUARK STAR. THESIS ADVISOR : PIYABUT  
BURIKHAM, Ph.D., 75 pp.

The gauge-gravity duality or the holographic principle is briefly reviewed starting from the AdS/CFT correspondence continuing to the more realistic model of Sakai-Sugimoto. The holographic models of mesons and baryons, constructed in Sakai-Sugimoto model, are also investigated. Their physical properties, especially thermodynamic relations are explored for both confined and deconfined cases. Interestingly, in the deconfined phase, it is found that even though gluons are free to propagate, quarks could form a new bound state with color charges called a multiquark state. The thermodynamics of multiquark states are considered both analytically and numerically. In the core of a dense warm star, it is conceivable that multiquark phase is preferred over the other nuclear phases, provided that the density is sufficiently large and the temperature is not too high. The massive star is assumed to be spherical symmetric and entirely in a deconfined phase due to the high density and a uniform moderate temperature throughout the star therefore it is called a multiquark star. Using the Tolman-Oppenheimer-Volkoff (TOV) equation and the equation of states of the multiquark from the Sakai-Sugimoto model, we established the mass limits of the multiquark star. For typical energy density  $10 \text{ GeV}/\text{fm}^3$ , the estimated mass and radius of the hypothetical multiquark star in the limit of large central density are approximately 2.6 - 3.9 solar mass and 15-27 km. The adiabatic index and sound speed distributions of the star are also discussed. It turns out that the sound speed never exceed the speed of light which confirms the compressibility of the multiquark matter at high density and pressure.

Department:..... Physics..... Student's Signature .....

Field of Study:..... Physics..... Advisor's Signature .....

Academic Year:.....2010.....



## ACKNOWLEDGEMENTS

I am extremely grateful to be under supervision of Dr. Piyabut Burikham. I can absorb many valuable things from him e.g. the way he manages to solve problems, the knowledge he gave, the good attitude toward doing this kind of research, and the way he trained his disciples. Without his helps and suggestions, I don't think I can fully overwhelm all obstacles to the research myself from the beginning.

I am very grateful to Dr. Auttakit Chatrabhuti, Dr. Burin Asavapibhop and Dr. Khamphree Karwan for serving as my thesis committee.

It was a very great chance to work with my colleague Mr. Ekapong Hirunsirisawat. Most of reviews and the contribution on thermodynamics of the multi-quark state in this work can be achieved by his support.

Finally, my gratitude goes to my parents and my family. May I dedicate this work to them. I am deeply indebted to them for their encouragement and consolation.

ศูนย์วิทยทรัพยากร  
จุฬาลงกรณ์มหาวิทยาลัย

# CONTENTS

|  | page      |
|--|-----------|
| Abstract (Thai) .....                                | iv        |
| Abstract (English) .....                             | v         |
| Acknowledgements .....                               | vi        |
| List of Tables .....                                 | ix        |
| List of Figures .....                                | x         |
| <b>Chapter</b>                                       |           |
| <b>I INTRODUCTION .....</b>                          | <b>1</b>  |
| <b>II REVIEW OF HOLOGRAPHIC PRINCIPLE .....</b>      | <b>5</b>  |
| 2.1 AdS/CFT duality .....                            | 6         |
| 2.2 More about AdS space .....                       | 7         |
| 2.3 Supporting evidences of AdS/CFT conjecture ..... | 9         |
| 2.4 Addition of fundamental matters .....            | 9         |
| <b>III REVIEW OF SAKAI-SUGIMOTO MODEL .....</b>      | <b>11</b> |
| 3.1 Finite Brane Configurations .....                | 12        |
| 3.2 Confined background .....                        | 13        |
| 3.2.1 Balance condition .....                        | 20        |
| 3.3 Deconfined background .....                      | 21        |
| 3.3.1 D4-brane sources .....                         | 24        |
| 3.3.2 String sources .....                           | 25        |
| 3.3.3 Balance condition .....                        | 26        |

|  |           |
|--|-----------|
| <b>IV THERMODYNAMICS WITH FINITE CHEMICAL POTENTIAL</b> .....                          | <b>28</b> |
| 4.1 Baryon chemical potential .....  | 28        |
| 4.2 Confined phase .....   | 29        |
| 4.3 Deconfined phase .....   | 32        |
| 4.3.1 Unstable quark matter .....  | 32        |
| 4.3.2 Comparison of the possible phase .....   | 33        |
| 4.3.3 Entropy and equation of state .....  | 35        |
| <b>V HOLOGRAPHIC MULTIQUARK AND ITS THERMODYNAMICS</b> .....                           | <b>38</b> |
| 5.1 Balance conditions .....   | 38        |
| 5.2 Thermodynamics of holographic multiquark .....                                     | 40        |
| 5.3 Calculation of the equation of state .....   | 41        |
| 5.4 Numerical studies of the thermodynamic relations .....                             | 48        |
| <b>VI GRAVITATIONAL STABILITY OF THE DENSE WARM STAR IN THE DECONFINED PHASE</b> ..... | <b>53</b> |
| <b>VII DISCUSSION AND SUMMARY</b> .....  | <b>63</b> |
| <b>References</b> .....  | <b>65</b> |
| <b>Appendices</b> .....  | <b>71</b> |
| <b>Appendix A: BALANCE CONDITION FROM VARIATIONAL PRINCIPLE</b> .....                  | <b>72</b> |
| <b>Appendix B: DIMENSIONAL TRANSLATION TABLE</b> .....                                 | <b>74</b> |
| <b>Vitae</b> .....   | <b>75</b> |



## LIST OF TABLES

| Table |   | page |
|-------|---|------|
| B.1   | Dimensional translation table of relevant physical quantities, $r_0 \equiv \left(\frac{GN}{c^4\tau V_3}\right)^{-1/2} = \left(\frac{G}{c^4}(\text{energy density scale})\right)^{-1/2}$ . . . . . | 74   |



ศูนย์วิทยทรัพยากร  
 จุฬาลงกรณ์มหาวิทยาลัย

## LIST OF FIGURES

| Figure | page   |    |
|--------|--|----|
| 5.1    | Different configurations of D8 and $\overline{\text{D8}}$ -branes in the background field following the Sakai-Sugimoto model that are dual to the phases of (a) $\chi_S$ -QGP, (b) vacuum and (c) multiquark phase. . . . .  | 39 |
| 5.2    | The graphs show the relations between $u_c$ and $T$ at small density (left) and at large density (right). . . . .  | 47 |
| 5.3    | Pressure and density in logarithmic scale at $T = 0.03$ . . . . .  | 50 |
| 5.4    | Pressure and density in logarithmic scale at $T = 0.03$ , zoomed in around the transition region. . . . .  | 50 |
| 5.5    | Pressure and density in linear scale. . . . .  | 51 |
| 5.6    | Relation between entropy and temperature in logarithmic scale for $n_s = 0$ (left), 0.3 (right). . . . .   | 51 |
| 5.7    | The baryon chemical potential and number density in logarithmic scale at $T = 0.03$ . . . . .  | 52 |
| 6.1    | The relation between mass and central density of the multiquark star for multiquarks with $n_s = 0$ (upper), 0.3 (lower). . . . .  | 57 |
| 6.2    | The accumulated mass distribution in the hypothetical multiquark star for the central density $\rho_0 = 20$ and $n_s = 0$ . The inner (outer) red (dashed-blue) line represents the core (crust) region. . . . .   | 57 |
| 6.3    | The density, and pressure distribution in the hypothetical multi-quark star for the central density $\rho_0 = 20$ and $n_s = 0$ . The inner (outer) red (dashed-blue) line represents the core (crust) region. . . . .   | 57 |
| 6.4    | The adiabatic index at constant entropy ( $\Gamma$ ) and the sound speed ( $c_s$ ) distribution in the hypothetical multiquark star for the central density $\rho_0 = 20$ and $n_s = 0$ . The inner (outer) red (dashed-blue) line represents the core (crust) region. . . . . | 58 |

- 6.5 Comparison of the accumulated mass distribution in the hypothetical multiquark star for the central density  $\rho_0 = 20$  between  $n_s = 0$  and 0.3. The (dashed) blue line represents the crust region of multiquark star with  $n_s = 0.3$  (0). The red lines represent the core region of which both cases are almost the same. . . . . 58
- 6.6 Comparison of the density, and pressure distribution in the hypothetical multiquark star for the central density  $\rho_0 = 20$  between  $n_s = 0$  and 0.3. The (dashed) blue line represents the crust region of multiquark star with  $n_s = 0.3$  (0). The red lines represent the core region of which both cases are almost the same. . . . . 58
- 6.7 Comparison of the baryon chemical distributions in the hypothetical multiquark star for the central density  $\rho_0 = 20$  between  $n_s = 0$  (left) and 0.3 (right). The solid (dashed) red (blue) line represents the core (crust) region. . . . . 59
- 6.8 The adiabatic index at constant entropy ( $\Gamma$ ) and the sound speed ( $c_s$ ) distribution in the hypothetical multiquark star for the central density  $\rho_0 = 20$  and  $n_s = 0.3$ . The inner (outer) red (dashed-blue) line represents the core (crust) region. . . . . 59
- 6.9 The relation between mass and radius of the multiquark star with (a)  $n_s = 0$ , (b)  $n_s = 0$  (red) and  $n_s = 0.3$  (black). . . . . 61
- 6.10 The relation between mass and radius of the core of the multiquark star with (a)  $n_s = 0$ , (b)  $n_s = 0$  (blue) and  $n_s = 0.3$  (black). . . . . 61

# Chapter I

## INTRODUCTION

In Quantum Chromodynamics (QCD), there is an important problem that the coupling constant of the strong interaction becomes nonperturbatively strong in the low energy regime. Quarks and gluons are confined within colorless hadrons and the chiral symmetry is broken. However, as the energy scale or the temperature of the system increases, the coupling tends to get weaker and eventually quarks and gluons become deconfined. Additionally, if quarks and gluons are extremely compressed, quarks strongly interact with other quarks from neighbouring hadrons and become effectively deconfined from the mesonic and baryonic bound state despite of the strong coupling. Even though the coupling is strong, the effective deconfinement is possible because of the extremely high density.

Lately, there are many experimental evidences from heavy ions collision suggesting that quark-gluon plasma (QGP), the nuclear matter in which the quarks and gluons become deconfined, might have been produced. The results from the relativistic heavy ions collider (RHIC) show that QGP act like a fluid with a small viscosity. This behavior cannot be explained by thinking of quarks and gluons as a hot gas system consisting of high energy particles. For example, the lattice simulations show that the pressure of QGP is relatively high above deconfinement temperature  $T_c$  which again cannot be described by weakly coupled quarks and gluons gas [1, 2]. Additionally, it is proposed that non color singlet and color-singlet bound states of quarks and gluons could exist in the plasma at the temperature  $(1 - 3)T_c$  [3, 2, 4]. The additional existence of the colored bound states could solve the high pressure problem and the small viscosity problem at once.

To study QCD in the large coupling limit, the use of perturbative method in QCD is meaningless. The attempt to find the suitable way to perform reliable calculation in this region has been developed. For instance, available tools for non-perturbative QCD at low energy such as MIT bag model and Lattice QCD have been proposed. The bag model promotes the nature of quark confinement and

asymptotic freedom. One can think of behavior of quarks inside a hadron as free quarks in an elastic bag. If one try to pull a quark out of the hadron, the energy required to separate will be greater than quark-antiquark pair creation. Consequently instead of pulling out a single quark, one surprisingly produces mesons. Accordingly the bag model is suitable for the nuclear matter in confined phase but it originally does not address the situation in the deconfined phase. For more information on MIT bag model, one can consult a good review for this topic in [5]. The lattice QCD is famous as a nonperturbative tool for low energy QCD. Originally, it is formulated on a discrete Euclidean spacetime grid which introduces a new kind of parameters relating to lattice spacing. The discrete Euclidean spacetime behave like a nonperturbative regularization scheme. At the finite value of a lattice spacing  $a$ , the discrete spacetime automatically introduces a cutoff at  $\frac{\pi}{a}$ . At the moment, this technique is reliable in the domain of low density and high temperature. At higher densities, the fermion sign problem and the slow convergence of statistical fluctuation in the numerical integration procedure make results of the calculation problematic. A good introductory review on lattice QCD can be found in [6] while the review on recent development in lattice QCD at finite density can be found in [1] and [7].

Apart from the mainstream researches in QCD mentioned above, there is an alternative approach to nonperturbative gauge theory using holographic principle. The prototype one is Anti-de Sitter space and Conformal Field Theory (AdS/CFT) duality proposed by Maldacena [8]. It is an important outcome from superstring theories conjecturing that a gauge theory in the spacetime boundary is equivalent to a superstring theory defined in higher dimensional space of that boundary. The duality comes with an outstanding feature that there is a strong-weak coupling duality associated with the gauge-gravity duality in a particular background. This allows us to solve the strongly coupled gauge theory by the weakly coupled superstring theory. By using the known relation between those two theories called “dictionary”, one can interpret the result of the weakly coupled superstring theory and identify with that of the strongly coupled gauge theory. This is an excellent way to solve the strong coupling problem; therefore this work will focus on the applications based upon this idea.

After the development of AdS/CFT correspondence, many holographic models have been proposed. Holographic models of meson were proposed by J. Maldacena, S. Rey, S. Theisen, and J. Yee [9, 10, 11]. The Coulomb type potential and screening effect of the potential between quark and antiquark are calculated from

Nambu-Goto action of the string in the bulk spacetime at zero and finite temperature. Additionally, the holographic baryons are proposed, by E. Witten, D. Gross, and H. Ooguri, to be a D5-brane wrapping the  $S^5$  subspace of the background spacetime with  $N_c$  strings connected and stretching out to the boundary. The fundamental requirement is the cancellation between a total of  $N_c$  charges from the endpoint of the strings and the charges of the vertex itself. Generally this condition allows more strings coming in and out of the vertex on the condition that the total charges of the string endpoints amount to  $N_c$  [12, 13, 14, 15, 16, 17]. Baryon vertex together with string configuration of the latter case represents the holographic model of color charged bound state called multiquark state which can exist only in deconfined phase.

The color multiquark phase was studied in the Sakai-Sugimoto model (SS) at the moderate temperature ranging from the gluon deconfinement (lower) to the chiral symmetry restoration temperature (higher) [20]. The multiquark phase was found to be thermodynamically stable and preferred to the other phase in gluon-deconfined plasma only if the density is sufficiently large [17]. The condition that the high density and the intermediate temperature coexist can be found in a dense warm star. Therefore it is interesting to explore the thermodynamical properties of multiquark nuclear matter and its influence on the stability of the dense star. In this thesis, The massive star was assumed to be spherical symmetric and entirely in a multiquark state due to the high density and a uniform moderate temperature throughout the star. The equation of state for multiquark star can be obtained from the Sakai-Sugimoto(SS) model and simplified by the power-law approximation. Finally, using the Tolman-Oppenheimer-Volkoff (TOV) equation [21, 22] and the equation of states of the multiquarks from the Sakai-Sugimoto model, the mass, density, and pressure distribution of the star are acquired numerically. The mass-radius relation and the mass limits of the multiquark star are also analyzed. Additionally the important hydrodynamical properties such as sound speed within the star are investigated.

This thesis is organized as the following. In Chapter 2, the general idea of the AdS/CFT correspondence will be introduced briefly. Chapter 3 provides the basics to understand the entire work in this thesis. This chapter reviews the specific holographic model, namely the Sakai-Sugimoto model which is used in most calculation to find the thermodynamics relation of nuclear matter for many possible cases in the chapter 4. In chapter 4, the equation of the states and calculation of various phases for nuclear matter with finite baryon number density are described.



Chapter 5 introduces a special kind of bound state called multiquark state which is a new state with color charges. We study the stability of the multiquarks state by examining the force condition on the superstring configuration of multiquark in the bulk. Chapter 6 is the main theme of this work. It focuses on thermodynamics of multiquark to acquire an equation of the state for the multiquark. A hypothetical multiquark star is the studied using the Tolmann-Oppenheimer-Volkov equation [21, 22] and equation of state for multiquark obtained from Sakai-Sugimoto model. Translation of unit from the superstring theory in Sakai-Sugimoto model to SI unit is provided in the Appendices.



ศูนย์วิทยทรัพยากร  
จุฬาลงกรณ์มหาวิทยาลัย

# Chapter II

## REVIEW OF HOLOGRAPHIC PRINCIPLE

Holographic principle is an equivalence between the description of physics in the volume and that is encoded on its lower dimensional boundary. It was first proposed by 't Hooft and Susskind and was inspired by a study of black hole thermodynamics near the Planck's scale. After the second revolution of superstrings theories, a new kind of holographic principle exists in the framework of superstrings theory called gauge-gravity duality relating superstring theories in the bulk to supersymmetric gauge theories defined at the spacetime boundary (sometime we interchange the word supergravity with superstrings since supergravity is a low energy limit of superstring theory). Additionally, it comes with some exciting features giving us an alternative description of the strongly coupled gauge theory due to the fact that there is a strong-weak duality between those two classes of theories. Despite of the disadvantage in describing real nuclear matter that there is still no exact (super) gravity dual of QCD, the duality has made a remarkable contribution on the understanding of QCD-like gauge theories which shares certain common properties with the QCD and offers a geometrical perspective of confinement and quark-gluon plasma. In this section we will focus on basics of gauge-gravity duality via the prototype one, namely the AdS/CFT duality following the Ref. [23, 24].

Originally, a study of the gauge-gravity duality depends on the understanding of D3-branes. Other type of branes have been studied but the best understood ones are D-branes based on the work of Polchinski [28]. D-branes are primarily locations in the ten-dimensional spacetime at which open strings can end. D3-branes is D-brane with 3 extending spatial dimension as well as in the time direction. At low energy, excitation of a single D3-brane can be described by  $\mathcal{N} = 4$  supersymmetric  $U(1)$  gauge theory. Stack of  $N$  D3-branes corresponds to  $\mathcal{N} = 4$  supersymmetric  $U(N)$  Yang-Mills theory ( $\mathcal{N} = 4$  SYM theory). The theory can be divided into (a) the  $U(1)$  component which is free and relating to center of mass motion of the stack of the branes: (b) the  $SU(N)$  component which refers to the interaction among each brane in the stack. In this kind of gauge theories, a

gluon is represented by a string having its ends on the  $N$  stack of brane where  $N$  is a number of color charges associated with the theory. For QCD-like gauge theory ( $N = 3$  labeling  $R$ -brane,  $G$ -brane, and  $B$ -brane.), a gluon with color charges  $\bar{R}B$  is represented by a strings having one end on  $R$ -brane and the other end on  $B$ -brane. Without mentioning to spin, all particles are in the adjoint representation of the gauge group.

D3-branes have a fixed mass density and a certain charge under five-form field strength. Placing D3-branes in the 10-dimensional spacetime, it will curve the spacetime into 10-dimensional Einstein equation coupled to a five-form field. It is found that the problem of finding black branes solution reduce to the problem of finding black hole solution [25, 26, 27]. In the near horizon limit, the solution to the Einstein equation becomes the direct product form of  $AdS_5 \times S^5$  where  $AdS_5$  is 5-dimensional Anti de Sitter space which is a type of space with negative (attractive) cosmological constant and  $S^5$  is a 5-dimensional sphere.

## 2.1 AdS/CFT duality

To understand the gauge-gravity duality, one can get the first step by starting with the prototype called AdS/CFT correspondence. In short it is an equivalence between string theory in the bulk  $AdS_5 \times S^5$  and  $\mathcal{N} = 4$  SYM in 4-dimensional boundary of the bulk spacetime [8].

First, we need to understand the metric of extremal D3-branes. The word extremal means that the branes is at the zero temperature which can be described by a vacuum state and satisfies the Bogomol'nyi-Sommerfield-Prasad (BPS) condition. The metric for the spacetime outside the horizon is given by

$$ds^2 = H^{-1/2} (-dt^2 + d\vec{x}^2) + H^{1/2} (dr^2 + r^2 d\Omega_5^2), \quad (2.1)$$

where  $H = 1 + \frac{R^4}{r^4}$ ,  $R^4 = \frac{\kappa}{2\pi^{5/2}} N$ ,  $\kappa = \sqrt{8\pi G}$  = gravitational coupling in 10-dimensional supergravity,  $N$  is the number of D3-branes and  $\alpha'$  is Regge slope parameter of fundamental string which is inversely proportional to the string tension. The horizon now locates at  $r = 0$ . In the large  $r$  limit ( $r \gg R$ ), the metric becomes asymptotically flat. D3-branes can be thought of a defect in the bulk spacetime; however, in the small  $r$  limit, the metric takes the following form

$$ds^2 = \frac{r^2}{R^2} (-dt^2 + d\vec{x}^2) + \frac{R^2}{r^2} (dr^2 + r^2 d\Omega_5^2). \quad (2.2)$$

It means that if we zoom in close to the horizon of the D3-branes, the resulting geometry takes  $AdS_5 \times S^5$  product space. This is how D3-branes are replaced by a curved geometry. Accordingly, the essential claim of AdS/CFT is that;

“Dynamics of SYM gauge theory on the boundary of string theory is equivalently described by the superstring theory in the curved geometry given in Eq.(2.2)”.

The  $AdS_5$  geometry can be clearly seen by considering transformation of radial variable. Usually, there are two common choices:  $z = \frac{R^2}{r}$  and  $u = \frac{r}{R^2}$ . Using

$$\begin{aligned}
 z &= \frac{R^2}{r}, \rightarrow \frac{r}{R} = \frac{R}{z}, \rightarrow \frac{r^2}{R^2} = \frac{R^2}{z^2}, \\
 dz &= -\frac{R^2}{r^2} dr, \\
 dz^2 &= \left(\frac{R^2}{r^2}\right)^2 dr^2, \\
 &= \left(\frac{z^2}{R^2}\right) \left(\frac{R^2}{r^2}\right) dr^2, \\
 \frac{R^2}{z^2} dz^2 &= \frac{R^2}{r^2} dr^2,
 \end{aligned} \tag{2.3}$$

the metric becomes

$$ds^2 = \frac{R^2}{z^2} (-dt^2 + d\vec{x}^2 + dz^2) + R^2 d\Omega_5^2. \tag{2.4}$$

The symmetry of this solution takes form of  $AdS_5 \times S^5$ .  $AdS_5$  is conformal to the region  $z > 0$  of half 5-dimensional  $\mathbb{R}^{4,1}$ . It has a boundary at  $z = 0$  which is Minkowski spacetime  $\mathbb{R}^{3,1}$ . The dual supersymmetric gauge theory lives on this boundary whereas strings theory live in bulk of  $AdS_5 \times S^5$ . The precise correspondence is given in Ref.[8]

“String theory on the whole of  $AdS_5 \times S^5$  is equivalent to  $\mathcal{N} = 4$  SYM theory on  $\mathbb{R}^{3,1}$ .”

## 2.2 More about AdS space

To become more familiar with  $AdS_5$ , let's consider two thought experiments described as the following: (a) An observer at fixed  $z_0$  sends light to the boundary at  $z = 0$  ( $r \rightarrow \infty$ ) away from horizon of D3-branes. A light ray has to propagate along  $z(t) = z_0 - t$ , therefore it reaches the boundary at  $t = z_0$ . It is assumed that some light reflects at boundary and comes back at the finite time interval

$t = 2z_0$  for the observer at  $z > 0$ . (b) The observer continues extending the rod toward the boundary. Surprisingly, the rod never reaches the boundary. The reason is the proper distance  $l$  between the observer and the boundary goes to infinity according to the integral below

$$\int_0^s ds = l = \int_0^{z_0} dz \frac{R}{z}. \quad (\text{spacelike distance}) \quad (2.5)$$

The integral diverges as  $z \rightarrow 0$ . In brief, AdS becomes infinitely large near the boundary but light can take a complete tour within a finite time interval. What a strange universe!

Interestingly, there is an indispensable symmetry associated with the action of dilaton in the AdS/CFT correspondence. On gauge theory side, the  $\beta$  function of  $\mathcal{N} = 4$  SYM theory vanishes identically. In the theory that the stress tensor is traceless, the renormalization group demands that dilaton acts trivially as an identity operator. On the other side of the duality, dilaton should only act as a coordinate transformation  $x^m \rightarrow Kx^m$  where  $x^m = (t, x, y, z)$  and  $K$  is a constant. Obviously, the coordinate transformation does not preserve the metric in (2.2) or (2.4). However, if one associates dilaton symmetry of  $\mathcal{N} = 4$  SYM theory with the radial part of the metric i.e.  $r \rightarrow \frac{r}{K}$  or equivalently  $u \rightarrow \frac{u}{K}$  and  $z \rightarrow Kz$ , preservation of the metric is restored. Choosing  $K > 1$  means that things become bigger in  $x^m$  direction and  $u \rightarrow \frac{u}{K}$  means that location in the radial direction becomes smaller as one goes further from the boundary.

The geometry of  $AdS_5$  plays a significant role to supersymmetric gauge theory. In large limit of  $u$ , the geometry corresponds to ultraviolet (UV) physics, whereas in small limit of  $u$ , the geometry relates to infrared (IR) physics. To make a distinction clearer, consider the more generalization of  $AdS_5$  part to the Eq.(2.4):

$$ds^2 = R^2 [u^2 (-h dt^2 + d\vec{x}^2) + h^{-1} du^2] + R^2 d\Omega_5^2. \quad (2.6)$$

where  $h = 1 - \frac{u_h^4}{u^4}$ . This geometry satisfies Einstein equation with the five-form field supporting as same as the original  $AdS_5 \times S^5$  metric. Eq.(2.6) describes near horizon geometry of near extremal D3-branes which means that small amount of mass in form of thermal energy has been added to the brane. The background metric introduces a finite temperature which manifests itself as a Hawking temperature of the horizon at  $u = u_h$  ( $T = \frac{u_h}{\pi}$ ). One can consider  $u$  as a typical energy scale connecting to the process in  $AdS_5$  at a depth  $u$ .



## 2.3 Supporting evidences of AdS/CFT conjecture

Although, the AdS/CFT duality has not been proved exactly, there are some evidences supporting the conjecture: (a) The symmetry structure between those dual theories are identical. (b) many study on Green's function of the gauge invariance operator, Wilson loop operator [8, 10] and thermal state [29, 30] lead to the dictionary for physical translation between the dual theories.

To understand the calculation of Green's function in AdS/CFT or other gauge-gravity duality, it is helpful to consider string theory in the asymptotically flat region where D3-branes is just a defect. To explore D3-branes physical properties, the matter wave was sent into the branes, then observing how it is reflected or get absorbed. A large number of literature reviews devoted to this kind of study are [31, 32, 33, 34, 35, 36]. The main goal is to compute absorption cross section of graviton by D3-brane. By means of the optical theorem, the cross section relates to the two points Green's function of the vertex operator. Higher points function can be treated as a linearized approximation. Heuristically, calculations of Green's function in supersymmetric gauge theory using  $AdS_5 \times S^5$  background based on the following ideas: (1) A graviton perturbation  $h_{mn}$  creates environment that the D3-branes can sense and respond to it. (2) On the gravity side, the graviton perturbs 10-dimensional spacetime in  $AdS_5 \times S^5$  causing a metric deformation at the large value of  $u$ . Consequently, the process to calculate the Green's function can be summarized as the following: (a) Enforce the metric deformation in the large  $u$  limit. (b) Take the calculation of path integral in the  $AdS_5 \times S^5$  depending on the boundary condition of the deformation. Outcome of the path integral in  $AdS_5 \times S^5$  must be the generating functional for color singlet operator in the dual field theory. However, path integral in the  $AdS_5 \times S^5$  is poorly understood. The best-known one is its approximation, the saddle point expression  $e^{iS}$  where  $S$  is an extremized gravitational action which is subjected to appropriate boundary conditions. This approximation is good when the curvature of  $AdS_5$  is small comparing to Plank scale ( $N \gg 1$ ) and to the string scale ( $g_{YM}^2 \gg 1$ ).

## 2.4 Addition of fundamental matters

To include fundamental matters or quarks into the large number of color supersymmetric gauge theory in AdS/CFT, one must admit the big difference from the



real QCD. Topologically, the fundamental representation quarks introduce the boundaries into double lined Feynman diagram. Each fundamental loop diagram associates with a power of  $N$ . Consequently, the dynamics of fermionic loop are suppressed at large  $N$  taking place in the background of the strongly coupled gluon. Addition of fundamental matters to the conformal  $\mathcal{N} = 4$  SYM gauge theory will make the  $\beta$  function become positive and lose their asymptotic freedom. The coefficient of  $\beta$  function would be of order  $\frac{1}{N}$ , so that the conformal symmetry breaking and the appearance of Landau pole can be ignored at large  $N$ .

Consequently, the addition of fundamental matters leads to the introduction of additional flavor branes on the dual gravity side in the bulk. Individually, quark in the gauge-gravity model can be thought of as a string having its ends on the boundary. There must be an additional brane apart from the D3-branes that the other end of the string can end. Existence of Additional D-branes cause spacetime to curve; however, the source term to Einstein equation is of order  $G_N T_{\mu\nu}^{D-branes} \sim \frac{1}{N}$  which vanish at large  $N$  limit. The effect of adding branes is minimized in the presence of the given background geometry. In this situation, there are also fermionic field on the brane. In gauge theory, the dynamics of gluons are unchanged in the presence of flavor branes at leading order  $N$ . A good example can be found in D3-D7 system where D7 acts as a probe brane (branes in the limit that back reaction can be neglected) in  $AdS_5 \times S^5$ .

Recently, several holographic models have been developed in order to imitate the dynamics of QCD. The first advancement in the progress was the construction of a non-conformal gauge-gravity duality without an introduction of flavor brane [20]. On the contrary, the construction of a gauge-gravity duality in cooperation with flavor degrees of freedom can be found in [37]. As mentioned before, adding flavor branes can be thought of a small perturbation on the background spacetime; therefore, the back reaction of the brane can be neglected at the large number of color,  $N_c$ , limit. The approximation is trustable when  $N_f \ll N_c$  where  $N_f$  is the number of flavor. Additionally, there is a large number of research [38, 39, 40, 41, 42, 43, 44, 45, 46, 47, 48, 49, 50, 51, 52, 53, 54, 55, 56, 57, 58, 59, 60] which apply the approximation to several supergravity models.

Despite of the excitement in the mainstream development of gauge-gravity duality, it is still considered to be far from an acceptably good theory to describe the dynamics of QCD. Their works investigate many aspects of low energy QCD; however, one crucial disadvantage is the absence of massless pions as Nambu-Goldstone bosons associated with chiral symmetry breaking in real QCD.

# Chapter III

## REVIEW OF SAKAI-SUGIMOTO MODEL

Recently, there is a holographic model of QCD which addresses the chiral symmetry breaking, called Sakai-Sugimoto model. The model is built based on Witten's model for pure Yang-Mills gauge theory that introduces 4-branes wrapped on Scherk-Schwarz circle [30], and  $N_f$  probe D8-branes and  $N_f$  probe anti D8-branes are added transverse to the circle. The construction provides massless chiral fermions (left-handed from 8-branes and right-handed from anti 8-branes) in fundamental representation of both gauge group  $U(N_c)$  and the flavor group  $U(N_f)_L \times U(N_f)_R$ . In this chapter, we will study Sakai-Sugimoto model in more details.

Sakai-Sugimoto model is a holographic model of massless QCD constructed by using D4-branes and D8-branes in type IIA string theory. Additionally, the  $x^4$  direction is compactified on a circle of a radius  $M_{KK}^{-1}$  with anti-periodic boundary condition for fermions where  $M_{KK}$  is a mass scale obtained from Kaluza-Klein compactification. In the low energy limit, the dual gauge theory effectively becomes 4-dimensional  $U(N_c)$  gauge theory in D4-brane world volume. D8-branes and anti D8-branes are introduced as probe branes. In the decoupling limit, the D4/D8/ $\bar{D}8$  system will give a holographic dual of large  $N_c$  gauge theory with chiral fermions.

One of the most exiting feature of the Sakai-Sugimoto model is that the model breaks chiral symmetry in a simple geometrical way. In the near horizon limit, the Scherk-Schwarz circle disappears in a finite radial coordinate. D8-branes and anti D8-branes smoothly connect into U-shaped configuration with an asymptotic separation  $L$  at infinity. Indeed the brane dynamics can be obtained by solving the DBI equation of motion with this boundary condition.

The model exhibits various properties similar to QCD [19, 61, 62, 63, 64, 65, 66, 67, 68, 69, 70]. Particularly, its phase structure at finite temperature is interesting. At low temperature, the phase structure of the model is required to be the same as that of zero temperature to describe confined gauge theory with broken

chiral symmetry. At high temperature, the gauge theory becomes deconfined and the chiral symmetry is restored. The situations can be described geometrically by the separation between D8-branes and anti D8-branes. Decreasing of the separation  $L$  leads to decreasing in the phase transition temperature of the model. For the sufficiently small  $L$ , there is a possible phase structure that the gauge theory is deconfined but chiral symmetry is still broken.

In brief, we review the Sakai-Sugimoto model following Ref.[71]. First, we focus on basic brane configuration of the model. Second, the configuration of confined phase is discussed in great details. Finally, many superstring constructions in deconfined phase are explored in various aspects.

### 3.1 Finite Brane Configurations

The basic brane configuration, corresponding to the gauge theory which is confined with broken chiral symmetry, consists of  $N_f$  D8-branes and  $N_f$  anti D8-branes in the near horizon background of  $N_c$  D4-branes wrapping  $x^4$  direction into a circle for  $N_c \gg N_f$ . At zero temperature, the background is sealed and the circle become topologically insignificant. Consequently, D8-branes and anti D8-branes connects into a U-shaped configuration. At the finite temperature, the model is heated up and could become deconfined. Equivalently, the background metric is replaced by the black hole geometry. Therefore the configuration will experience Hawking temperature which is considered to be the temperature of a whole configuration. In this case, both U-shaped 8-branes and the separated parallel 8-branes and anti 8-branes exist. Additionally, there is a chiral restoration at the second critical temperature for the sufficiently small value of  $L$  [72]. At this temperature, the separated 8-branes and anti 8-branes begin to outweigh.

In the superstring configuration, baryon number current is related holographically to diagonal  $U(1)$  part of the gauge field living on the 8-branes. To study the configurations duals to the plasma with finite baryon number density, it is necessary to include this gauge field into the 8-branes action. The first place for the gauge field to enter is DBI action of the D8 brane which takes the following form

$$S_{D8} = -\mu_8 \int d^9 X e^{-\phi} \sqrt{-\det(g_{MN} + 2\pi\alpha' \text{Tr}(\mathcal{F}_{MN}))}, \quad (3.1)$$

where

$$\mathcal{F} = d\mathcal{A} + i\mathcal{A} \wedge \mathcal{A}, \quad (3.2)$$

and  $\mathcal{F}$  is  $U(N_f)$  field strength and  $\mathcal{A}$  is the  $U(N_f)$  non abelian gauge field. The  $U(N_f)$  gauge field can be decomposed into  $SU(N_f)$  part and  $U(1)$  part as follows

$$\mathcal{A} = A + \frac{1}{\sqrt{2N_f}} \hat{A}, \quad (3.3)$$

where  $A$  is  $SU(N_f)$  non abelian gauge field, and  $\hat{A}$  is  $U(1)$  abelian gauge field. The effect of turning on this gauge field on the brane configuration will be clearly seen in various different phases.

## 3.2 Confined background

The near horizon background, corresponding to the confined gauge theory, is given by

$$ds^2 = \left(\frac{U}{R}\right)^{\frac{3}{2}} \left(- (dX_0)^2 + (d\mathbf{X})^2 + f(U)(dX_4)^2\right) + \left(\frac{R}{U}\right)^{\frac{3}{2}} \left(\frac{(dU)^2}{f(U)} + U^2 d\Omega_4^2\right). \quad (3.4)$$

After it is Euclideanized, the metric takes the following form

$$ds^2 = \left(\frac{U}{R}\right)^{\frac{3}{2}} \left((dX_0^E)^2 + (d\mathbf{X})^2 + f(U)(dX_4)^2\right) + \left(\frac{R}{U}\right)^{\frac{3}{2}} \left(\frac{(dU)^2}{f(U)} + U^2 d\Omega_4^2\right),$$

$$e^\phi = g_s \left(\frac{U}{R}\right)^{3/4}, \quad F_4 = \frac{(2\pi)^3 (\alpha')^{3/2} N_c}{\Omega_4} \epsilon_4, \quad f(U) = 1 - \frac{U_{KK}^3}{U^3}, \quad (3.5)$$

where  $X_0^E \sim X_0^E + \beta$  and  $X_4 \sim X_4 + \beta_4$ ,  $\epsilon_4$  and  $\Omega_4 = 8\pi^2/3$  are the volume form and the volume of a unit  $S^4$ , respectively.  $R$  and  $U_{KK}$  are constant parameters.  $R$  is related to the string coupling  $g_s$  and string length  $l_s$  as  $R^3 = \pi g_s N_c l_s^3$ . For convenience, we define dimensionless quantities

$$u = \frac{U}{R}, \quad \tau = \frac{X_0^E}{R}, \quad x^i = \frac{X^i}{R}, \quad x^4 = \frac{X^4}{R}, \quad \hat{a} = \frac{2\pi\alpha'\hat{A}}{\sqrt{2N_f}R}. \quad (3.6)$$

The metric and the parameters become

$$ds^2 = R^2 u^{3/2} \left((d\tau)^2 + (d\mathbf{x})^2 + f(u)(dx_4)^2\right) + R^2 u^{-3/2} \left(\frac{(du)^2}{f(u)} + u^2 d\Omega_4^2\right), \quad (3.7)$$

$$e^\phi = g_s u^{3/4}.$$

Consider the contribution of field strength to the D8-branes. In general  $\mathcal{A} = A + \frac{\hat{A}}{\sqrt{2N_f}} = A^{(i)} T^i + \frac{\hat{A}}{\sqrt{2N_f}}$  where  $T^i$  is the  $SU(N_f)$  generators normalized as

$Tr[T^i, T^j] = \frac{1}{2}\delta^{ij}$ . The field strength takes the following form

$$\begin{aligned}
\mathcal{F} &= dA^{(i)}T^i + \frac{d\hat{A}}{\sqrt{2N_f}} + i(A^{(i)}T^i + \frac{\hat{A}}{\sqrt{2N_f}}) \wedge (A^{(i)}T^i + \frac{\hat{A}}{\sqrt{2N_f}}), \\
F_{MN} &= [\partial_M A_N^{(i)} - \partial_N A_M^{(i)}]T^i + \frac{1}{\sqrt{2N_f}}[\partial_M \hat{A}_N - \partial_N \hat{A}_M] \\
&\quad + i(A_M^{(i)}A_N^{(j)} - A_N^{(j)}A_M^{(i)})T^i T^j, \\
&= [\partial_M A_N^{(i)} - \partial_N A_M^{(i)}]T^i + \frac{1}{\sqrt{2N_f}}[\partial_M \hat{A}_N - \partial_N \hat{A}_M] + i(A_M^{(i)}A_N^{(j)}[T^i, T^j]), \\
&= [\partial_M A_N^{(i)} - \partial_N A_M^{(i)}]T^i + \frac{1}{\sqrt{2N_f}}[\partial_M \hat{A}_N - \partial_N \hat{A}_M] - \epsilon^{ijk}A_M^{(i)}A_N^{(j)}T^k, \\
&= F_{MN}^{(i)}T^{(i)} + \frac{\hat{F}_{MN}}{\sqrt{2N_f}},
\end{aligned}$$

where

$$F_{MN}^{(i)} = \partial_M A_N^{(i)} - \partial_N A_M^{(i)} - \epsilon^{ijk}A_M^{(i)}A_N^{(j)}, \quad (3.8)$$

$$\hat{F}_{MN} = \partial_M \hat{A}_N - \partial_N \hat{A}_M. \quad (3.9)$$

Let's consider the case that only  $U(1)$  part is turned on,

$$g_{MN} + 2\pi\alpha'R^2\mathcal{F}_{MN} = g_{MN} + 2\pi\alpha'R^2\frac{\hat{F}_{MN}}{\sqrt{2N_f}}. \quad (3.10)$$

The  $U(1)$  gauge field consists of nine components:  $A_\mu(\mu = 0, 1, 2, 3)$ ,  $A_u$ ,  $A_\alpha(\alpha = 5, 6, 7, 8) \rightarrow S^4$ . Let's consider only the fields on  $S^4$ , by setting  $A_\alpha = 0$  to get  $SO(5)$  singlet state [18]. Choosing the gauge  $A_u = 0$  and turning on only  $A_0$ , the construction provides baryon number current. Accordingly, the field strength tensor becomes

$$\begin{aligned}
\hat{F}_{MN} \rightarrow \hat{F}_{ou} &= \partial_o \hat{A}_u - \frac{1}{R}\partial_u \hat{A}_0 = -\hat{F}_{ou}, \\
\frac{2\pi\alpha'R}{\sqrt{2N_f}}\hat{F}_{ou} &= -R^2\partial_u \frac{2\pi\alpha'\hat{A}_0}{\sqrt{2N_f}R} = -\hat{a}'_o,
\end{aligned} \quad (3.11)$$

where  $\hat{a}'_o = \frac{2\pi\alpha'\hat{A}_0}{\sqrt{2N_f}R}$ . Consequently,

$$g_{MN} + 2\pi\alpha'R^2\mathcal{F}_{MN} = \begin{pmatrix} g_{00} & 0 & \cdots & -R^2\hat{a}'_o & \cdots & 0 \\ 0 & g_{11} & & & & \vdots \\ \vdots & & \ddots & & & \\ R^2\hat{a}'_o & & & g_{uu} & & \\ \vdots & & & & \ddots & \\ 0 & \cdots & & & & g_{88} \end{pmatrix}.$$



where the spacetime metric can be calculated from the induced metric  $g_{MN} = G_{\mu\nu}\partial_M X^\mu\partial_N X^\nu$ . The determinant turns into

$$\det(g_{MN} + 2\pi\alpha'R^2\mathcal{F}_{MN}) = g_{00}g_{11}g_{22}\cdots g_{88} + R^2\hat{a}'_0(-R^2\hat{a}'_0)g_{11}g_{22}g_{33}g_{55}\cdots g_{88}. \quad (3.12)$$

where  $g_{00} = g_{11} = g_{22} = g_{33} = R^2u^{3/2}$ ,  $g_{uu} = R^2\left(\frac{u^{-3/2}}{f(u)} + u^{3/2}f(u)(x'_4(u))^2\right)$ , and  $g_{55}g_{66}g_{77}g_{88} = R^2u^2\sin^6(\theta_1)\sin^4(\theta_2)\sin^2(\theta_3)$ . Eventually, the determinant becomes

$$\begin{aligned} \det(g_{MN} + 2\pi\alpha'R^2\mathcal{F}_{MN}) &= -R^{18}\sin^6(\theta_1)\sin^4(\theta_2)\sin^2(\theta_3) \times \left\{ \right. \\ &\quad \left. u^8\left[u^{-3/2}f^{-1}(u) + u^{3/2}f(u)(x'_4(u))^2\right] \right. \\ &\quad \left. -u^{13/2}(\hat{a}'_0)^2\right\}, \\ &= -R^{18}u^{13/2}\sin^6(\theta_1)\sin^4(\theta_2)\sin^2(\theta_3) \times \left\{ \right. \\ &\quad \left. u^3f(u)(x'_4(u))^2 + \left[\frac{1}{f(u)} - (\hat{a}'_0)^2\right]\right\}. \quad (3.13) \end{aligned}$$

Consider the  $N_f$  stack of D8-branes configuration for the confined gauge theory. According to Eq.(3.1) and (3.13), the D8-brane action takes the form

$$\begin{aligned} S_{D8} &= \mu_8 N_f \int d\tau d^3x d\Omega_4 du \left(\frac{u^{-3/4}}{g_s}\right) R^9 u^{13/4} \sqrt{u^3 f(u)(x'_4(u))^2 + \left[\frac{1}{f(u)} - (\hat{a}'_0)^2\right]}, \\ &= \frac{\mu_8 N_f R^9}{g_s} \left(\frac{\beta}{R}\right) \left(\frac{V_3}{R^3}\right) \int du u^4 \sqrt{f(u)(x'_4(u))^2 + \frac{1}{u^3} \left[\frac{1}{f(u)} - (\hat{a}'_0)^2\right]}, \\ &= \frac{\mu_8 N_f \Omega_4 V_3 \beta R^5}{g_s} \int du u^4 \sqrt{f(u)(x'_4(u))^2 + \frac{1}{u^3} \left[\frac{1}{f(u)} - (\hat{a}'_0)^2\right]}, \\ &= \mathcal{N} \int du u^4 \sqrt{f(u)(x'_4(u))^2 + \frac{1}{u^3} \left[\frac{1}{f(u)} - (\hat{a}'_0)^2\right]}, \quad (3.14) \end{aligned}$$

where we define  $\mathcal{N} \equiv \frac{\mu_8 N_f \Omega_4 V_3 \beta R^5}{g_s}$ .

The Legendre-transformed action is given by

$$\tilde{S}_{D8} = S_{D8} + \int du d(u)\hat{a}'_0(u), \quad (3.15)$$

where

$$d(u) \equiv -\frac{1}{\mathcal{N}} \frac{\delta S_{D8}}{\delta \hat{a}'_0(u)} = \frac{u\hat{a}'_0}{\sqrt{f(u)(x'_4(u))^2 + \frac{1}{u^3} \left[\frac{1}{f(u)} - (\hat{a}'_0)^2\right]}}. \quad (3.16)$$



Clearly we found that

$$\begin{aligned}
d^2(u) \left( f(u)(x'_4(u))^2 + \frac{1}{u^3} \left[ \frac{1}{f(u)} - (\hat{a}'_0)^2 \right] \right) &= u^2(\hat{a}'_0)^2, \\
d^2(u) \left( f(u)(x'_4(u))^2 + \frac{1}{f(u)u^3} \right) &= (\hat{a}'_0)^2 \left( u^2 + \frac{d^2(u)}{u^3} \right), \\
\hat{a}'_0 &= \frac{d(u)u^{3/2}}{\sqrt{d^2(u) + u^5}} \sqrt{f(u)(x'_4(u))^2 + \frac{1}{f(u)u^3}}. \tag{3.17}
\end{aligned}$$

Consequently, the Legendre-transformed D8-brane action turns into

$$\begin{aligned}
\tilde{S}_{D8} &= \mathcal{N} \int du u^4 \left( f(u)(x'_4(u))^2 + \frac{1}{u^3} \left[ \frac{1}{f(u)} - \frac{d^2(u)u^3}{d^2(u) + u^5} \left( f(u)(x'_4(u))^2 + \frac{1}{f(u)u^3} \right) \right] \right)^{1/2} \\
&\quad + \mathcal{N} \int du \frac{d^2(u)u^{3/2}}{\sqrt{d^2(u) + u^5}} \sqrt{f(u)(x'_4(u))^2 + \frac{1}{f(u)u^3}}, \\
&= \mathcal{N} \int du u^4 \left\{ f(u)(x'_4(u))^2 + \frac{1}{f(u)u^3} - \frac{d^2(u)}{d^2(u) + u^5} f(u)(x'_4(u))^2 \right. \\
&\quad \left. - \frac{d^2(u)}{d^2(u) + u^5} \frac{1}{f(u)u^3} \right\}^{1/2} + \mathcal{N} \int du \frac{d^2(u)u^{3/2}}{\sqrt{d^2(u) + u^5}} \sqrt{f(u)(x'_4(u))^2 + \frac{1}{f(u)u^3}}, \\
&= \mathcal{N} \int du u^4 \left[ 1 - \frac{d^2(u)}{d^2(u) + u^5} \right]^{1/2} \left[ f(u)(x'_4(u))^2 + \frac{1}{f(u)u^3} \right]^{1/2} \\
&\quad + \mathcal{N} \int du u^4 \left[ \frac{d^4(u)}{u^5(d^2(u) + u^5)} \right]^{1/2} \left[ f(u)(x'_4(u))^2 + \frac{1}{f(u)u^3} \right]^{1/2}, \\
&= \mathcal{N} \int du u^4 \left[ \frac{u^{5/2}}{\sqrt{d^2(u) + u^5}} + \frac{d^2(u)}{u^{5/2}\sqrt{d^2(u) + u^5}} \right] \left[ f(u)(x'_4(u))^2 + \frac{1}{f(u)u^3} \right]^{1/2}, \\
&= \mathcal{N} \int du u^4 \sqrt{\frac{d^2(u) + u^5}{u^5}} \left[ f(u)(x'_4(u))^2 + \frac{1}{f(u)u^3} \right]^{1/2}, \\
&= \mathcal{N} \int du u^4 \left[ f(u)(x'_4(u))^2 + \frac{1}{f(u)u^3} \right]^{1/2} \left[ 1 + \frac{d^2(u)}{u^5} \right]^{1/2}. \tag{3.18}
\end{aligned}$$

Consider the constants of motion associated with the D8-brane action. Since  $S_{D8}(\hat{a}_0, x_4, u)$  is independent of  $\hat{a}_0$ , therefore  $\frac{\delta S_{D8}}{\delta \hat{a}_0} = -d'(u) = 0$ ,  $d(u) = d$  (a constant of motion). In the same manner, the other constant of motion can be obtained from  $\tilde{S}_{D8}(\hat{a}_0, x_4, u)$ ,

$$\begin{aligned}
\frac{\delta \tilde{S}_{D8}}{\delta x'_4(u)} &= u^4 \left[ 1 + \frac{d^2}{u^5} \right]^{1/2} \frac{f(u)x'_4(u)}{\left[ f(u)(x'_4(u))^2 + \frac{1}{f(u)u^3} \right]^{1/2}}, \\
&= u_0^4 \left[ 1 + \frac{d^2}{u_0^5} \right]^{1/2} (f(u_0))^{1/2}, \\
&= \text{const.} \tag{3.19}
\end{aligned}$$

The shape of D8-branes configuration can be determined from

$$(f(u))^2(x'_4(u))^2 = f(u_0) \frac{u_0^8 \left(1 + \frac{d^2}{u_0^5}\right)}{u^8 \left(1 + \frac{d^2}{u^5}\right)} \left( f(u)(x'_4(u))^2 + \frac{1}{f(u)u^3} \right),$$

$$f(u)(x'_4(u))^2 \left[ f(u) - f(u_0) \frac{u_0^8 + u_0^3 d^2}{u^8 + u^3 d^2} \right] = f(u_0) \frac{u_0^8 + u_0^3 d^2}{u^8 + u^3 d^2} \frac{1}{f(u)u^3}$$

$$(x'_4(u))^2 = \frac{1}{f^2(u)u^3} \left[ \frac{f(u)(u^8 + u^3 d^2)}{f(u_0)(u_0^8 + u_0^3 d^2)} - 1 \right]^{-1}. \quad (3.20)$$

In the case that  $d = 0$ , D8-branes and anti D8-branes deform into U-shape in  $(u, x_4)$  plane and coincide at  $u_0$ . For the case that  $d \neq 0$ , D8-branes and anti D8-branes do not coincide but they will intersect at  $u_c$  with additional structure. Instantons, or equivalently D4-branes wrapped on  $S^4$ , are only sources for  $d \neq 0$  case. For a uniform  $d$  we need a uniform distribution in  $\mathbb{R}^3$  of D4-branes. Another source term comes from the D8-brane CS action,

$$S_{CS} = \frac{\mu_8}{6} \int_{R^4 \times R_+ \times S^4} C_3 \text{Tr}(2\pi\alpha' \mathcal{F})^3 = \frac{N_c}{24\pi^2} \int_{R^4 \times R_+} \omega_5(\mathcal{A}). \quad (3.21)$$

The relevant term is the one coupling the  $U(1)$  to the  $SU(N_f)$ :

$$\frac{N_c}{24\pi^2} \int_{R^4 \times R_+} \frac{3}{\sqrt{2N_f}} \hat{A}_0 \text{Tr} F^2. \quad (3.22)$$

Assuming D4-branes in  $\mathbb{R}^3$  at  $u = u_c$ ,

$$\frac{1}{8\pi^2} \text{Tr} F^2 = n_4 \delta(u - u_c) d^3 x du, \quad (3.23)$$

where  $n_4$  is the (dimensionless) density of D4-branes wrapped on  $S^4$ . The D8-brane CS action then becomes

$$\begin{aligned} S_{CS} &= \frac{\beta N_c n_4}{\sqrt{2N_f}} \int du' d^3 x \hat{A}_0(u') \delta(u - u_c), \\ &= \frac{\beta N_c R n_4}{2\pi\alpha'} \int du' d^3 x \hat{a}_0(u') \delta(u - u_c), \\ &= \frac{\beta N_c n_4 V_3}{2\pi\alpha' R^2} \int du' \hat{a}_0(u') \delta(u - u_c). \end{aligned} \quad (3.24)$$

Recalling  $S_{total} = S_{D8} + S_{CS}$ , the equation of motion for the  $U(1)$  gauge field can be determined from

$$\begin{aligned}
-\frac{1}{\mathcal{N}} \frac{\partial}{\partial u} \frac{\delta S}{\delta \hat{a}'_0} &= -\frac{1}{\mathcal{N}} \frac{\delta S}{\delta \hat{a}_0}, \\
\frac{\partial d(u)}{\partial u} &= \frac{1}{\mathcal{N}} \frac{\beta N_c n_4 V_3}{2\pi\alpha' R^2} \delta(u - u_0), \\
d'(u) &= \frac{\beta N_c n_4 V_3}{2\pi\alpha' R^2 \mathcal{N}} \delta(u - u_0), \\
d(u) &= \frac{\beta N_c n_4 V_3}{2\pi\alpha' R^2 \mathcal{N}}.
\end{aligned} \tag{3.25}$$

Therefore

$$n_4 = \frac{2\pi\alpha' R^2 \mathcal{N}}{\beta V_3 N_c} d. \tag{3.26}$$

The instanton distribution in Eq.(3.23) can also be a source to the equation of motion for  $x_4(u)$  and will therefore distort the configuration of the D8-branes. Physically, the D4-branes pull down on the D8-branes. Since the D4-branes distribution has a finite energy density per unit 7-volume (the  $S^4$  they wrap plus the  $\mathbb{R}^3$ ), it will form a cusp in the D8-branes (like a bead on a string). Away from the cusp the D8-branes will follow two opposite pieces of a U-shaped solution, which are truncated at some radial position  $u_c$  above  $u_0$ . The value of  $u_c$  can be determined by the zero-force condition in the  $(x_4, u)$  plane. Consider the proper coordinate along D8-branes, the proper length is given by

$$dl^2 = u^{3/2} f(u) dx_4^2 + u^{-3/2} f^{-1}(u) du^2, \tag{3.27}$$

$$dl = du u^{3/4} \sqrt{f(u) (dx_4'(u))^2 + \frac{1}{f(u) u^3}}. \tag{3.28}$$

From

$$\tilde{S}_{D8} = \mathcal{N} \int du u^4 \left[ f(u) (x_4'(u))^2 + \frac{1}{f(u) u^3} \right]^{1/2} \left[ 1 + \frac{d^2(u)}{u^5} \right]^{1/2},$$

using proper length coordinate along D8-branes, the Legendre-transformed action becomes

$$\tilde{S}_{D8} = \mathcal{N} \int dl u^{13/4} \left[ 1 + \frac{d^2(u)}{u^5} \right]^{1/2}.$$

Therefore

$$f_{D8} = \left. \frac{\delta \tilde{S}_{D8}}{\delta l} \right|_{u_c} = \mathcal{N} u_c^{13/4} \left[ 1 + \frac{d^2(u_c)}{u_c^5} \right]^{1/2}. \tag{3.29}$$

In order to calculate the D4-branes action, let's consider the wrapped 4-sphere metric by identifying

$$\begin{aligned} x^0 &= \frac{X_E^0}{R} = \tau, \\ x^1 &= x^6 = \theta_1, \\ x^2 &= x^7 = \theta_2, \\ x^3 &= x^8 = \theta_3, \\ x^4 &= x^9 = \theta_4. \end{aligned}$$

The metric of D4-branes locating at  $u = u_c$  takes the following form

$$g_{MN} = \text{diag}(R^2 u_c^{3/2}, R^2 u_c^{1/2}, R^2 u_c^{1/2} \sin^2 \theta_1, R^2 u_c^{1/2} \sin^2 \theta_1 \sin^2 \theta_2, R^2 u_c^{1/2} \sin^2 \theta_1 \sin^2 \theta_2 \sin^2 \theta_3), \quad (3.30)$$

therefore

$$\det(g_{MN}) = R^{10} u_c^{7/2} \sin^6 \theta_1 \sin^4 \theta_2 \sin^2 \theta_3. \quad (3.31)$$

From

$$\begin{aligned} S_{D4} &= \frac{n_4 V_3 \mu_4}{R^3} \int d\theta_1 d\theta_2 d\theta_3 d\theta_4 d\tau e^{-\phi} \sqrt{\det(g_{MN})}, \\ &= \frac{n_4 V_3 \mu_4}{R^3} \int d\theta_1 d\theta_2 d\theta_3 d\theta_4 d\tau \left( \frac{1}{g_s u_c^{3/4}} \right) \sqrt{\det(g_{MN})}, \\ &= \frac{n_4 V_3 \mu_4 \beta \Omega_4}{g_s R^4} u_c^{-3/4} (R^5 u_c^{7/4}), \\ &= \frac{n_4 V_3 \mu_4 \beta \Omega_4 R}{g_s} u_c. \end{aligned} \quad (3.32)$$

Using (3.26)

$$n_4 = \frac{2\pi\alpha' R^2 \mathcal{N}}{\beta V_3 N_c} d, \quad (3.33)$$

the D4-branes action can be obtained as follows

$$\begin{aligned} S_{D4} &= \frac{2\pi\alpha' R^2 \mu_4 \mathcal{N} \Omega_4 R}{g_s N_c} u_c d, \\ &= \frac{2\pi\alpha' R^3}{g_s N_c} \left( \frac{1}{2^4 \pi^4 (\alpha')^{5/2}} \right) \left( \frac{2^3 \pi^2}{3} \right) \mathcal{N} u_c d, \\ &= 2\pi\alpha' (\pi(\alpha')^{3/2}) \left( \frac{1}{2^4 \pi^4 (\alpha')^{5/2}} \right) \left( \frac{2^3 \pi^2}{3} \right) \mathcal{N} u_c d, \\ S_{D4} &= \frac{1}{3} \mathcal{N} u_c d, \end{aligned} \quad (3.34)$$

where we use  $\frac{R^3}{g_s N_c} = \pi(\alpha')^{3/2}$  in the last equation.

### 3.2.1 Balance condition

The force due to D4-brane can be obtained from

$$f_{D4} = \frac{\partial S_{D4}}{\partial u_c} \frac{1}{\sqrt{g_{uu}}} \Big|_{u=u_c} = \frac{1}{3} \mathcal{N} d u_c^{3/4} f^{1/2}. \quad (3.35)$$

The configuration is in equilibrium when these forces are balanced,

$$f_{D8} \cos \theta = f_{D4}, \quad (3.36)$$

where  $\theta$  is the proper angle between the D8-branes and the  $x_4$  direction at  $u_c$ . The angle can be determined by substituting  $f_{D8}$  and  $f_{D4}$  into the Eq.(3.36).

$$\cos \theta = \frac{\frac{1}{3} \mathcal{N} d u_c^{3/4} f^{1/2}(u_c)}{\mathcal{N} u_c^{13/4} \left[ 1 + \frac{d^2(u_c)}{u_c^5} \right]^{1/2}} = \frac{d}{3} u_c^{-5/2} \sqrt{\frac{f(u_c)}{1 + \frac{d^2(u_c)}{u_c^5}}}. \quad (3.37)$$

From the configuration,

$$\cos \theta = \frac{\Delta u}{\Delta l} = \frac{\sqrt{g_{uu}} du}{\sqrt{g_{uu} du^2 + g_{x_4 x_4} dx_4^2}} \Big|_{u_c}, \quad (3.38)$$

$$= \frac{u^{-3/4} f^{-1/2}(u) du}{u^{3/4} \sqrt{f(u)(x'_4(u))^2 + \frac{1}{f(u)u^3}}} du \Big|_{u_c}, \quad (3.39)$$

$$= \frac{u_c^{-3/2} f^{-1/2}(u_c)}{\sqrt{f(u_c)(x'_4(u_c))^2 + \frac{1}{f(u_c)u_c^3}}}, \quad (3.40)$$

$$= \frac{1}{\sqrt{f^2(u_c)u_c^3(x'_4(u_c))^2 + 1}}. \quad (3.41)$$

Using,

$$\begin{aligned} (x'_4(u))^2 &= \frac{1}{f^2(u) u^3} \left[ \frac{f(u)(u^8 + u^3 d^2)}{f(u_0)(u_0^8 + u_0^3 d^2)} - 1 \right]^{-1}, \\ &\equiv \frac{1}{f^2(u) u^3} [\Psi(u) - 1]^{-1}. \end{aligned} \quad (3.42)$$

The cosine becomes

$$\begin{aligned}
\cos \theta &= \frac{1}{\sqrt{\frac{1}{\Psi(u_c) - 1} + 1}}, \\
&= \frac{1}{\sqrt{\frac{\Psi(u_c)}{\Psi(u_c) - 1}}}, \\
&= \sqrt{\frac{\Psi(u_c) - 1}{\Psi(u_c)}}, \\
&= \sqrt{1 - \Psi^{-1}(u_c)}, \\
&= \left[ 1 - \frac{f(u_0) (u_0^8 + u_0^3 d^2)}{f(u_c) (u_c^8 + u_c^3 d^2)} \right]^{1/2}. \tag{3.43}
\end{aligned}$$

Therefore,

$$\cos \theta = \frac{d}{3} u_c^{-5/2} \left[ \frac{f(u_c)}{1 + \frac{d^2(u_c)}{u_c^5}} \right]^{1/2} = \left[ 1 - \frac{f(u_0) (u_0^8 + u_0^3 d^2)}{f(u_c) (u_c^8 + u_c^3 d^2)} \right]^{1/2}. \tag{3.44}$$

Aiming to solve for the value of  $u_c$  while holding the asymptotic separation of D8-branes and anti D8-branes fixed, the asymptotic separation is given by

$$l = 2 \int_{u_c}^{\infty} du x'_4(u). \tag{3.45}$$

### 3.3 Deconfined background

The near horizon solution to the deconfined background is

$$ds^2 = \left( \frac{U}{R} \right)^{\frac{3}{2}} (-f(U)(dX_0)^2 + (d\mathbf{X})^2 + (dX_4)^2) + \left( \frac{R}{U} \right)^{\frac{3}{2}} \left( \frac{(dU)^2}{f(U)} + U^2 d\Omega_4^2 \right). \tag{3.46}$$

After it is Euclideanized, the metric takes the following form

$$\begin{aligned}
ds^2 &= \left( \frac{U}{R} \right)^{\frac{3}{2}} (f(U)(dX_0^E)^2 + (d\mathbf{X})^2 + (dX_4)^2) + \left( \frac{R}{U} \right)^{\frac{3}{2}} \left( \frac{(dU)^2}{f(U)} + U^2 d\Omega_4^2 \right), \\
e^\phi &= g_s \left( \frac{U}{R} \right)^{3/4}, F_4 = \frac{(2\pi)^3 (\alpha')^{3/2} N_c}{\Omega_4} \epsilon_4, f(U) = 1 - \frac{U_{KK}^3}{U^3}, \tag{3.47}
\end{aligned}$$

where  $X_0^E \sim X_0^E + \beta$  and  $X_4 \sim X_4 + \beta_4$ .  $\epsilon_4$  and  $\Omega_4 = 8\pi^2/3$  are the volume form and the volume of a unit  $S^4$ , respectively.  $R$  and  $U_{KK}$  are constant parameters.



$R$  is related to the string coupling  $g_s$  and string length  $l_s$  as  $R^3 = \pi g_s N_c l^3$ . For convenience, we define dimensionless quantities

$$u = \frac{U}{R}, \quad \tau = \frac{X_0^E}{R}, \quad x^i = \frac{X^i}{R}, \quad x^4 = \frac{X^4}{R}, \quad \hat{a} = \frac{2\pi\alpha' \hat{A}}{\sqrt{2N_f} R}. \quad (3.48)$$

The metric and the parameters become

$$\begin{aligned} ds^2 &= R^2 u^{3/2} \left( f(u) (d\tau)^2 + (d\mathbf{x})^2 + (dx_4)^2 \right) + R^2 u^{-3/2} \left( \frac{(du)^2}{f(u)} + u^2 d\Omega_4^2 \right), \\ e^\phi &= g_s u^{3/4}. \end{aligned} \quad (3.49)$$

Similarly, the DBI action can be obtained in the same manner as the confined case. Therefore

$$\det(g_{MN} + 2\pi\alpha' R^2 \mathcal{F}_{MN}) = g_{00} g_{11} g_{22} \cdots g_{88} + R^2 \hat{a}'_0 (-R^2 \hat{a}'_0) g_{11} g_{22} g_{33} g_{55} \cdots g_{88}, \quad (3.50)$$

where  $g_{00} = R^2 f(u) u^{3/2}$ ,  $g_{11} = g_{22} = g_{33} = R^2 u^{3/2}$ ,  $g_{uu} = G_{\mu\nu} \partial_u X^\mu \partial_u X^\nu = R^2 \left( \frac{u^{-3/2}}{f(u)} + u^{3/2} (x'_4(u))^2 \right)$ , and  $g_{55} g_{66} g_{77} g_{88} = R^2 u^2 \sin^6(\theta_1) \sin^4(\theta_2) \sin^2(\theta_3)$ . The determinant turn into

$$\begin{aligned} \det(g_{MN} + 2\pi\alpha' R^2 \mathcal{F}_{MN}) &= -R^{18} \sin^6(\theta_1) \sin^4(\theta_2) \sin^2(\theta_3) \times \left\{ \right. \\ &\quad \left. u^8 \left[ u^{-3/2} + u^{3/2} f(u) (x'_4(u))^2 \right] - u^{13/2} (\hat{a}'_0)^2 \right\}, \\ &= -R^{18} u^{13/2} \sin^6(\theta_1) \sin^4(\theta_2) \sin^2(\theta_3) \times \left\{ \right. \\ &\quad \left. u^3 f(u) (x'_4(u))^2 + [1 - (\hat{a}'_0)^2] \right\}. \end{aligned} \quad (3.51)$$

Therefore  $N_f$  stack of D8-branes action becomes

$$\begin{aligned} S_{D8} &= \mu_8 N_f \int d\tau d^3x d\Omega_4 du \left( \frac{u^{-3/4}}{g_s} \right) R^9 u^{13/4} \sqrt{u^3 f(u) (x'_4(u))^2 + [1 - (\hat{a}'_0)^2]}, \\ &= \frac{\mu_8 N_f R^9}{g_s} \left( \frac{\beta}{R} \right) \left( \frac{V_3}{R^3} \right) \int du u^4 \sqrt{f(u) (x'_4(u))^2 + u^{-3} [1 - (\hat{a}'_0)^2]}, \\ &= \frac{\mu_8 N_f \Omega_4 V_3 \beta R^5}{g_s} \int du u^4 \sqrt{f(u) (x'_4(u))^2 + u^{-3} [1 - (\hat{a}'_0)^2]}, \\ &= \mathcal{N} \int du u^4 \sqrt{f(u) (x'_4(u))^2 + u^{-3} [1 - (\hat{a}'_0)^2]}, \end{aligned} \quad (3.52)$$

where we define  $\mathcal{N} \equiv \frac{\mu_8 N_f \Omega_4 V_3 \beta R^5}{g_s}$ . The Legendre-transformed action is given by

$$\tilde{S}_{D8} = S_{D8} + \int du d(u) \hat{a}'_0(u), \quad (3.53)$$

where

$$d(u) \equiv -\frac{1}{\mathcal{N}} \frac{\delta S_{D8}}{\delta \hat{a}'_0(u)} = \frac{u \hat{a}'_0}{\sqrt{f(u)(x'_4(u))^2 + u^{-3} [1 - (\hat{a}'_0)^2]}}, \quad (3.54)$$

Clearly we found that

$$\begin{aligned} d^2(u) (f(u)(x'_4(u))^2 + u^{-3} [1 - (\hat{a}'_0)^2]) &= u^2 (\hat{a}'_0)^2, \\ d^2(u) (f(u)(x'_4(u))^2 + u^{-3}) &= (\hat{a}'_0)^2 (u^2 + u^{-3} d^2(u)), \\ \hat{a}'_0 &= d(u) \left[ \frac{f(u)(x'_4(u))^2 + u^{-3}}{u^2 + u^{-3} d^2(u)} \right]^{1/2}. \end{aligned} \quad (3.55)$$

Consequently, the Legendre-transformed D8-brane action takes the form

$$\begin{aligned} \tilde{S}_{D8} &= \mathcal{N} \int du u^4 \left[ f(u)(x'_4(u))^2 + u^{-3} \left[ 1 - \frac{d^2(u)[f(u)(x'_4(u))^2 + u^{-3}]}{u^2 + u^{-3} d^2(u)} \right] \right]^{1/2} \\ &\quad + \mathcal{N} \int du d^2(u) \left[ \frac{f(u)(x'_4(u))^2 + u^{-3}}{u^2 + u^{-3} d^2(u)} \right]^{1/2}, \\ &= \mathcal{N} \int du u^4 \left[ f(u)(x'_4(u))^2 + u^{-3} \left[ \frac{u^2}{u^2 + u^{-3} d^2(u)} - \frac{d^2(u)f(u)(x'_4(u))^2}{u^2 + u^{-3} d^2(u)} \right] \right]^{1/2} \\ &\quad + \mathcal{N} \int du d^2(u) \left[ \frac{f(u)(x'_4(u))^2 u^3 + 1}{u^5 + d^2(u)} \right]^{1/2}, \\ &= \mathcal{N} \int du \left\{ u^4 \left[ f(u)(x'_4(u))^2 \left( 1 - \frac{d^2(u)}{u^5 + d^2(u)} \right) + \frac{u^2}{u^5 + d^2(u)} \right]^{1/2} \right. \\ &\quad \left. + d^2(u) \left[ \frac{f(u)(x'_4(u))^2 u^3 + 1}{u^5 + d^2(u)} \right]^{1/2} \right\}, \\ &= \mathcal{N} \int du \left\{ u^4 \left[ f(u)(x'_4(u))^2 \left( \frac{u^5}{u^5 + d^2(u)} \right) + \frac{u^2}{u^5 + d^2(u)} \right]^{1/2} \right. \\ &\quad \left. + d^2(u) \left[ \frac{f(u)(x'_4(u))^2 u^3 + 1}{u^5 + d^2(u)} \right]^{1/2} \right\}, \\ &= \mathcal{N} \int du \left( u^5 \left[ \frac{f(u)(x'_4(u))^2 u^3 + 1}{u^5 + d^2(u)} \right]^{1/2} + d^2(u) \left[ \frac{f(u)(x'_4(u))^2 u^3 + 1}{u^5 + d^2(u)} \right]^{1/2} \right), \\ &= \mathcal{N} \int du \left[ \frac{f(u)(x'_4(u))^2 u^3 + 1}{u^5 + d^2(u)} \right]^{1/2} [u^5 + d^2(u)], \\ &= \mathcal{N} \int du [f(u)(x'_4(u))^2 u^3 + 1]^{1/2} [u^5 + d^2(u)]^{1/2}, \\ &= \mathcal{N} \int du u^4 [f(u)(x'_4(u))^2 + u^{-3}]^{1/2} \left[ 1 + \frac{d^2(u)}{u^5} \right]^{1/2}, \end{aligned} \quad (3.56)$$

$$= \mathcal{N} \int du \tilde{\mathcal{L}}. \quad (3.57)$$

Similarly, the constant of motion associated with  $x'_4(u)$  can be obtained from

$$\begin{aligned}
\frac{\delta \tilde{S}_{D8}}{\delta x'_4(u)} &= u^4 \left[ 1 + \frac{d^2(u)}{u^5} \right]^{1/2} \frac{f(u)x'_4(u)}{[f(u)(x'_4(u))^2 + u^{-3}]^{1/2}}, \\
&= u_0^4 \left[ 1 + \frac{d^2}{u_0^5} \right]^{1/2} [f(u_0)]^{1/2}, \\
&= \text{const.}
\end{aligned} \tag{3.58}$$

The shape of D8-branes configuration can be determined from

$$\begin{aligned}
(f(u))^2(x'_4(u))^2 &= f(u_0) \frac{u_0^8 \left( 1 + \frac{d^2}{u_0^5} \right)}{u^8 \left( 1 + \frac{d^2}{u^5} \right)} (f(u)(x'_4(u))^2 + u^{-3}), \\
f(u)(x'_4(u))^2 \left[ f(u) - f(u_0) \frac{u_0^8 + u_0^3 d^2}{u^8 + u^3 d^2} \right] &= f(u_0) \frac{u_0^8 + u_0^3 d^2}{u^8 + u^3 d^2} \frac{1}{u^3}, \\
(x'_4(u))^2 &= \frac{1}{u^3 f(u)} \left[ \frac{f(u)(u^8 + u^3 d^2)}{f(u_0)(u_0^8 + u_0^3 d^2)} - 1 \right]^{-1}.
\end{aligned} \tag{3.59}$$

### 3.3.1 D4-brane sources

In order to calculate the D4-branes action, let's consider the wrapped 4-sphere metric which is given by identifying

$$\begin{aligned}
x^0 &= \frac{X_E^0}{R} = \tau, \\
x^1 &= x^6 = \theta_1, \\
x^2 &= x^7 = \theta_2, \\
x^3 &= x^8 = \theta_3, \\
x^4 &= x^9 = \theta_4.
\end{aligned}$$

The metric of D4-branes locating at  $u = u_c$  takes the following form,

$$\begin{aligned}
g_{MN} &= \text{diag}(R^2 u_c^{3/2} f(u_c), R^2 u_c^{1/2}, R^2 u_c^{1/2} \sin^2 \theta_1, R^2 u_c^{1/2} \sin^2 \theta_1 \sin^2 \theta_2, \\
&R^2 u_c^{1/2} \sin^2 \theta_1 \sin^2 \theta_2 \sin^2 \theta_3).
\end{aligned} \tag{3.60}$$

Therefore

$$\det(g_{MN}) = R^{10} u_c^{7/2} f(u_c) \sin^6 \theta_1 \sin^4 \theta_2 \sin^2 \theta_3. \tag{3.61}$$

From

$$\begin{aligned}
S_{D4} &= \frac{n_4 V_3 \mu_4}{R^3} \int d\theta_1 d\theta_2 d\theta_3 d\theta_4 d\tau e^{-\phi} \sqrt{\det(g_{MN})}, \\
&= \frac{n_4 V_3 \mu_4}{R^3} \int d\theta_1 d\theta_2 d\theta_3 d\theta_4 d\tau \left( \frac{1}{g_s u_c^{3/4}} \right) \sqrt{\det(g_{MN})}, \\
&= \frac{n_4 V_3 \mu_4 \beta \Omega_4}{g_s R^4} u_c^{-3/4} \left( R^5 u_c^{7/4} \sqrt{f(u_c)} \right), \\
&= \frac{n_4 V_3 \mu_4 \beta \Omega_4 R}{g_s} \sqrt{f(u_c)} u_c.
\end{aligned} \tag{3.62}$$

Using (3.26)

$$n_4 = \frac{2\pi\alpha' R^2 \mathcal{N}}{\beta V_3 N_c} d, \tag{3.63}$$

the D4-branes action can be obtained as follows

$$\begin{aligned}
S_{D4} &= \frac{2\pi\alpha' R^2 \mu_4 \mathcal{N} \Omega_4 R}{g_s N_c} \sqrt{f(u_c)} u_c d, \\
&= \frac{2\pi\alpha' R^3}{g_s N_c} \left( \frac{1}{2^4 \pi^4 (\alpha')^{5/2}} \right) \left( \frac{2^3 \pi^2}{3} \right) \mathcal{N} u_c \sqrt{f(u_c)} d, \\
&= 2\pi\alpha' (\pi(\alpha')^{3/2}) \left( \frac{1}{2^4 \pi^4 (\alpha')^{5/2}} \right) \left( \frac{2^3 \pi^2}{3} \right) \mathcal{N} u_c \sqrt{f(u_c)} d, \\
S_{D4} &= \frac{1}{3} \mathcal{N} u_c \sqrt{f(u_c)} d,
\end{aligned} \tag{3.64}$$

where we use  $\frac{R^3}{g_s N_c} = \pi(\alpha')^{3/2}$  for the last equation.

### 3.3.2 String sources

The remaining possible sources of electric displacement in this phase are strings stretching from D8-branes to the horizon at  $u_T$ . The precise relation between the density of string  $n_s$  and the electric displacement  $d$  can be determined by considering the  $B$ -field dependence of the supergravity, D8-branes and the string action [71]:

$$S_{SUG}[B] = -\frac{1}{4\kappa_{10}^2} \int d^{10}x \sqrt{-\det g} e^{-2\Phi} |\partial B|^2, \tag{3.65}$$

$$S_{D8}[B] = \mathcal{N} \int du u^4 \left[ f(u) (x'_4(u))^2 + u^{-3} - u^{-3} (B_{0u} + \hat{a}'_0(u))^2 \right]^{1/2}, \tag{3.66}$$

$$S_{F1}[B] = -\frac{n_s V_3}{2\pi\alpha' R^3} \int dt du \left( \sqrt{-\det g_{MN}} - B_{0u} \right). \tag{3.67}$$

Varying the actions with respect to  $B_{0u}$  gives,

$$\begin{aligned}\frac{\delta S_{SUG}}{\delta B_{0u}(u)} &= \frac{\partial \mathcal{L}_{SUG}}{\partial B_{0u}} - \partial_\mu \left( \frac{\partial \mathcal{L}_{SUG}}{\partial (\partial_\mu B_{0u})} \right), \\ &= \frac{1}{2\kappa_{10}^2} \partial_\mu (\sqrt{-g} e^{-2\phi} \partial^\mu B_{0u}) = 0,\end{aligned}\quad (3.68)$$

$$\begin{aligned}\frac{\delta S_{D8}}{\delta B_{0u}(u)} &= \mathcal{N} \frac{u^4(-u^3)(B_{0u} + \hat{a}'_0(u))}{[f(u)(x'_4(u))^2 + u^{-3} - u^{-3}(B_{0u} + \hat{a}'_0(u))^2]^{1/2}}, \\ &= \frac{\delta S_{D8}}{\delta \hat{a}'_0(u)} = \mathcal{N}d,\end{aligned}\quad (3.69)$$

$$\frac{\delta S_{F1}}{\delta B_{0u}(u)} = -\frac{n_s V_3}{2\pi\alpha'R} \int dt(-1) = \frac{n_s V_3 \beta}{2\pi\alpha'R^2}.\quad (3.70)$$

Consequently, invariance of the total actions gives,

$$\begin{aligned}\mathcal{N}d + \frac{n_s V_3 \beta}{2\pi\alpha'R^2} &= 0, \\ \frac{n_s V_3 \beta}{2\pi\alpha'R^2} &= -\mathcal{N}d, \\ n_s &= -\frac{2\pi\alpha'R^2 \mathcal{N}}{\beta V_3} d.\end{aligned}\quad (3.71)$$

For deconfined background,

$$\det g_{MN} = \begin{vmatrix} -R^2 f(u) u^{3/2} & \\ & R^2 f^{-1}(u) u^{-3/2} \end{vmatrix} = -R^4.\quad (3.72)$$

The string action in deconfined background takes the form

$$\begin{aligned}S_{F1} &= -\frac{n_s V_3}{2\pi\alpha'R} \int dt du, \\ &= -\frac{n_s V_3 \beta}{2\pi\alpha'R^2} \int du, \\ &= -\mathcal{N}d \int_{u_c}^{u_T} du, \\ &= \mathcal{N}(u_c - u_T)d.\end{aligned}\quad (3.73)$$

### 3.3.3 Balance condition

According to the configuration in the deconfined phase, addition of D4-brane source or string source suggests a new reference at  $u = u_c$ , however in (3.59), we use  $u_0$  as a reference position. Therefore we will use the  $u_c$  as a reference point instead of  $u_0$ . Consequently, the reference function  $f(u_0)(u_0^8 + u_0^3 d^2)$  turns into the new function  $F(u_c)$ . The relation in (3.59) becomes

$$(x'_4(u))^2 = \frac{1}{u^3 f(u)} \left[ \frac{f(u)(u^8 + u^3 d^2)}{F^2(u_c)} - 1 \right]^{-1},\quad (3.74)$$

where  $F(u_c)$  can be determined from

$$\begin{aligned}
 (x'_4(u_c))^2 &= \frac{1}{u_c^3 f(u_c)} \left[ \frac{f(u_c) (u_c^8 + u_c^3 d^2)}{F^2(u_c)} - 1 \right]^{-1}, \\
 \frac{f(u_c) (u_c^8 + u_c^3 d^2)}{F^2(u_c)} &= \frac{1}{u_c^3 f(u_c) (x'_4(u_c))^2} + 1, \\
 &= \frac{f(u_c) (x'_4(u_c))^2 + u_c^{-3}}{f(u_c) (x'_4(u_c))^2}. \\
 F(u_c) &= \frac{f(u_c) \sqrt{u_c^8 + u_c^3 d^2}}{\sqrt{f(u_c) (x'_4(u_c))^2 + u_c^{-3}}} (x'_4(u_c)). \tag{3.75}
 \end{aligned}$$

Note that we can determine  $x'_4(u_c)$  from the balance condition in Appendix A.





# Chapter IV

## THERMODYNAMICS WITH FINITE CHEMICAL POTENTIAL

We now consider the implication of configuration in the bulk to the gauge theory at the boundary based on Ref.[71]. The main goal of this chapter is to study many different phases of the gauge theory at the finite temperature and finite baryon chemical potential  $\mu$ . The superstring construction in Sakai-Sugimoto model introduces an additional parameter apart from the parameters of QCD that is the asymptotic separation  $l$  between D8-branes and anti D8-branes. For convenience, we will fix  $l = 1$ . Generally we will later consider the variation of  $l$  that take no quantitative change in the results.

### 4.1 Baryon chemical potential

The grand canonical potential is naturally obtained by evaluating D8-branes action on the solution. For convenience, we will normalize the potential by dividing out the normalization constant  $\mathcal{N}$ ,

$$\Omega(t, \mu) = \frac{1}{\mathcal{N}} S_{D8} [t, x_4(u), \hat{a}_0(u)]_{solution}. \quad (4.1)$$

Note that the potential and all other thermodynamic quantities associated with the matter scales as  $N_f N_c$ . The (dimensionless) baryon chemical potential  $\mu$  can be identified using the asymptotic value of the  $U(1)$  gauge potential in the solution

$$\mu = \hat{a}_0(\infty). \quad (4.2)$$

With the normalization factor, the baryon number density  $d$  can be obtained from

$$n_b = -\frac{\partial \Omega(t, \mu)}{\partial \mu} = d, \quad (4.3)$$

For computational convenience, we will express  $\mu$  in terms of  $d$  using the canonical ensemble. Correspondingly, the free energy take the following form

$$F(t, d) = \Omega(t, \mu) + \mu d, \quad (4.4)$$

and the chemical potential is given by

$$\mu = \left. \frac{\partial F(t, d)}{\partial d} \right|_t. \quad (4.5)$$

The free energy is then related to the Legendre-transformed D8-branes action on the solution. In the cusp configuration, there is an influence of sources such as D4-branes or strings. Therefore, we have to include the contribution of the sources determined at position of the cusp.

$$F(t, d) = \frac{1}{\mathcal{N}} \left( \tilde{S}_{D8}[t, x_4(u), d(u)]_{solution} + S_{source}(t, d, u_c) \right). \quad (4.6)$$

The dependence on  $d$  comes from three reasons:  $\tilde{S}_{D8}$  and  $S_{source}$  are explicit function of  $d$ , the solution for  $x'_4$  on  $d$  is also an explicit function of  $d$ , and the dependence on  $d$  of  $u_c$ . Including all of them, the chemical potential becomes

$$\begin{aligned} \mu = & \frac{1}{\mathcal{N}} \left\{ \int_{u_c}^{\infty} du \left( \frac{\delta \tilde{S}_{D8}}{\delta d(u)} + \frac{\delta \tilde{S}_{D8}}{\delta x'_4(u)} \frac{\partial x'_4}{\partial d} \right) \Big|_{t,l,u_c}^{solution} \right. \\ & \left. + \frac{\partial u_c}{\partial d} \Big|_{t,l} \left( \frac{\partial \tilde{S}_{D8}}{\partial u_c} + \frac{\partial S_{source}}{\partial u_c} \right) \Big|_{d,t,l}^{solution} + \frac{\partial S_{source}}{\partial d} \Big|_{t,l,u_c} \right\}. \quad (4.7) \end{aligned}$$

The second term vanishes since  $\delta \tilde{S}_{D8}/\delta x'_4(u)$  is constant by the equation of motion for  $x_4$  and the integral term with  $\partial x'_4/\partial d$  at fixed  $u_c$  gives  $\partial l/\partial d = 0$  since  $l$  is fixed. The third and fourth terms are canceled by the zero-force condition at the cusp (see Appendix),

$$\mu = \int_{u_c}^{\infty} du \hat{a}'_0(u) + \frac{1}{\mathcal{N}} \left. \frac{\partial S_{source}}{\partial d} \right|_{t,l,u_c}. \quad (4.8)$$

where  $\hat{a}'_0(u)$  is related to  $d$  by solving for the inverse relation. The fact that chemical potential is identified with the value of gauge potential at infinity, reflects a specific choice of gauge, in which  $\hat{a}_0(u_c)$  is identified with mass of the source. In the parallel configuration the source is absent and the lower limit of the integral becomes the value at the horizon  $u = u_T$ . In this case the gauge choice (4.2) gives  $\hat{a}_0(u_T) = 0$ , which is in agreement with the fact that the source becomes massless at the horizon.

## 4.2 Confined phase

In confined phase, only connected D8-branes and anti-D8-branes is possible. For a given  $\mu$  which is at fixed  $\hat{a}_0(\infty)$ , there are two connected solutions, a U-shape

configuration with  $d = 0$  and a D4-branes sourced cusp configuration with  $d \neq 0$ . The former refers to the QCD vacuum, while the latter corresponds to a phase of nuclear matter. In vacuum phase,  $\hat{a}_0$  is constant, and the electric displacement  $d$  disappears. Therefore the grand canonical potential,  $\Omega$ , is independent of  $\mu$  in this phase. For nuclear matter phase  $\hat{a}_0(u)$  is sourced by D4-branes. Therefore using (4.8), (3.17), and (3.20) chemical potential for the confined phase yields

$$\begin{aligned} \mu &= \int_{u_c}^{\infty} du \hat{a}'_0(u) + \frac{1}{\mathcal{N}} \left. \frac{\partial S_{D4}}{\partial d} \right|_{t,l,u_c}, \\ &= \int_{u_c}^{\infty} du d \left[ \frac{u^3}{d^2 + u^5} \right]^{1/2} \left[ \frac{1}{u^3 f(u)} \left( \frac{f(u)u^3(d^2 + u^5)}{f(u_0)u_0^3(d^2 + u_0^5)} - 1 \right)^{-1} + \frac{1}{u^3 f(u)} \right]^{1/2} \\ &\quad + \frac{1}{3} u_c. \end{aligned} \quad (4.9)$$

Using  $\Theta(u) \equiv f(u)u^3(d^2 + u^5)$ , the chemical potential becomes

$$\begin{aligned} \mu &= \int_{u_c}^{\infty} du d \left[ \frac{1}{f(u)(d^2 + u^5)} \right]^{1/2} \left[ \left( \frac{\Theta(u)}{\Theta(u_0)} - 1 \right)^{-1} + 1 \right]^{1/2} \\ &\quad + \frac{1}{3} u_c, \\ &= \int_{u_c}^{\infty} du d \left[ \frac{1}{f(u)(d^2 + u^5)} \right]^{1/2} \left[ \left( \frac{\Theta(u_0)}{\Theta(u) - \Theta(u_0)} \right) + 1 \right]^{1/2} \\ &\quad + \frac{1}{3} u_c, \\ &= \int_{u_c}^{\infty} du d \left[ \frac{1}{f(u)(d^2 + u^5)} \right]^{1/2} \left[ \frac{\Theta(u)}{\Theta(u) - \Theta(u_0)} \right]^{1/2} + \frac{1}{3} u_c, \\ &= \int_{u_c}^{\infty} du d [u^3]^{1/2} \left[ \frac{1}{f(u)u^3(d^2 + u^5) - f(u_0)u_0^3(d^2 + u_0^5)} \right]^{1/2} + \frac{1}{3} u_c, \\ &= \int_{u_c}^{\infty} du \frac{d}{\sqrt{f(u)(d^2 + u^5) - \left(\frac{u_0}{u}\right)^3 f(u_0)(d^2 + u_0^5)}} + \frac{1}{3} u_c. \end{aligned} \quad (4.10)$$

The grand canonical potential for nuclear matter can be obtained by using Eq.(4.1), and (3.14),

$$\begin{aligned}
\Omega_{nuc}(\mu) &= \int du u^4 \sqrt{f(u)(x'_4(u))^2 + \frac{1}{u^3} \left[ \frac{1}{f(u)} - (\hat{a}'_0)^2 \right]}, \\
&= \int_{u_c}^{\infty} du u^4 \left[ 1 - \frac{d^2}{d^2 + u^5} \right]^{1/2} \left[ f(u)(x'_4(u))^2 + \frac{1}{f(u)u^3} \right]^{1/2}, \\
&= \int_{u_c}^{\infty} du u^4 \left[ \frac{u^5}{d^2 + u^5} \right]^{1/2} \left[ \frac{1}{u^3 f(u)} \left( \frac{f(u)u^3(d^2 + u^5)}{f(u_0)u_0^3(d^2 + u_0^5)} - 1 \right)^{-1} + \frac{1}{f(u)u^3} \right]^{1/2}, \\
&= \int_{u_c}^{\infty} du \frac{u^5}{f^{1/2}(u)} \left[ \frac{1}{d^2 + u^5} \right]^{1/2} \left[ \left( \frac{\Theta(u)}{\Theta(u_0)} - 1 \right)^{-1} + 1 \right]^{1/2}, \\
&= \int_{u_c}^{\infty} du \frac{u^5}{f^{1/2}(u) (d^2 + u^5)^{1/2}} \left[ \frac{\Theta(u)}{\Theta(u) - \Theta(u_0)} \right]^{1/2}, \\
&= \int_{u_c}^{\infty} du \frac{u^{13/2}}{[\Theta(u) - \Theta(u_0)]^{1/2}}, \\
&= \int_{u_c}^{\infty} du \frac{u^{13/2}}{\sqrt{f(u)(u^8 + u^3 d^2) - f(u_0)(u_0^8 + u_0^3 d^2)}}, \\
&= \int_{u_c}^{\infty} du \frac{u^{5/2}}{\sqrt{f(u)(1 + \frac{d^2}{u^5}) - \frac{u_0^8}{u^8} f(u_0)(1 + \frac{d^2}{u_0^5})}}. \tag{4.11}
\end{aligned}$$

For vacuum configuration in the confined phase,  $d = 0$ , the grand canonical potential takes the following form

$$\Omega_{vac}(\mu) = \int_{u_{0v}}^{\infty} du \frac{u^{5/2}}{\sqrt{f(u) - \frac{u_{0v}^8}{u^8} f(u_{0v})}}, \tag{4.12}$$

where  $u_0$  is the minimum value for the nuclear matter phase and  $u_{0v}$  is that of the vacuum phase. These grand chemical potentials are actually divergent at  $u \rightarrow \infty$ , however the difference is finite and is given by

$$\begin{aligned}
\Delta\Omega(\mu) &= \Omega_{nuc}(\mu) - \Omega_{vac}(\mu), \\
&= \int_{u_c}^{\infty} du \frac{u^{5/2}}{\sqrt{f(u)(1 + \frac{d^2}{u^5}) - \frac{u_0^8}{u^8} f(u_0)(1 + \frac{d^2}{u_0^5})}} - \int_{u_{0v}}^{\infty} du \frac{u^{5/2}}{\sqrt{f(u) - \frac{u_{0v}^8}{u^8} f(u_{0v})}}, \\
&= \int_{u_c}^{\infty} du \frac{u^{5/2}}{\sqrt{f(u)(1 + \frac{d^2}{u^5}) - \frac{u_0^8}{u^8} f(u_0)(1 + \frac{d^2}{u_0^5})}} - \frac{u^{5/2}}{\sqrt{f(u) - \frac{u_{0v}^8}{u^8} f(u_{0v})}} \\
&\quad - \int_{u_{0v}}^{u_c} du \frac{u^{5/2}}{\sqrt{f(u) - \frac{u_{0v}^8}{u^8} f(u_{0v})}}. \tag{4.13}
\end{aligned}$$

### 4.3 Deconfined phase

In deconfined phase, the thermodynamics turns to be more interesting since there are more possible configurations for a given value of  $\mu$ . Apart from the U-shaped and D4-branes cusp configurations, there are also the parallel configuration, with vanishing or non-vanishing density, and the string-cusp configuration. The parallel configuration represent a phase with restored chiral symmetry. At finite  $\mu$ , there is also the quark-gluon plasma (QGP). Interestingly, in the string cusp-configuration, there are strings stretched between 8-branes and the horizon. This refer to the quark matter in the corresponding gauge theory, however, it will become clear later that this phase is actually unstable at least for a uniform distribution of baryon charge. Consequently, the remaining three phase will be compared using phase diagram in the  $(t, \mu)$  plane.

#### 4.3.1 Unstable quark matter

In this section, we will show that the quark matter phase is thermodynamically unstable. Attempt to evaluate the chemical potential in the deconfined phase with string sources (3.73) yields

$$\begin{aligned}
\mu &= \int_{u_c}^{\infty} du \hat{a}'_0(u) + \frac{1}{\mathcal{N}} \left. \frac{\partial S_{F1}}{\partial d} \right|_{t,l,u_c}, \\
&= \int_{u_c}^{\infty} du d \left[ \frac{f(u)u^3(x'_4(u))^2 + 1}{u^5 + d^2} \right]^{1/2} + (u_c - u_T), \\
&= \int_{u_c}^{\infty} du \frac{d}{[u^5 + d^2(u)]^{1/2}} \left[ \left( \frac{f(u)u^3(u^5 + d^2)}{f(u_0)u_0^3(u_0^5 + d^2)} - 1 \right)^{-1} + 1 \right]^{1/2} + (u_c - u_T), \\
&= \int_{u_c}^{\infty} du \frac{d}{[u^5 + d^2]^{1/2}} \left[ \left( \frac{\Theta(u)}{\Theta(u_0)} - 1 \right)^{-1} + 1 \right]^{1/2} + (u_c - u_T), \\
&= \int_{u_c}^{\infty} du \frac{d}{[u^5 + d^2]^{1/2}} \left[ \frac{\Theta(u)}{\Theta(u) - \Theta(u_0)} \right]^{1/2} + (u_c - u_T), \\
&= \int_{u_c}^{\infty} du \frac{d u^{3/2} f^{1/2}(u)}{[\Theta(u) - \Theta(u_0)]^{1/2}} + (u_c - u_T), \\
&= \int_{u_c}^{\infty} du \frac{d \sqrt{f(u)}}{\sqrt{f(u)(u^5 + d^2) - \frac{u_0^3}{u^3} f(u_0)(u_0^5 + d^2)}} + (u_c - u_T). \tag{4.14}
\end{aligned}$$

It is obvious from the plot that

$$\frac{\partial \mu}{\partial d} < 0, \tag{4.15}$$

and therefore the string-cusp configuration is thermodynamically unstable to the fluctuations in density. Similarly the instability was found in the D3-D7 model at finite density.

### 4.3.2 Comparison of the possible phase

In this section we will compare the vacuum phase to the quark-gluon plasma phase. The vacuum phase can be described by the U-shape configuration, while the quark-gluon plasma phase can be described by the parallel configuration. The grand canonical potential of the vacuum can be obtained by using Eq.(4.1), and (3.52) with additional condition that  $d = 0$

$$\begin{aligned}
\Omega_{vac}(\mu) &= \int_{u_0}^{\infty} du u^4 \sqrt{f(u)(x'_4(u))^2 + u^{-3} [1 - (\hat{a}'_0)^2]} \Big|_{d=0}, \\
&= \int_{u_0}^{\infty} du u^5 \left[ \frac{f(u)(x'_4(u))^2 u^3 + 1}{d^2 + u^5} \right]^{1/2} \Big|_{d=0}, \\
&= \int_{u_0}^{\infty} du \frac{u^5}{[u^5 + d^2]^{1/2}} \left[ \left( \frac{f(u)u^3(u^5 + d^2)}{f(u_0)u_0^3(u_0^5 + d^2)} - 1 \right)^{-1} + 1 \right]^{1/2} \Big|_{d=0}, \\
&= \int_{u_0}^{\infty} du \frac{u^5}{[u^5 + d^2]^{1/2}} \left[ \left( \frac{\Theta(u)}{\Theta(u_0)} - 1 \right)^{-1} + 1 \right]^{1/2} \Big|_{d=0}, \\
&= \int_{u_0}^{\infty} du \frac{u^5}{[u^5 + d^2]^{1/2}} \left[ \frac{\Theta(u)}{\Theta(u) - \Theta(u_0)} \right]^{1/2} \Big|_{d=0}, \\
&= \int_{u_0}^{\infty} du \frac{u^5 u^{3/2} f^{1/2}(u)}{[\Theta(u) - \Theta(u_0)]^{1/2}} \Big|_{d=0}, \\
&= \int_{u_0}^{\infty} du \frac{u^5 \sqrt{f(u)}}{\sqrt{f(u)(u^5 + d^2) - \frac{u_0^3}{u^3} f(u_0)(u_0^5 + d^2)}} \Big|_{d=0}, \\
&= \int_{u_0}^{\infty} du \frac{u^{5/2} \sqrt{f(u)}}{\sqrt{f(u) - \frac{u_0^8}{u^8} f(u_0)}}. \tag{4.16}
\end{aligned}$$

The potential of the QGP is given by using Eq.(4.1), and (3.52) with  $x'_4(u) = 0$ ,

$$\begin{aligned}
\Omega_{qgp}(\mu) &= \int_{u_T}^{\infty} du u^4 \sqrt{f(u)(x'_4(u))^2 + u^{-3} [1 - (\hat{a}'_0)^2]} \Big|_{x'_4(u)=0}, \\
&= \int_{u_T}^{\infty} du u^5 \left[ \frac{f(u)(x'_4(u))^2 u^3 + 1}{d^2 + u^5} \right]^{1/2} \Big|_{x'_4(u)=0}, \\
&= \int_{u_T}^{\infty} du \frac{u^5}{\sqrt{d^2 + u^5}}. \tag{4.17}
\end{aligned}$$



The chemical potential is obtained as a function of density  $d$ , by using Eq.(3.55), (3.59), and (4.8)

$$\begin{aligned}
\mu &= \int_{u_T}^{\infty} du \hat{a}'_0(u) \Big|_{x'_4(u)=0}, \\
&= \int_{u_T}^{\infty} du d \left[ \frac{f(u)u^3(x'_4(u))^2 + 1}{u^5 + d^2} \right]^{1/2} \Big|_{x'_4(u)=0}, \\
&= \int_{u_T}^{\infty} du \frac{d}{\sqrt{u^5 + d^2}}.
\end{aligned} \tag{4.18}$$

The grand chemical potentials for both quark-gluon plasma phase and vacuum phase diverge as  $u \rightarrow \infty$  but the difference is finite,

$$\Delta\Omega_1 = \Omega_{qgp} - \Omega_{vac}. \tag{4.19}$$

We now turn to the comparison between the vacuum phase and the nuclear deconfined matter phase. Since there is chiral-symmetry breaking in deconfined phase, based on the Sakai-Sugimoto model, it is sensible to expect that nuclear matter could also form in this case. The potential of nuclear phase is given by

$$\begin{aligned}
\Omega_{nuc}(\mu) &= \int_{u_0}^{\infty} du u^4 \sqrt{f(u)(x'_4(u))^2 + u^{-3} [1 - (\hat{a}'_0)^2]}, \\
&= \int_{u_0}^{\infty} du u^5 \left[ \frac{f(u)(x'_4(u))^2 u^3 + 1}{d^2 + u^5} \right]^{1/2}, \\
&= \int_{u_0}^{\infty} du \frac{u^5}{[u^5 + d^2]^{1/2}} \left[ \left( \frac{f(u)u^3(u^5 + d^2)}{f(u_0)u_0^3(u_0^5 + d^2)} - 1 \right)^{-1} + 1 \right]^{1/2}, \\
&= \int_{u_0}^{\infty} du \frac{u^5}{[u^5 + d^2]^{1/2}} \left[ \left( \frac{\Theta(u)}{\Theta(u_0)} - 1 \right)^{-1} + 1 \right]^{1/2}, \\
&= \int_{u_0}^{\infty} du \frac{u^5}{[u^5 + d^2]^{1/2}} \left[ \frac{\Theta(u)}{\Theta(u) - \Theta(u_0)} \right]^{1/2}, \\
&= \int_{u_0}^{\infty} du \frac{u^5 u^{3/2} f^{1/2}(u)}{[\Theta(u) - \Theta(u_0)]^{1/2}}, \\
&= \int_{u_0}^{\infty} du \frac{u^5 \sqrt{f(u)}}{\sqrt{f(u)(u^5 + d^2) - \frac{u_0^3}{u^3} f(u_0)(u_0^5 + d^2)}}, \\
&= \int_{u_0}^{\infty} du \frac{u^{5/2} \sqrt{f(u)}}{\sqrt{f(u)(1 + \frac{d^2}{u^5}) - \frac{u_0^8}{u^8} f(u_0)(1 + \frac{d^2}{u_0^5})}},
\end{aligned} \tag{4.20}$$

where  $d$  is again given implicitly in terms of  $\mu$  using with 4-branes sources (3.64). The chemical potential becomes

$$\begin{aligned}
\mu &= \int_{u_c}^{\infty} du \hat{a}'_0(u) + \frac{1}{\mathcal{N}} \frac{\partial S_{D4}}{\partial d} \Big|_{t,l,u_c}, \\
&= \int_{u_c}^{\infty} du d \left[ \frac{f(u)u^3(x'_4(u))^2 + 1}{u^5 + d^2} \right]^{1/2} + \frac{1}{3}u_c\sqrt{f(u_c)}, \\
&= \int_{u_c}^{\infty} du \frac{d}{[u^5 + d^2(u)]^{1/2}} \left[ \left( \frac{f(u)u^3(u^5 + d^2)}{f(u_0)u_0^3(u_0^5 + d^2)} - 1 \right)^{-1} + 1 \right]^{1/2} + \frac{1}{3}u_c\sqrt{f(u_c)}, \\
&= \int_{u_c}^{\infty} du \frac{d}{[u^5 + d^2]^{1/2}} \left[ \left( \frac{\Theta(u)}{\Theta(u_0)} - 1 \right)^{-1} + 1 \right]^{1/2} + \frac{1}{3}u_c\sqrt{f(u_c)}, \\
&= \int_{u_c}^{\infty} du \frac{d}{[u^5 + d^2]^{1/2}} \left[ \frac{\Theta(u)}{\Theta(u) - \Theta(u_0)} \right]^{1/2} + \frac{1}{3}u_c\sqrt{f(u_c)}, \\
&= \int_{u_c}^{\infty} du \frac{d u^{3/2} f^{1/2}(u)}{[\Theta(u) - \Theta(u_0)]^{1/2}} + \frac{1}{3}u_c\sqrt{f(u_c)}, \\
&= \int_{u_c}^{\infty} du \frac{d\sqrt{f(u)}}{\sqrt{f(u)(u^5 + d^2) - \frac{u_0^3}{u^3}f(u_0)(u_0^5 + d^2)}} + \frac{1}{3}u_c\sqrt{f(u_c)}. \tag{4.21}
\end{aligned}$$

The difference between the potential of the nuclear phase and the vacuum phase is then

$$\Delta\Omega_2 = \Omega_{nuc} - \Omega_{vac}. \tag{4.22}$$

The final part of phase diagram comes from comparison between grand canonical potential of the nuclear matter phase and that of QGP phase:

$$\Delta\Omega_3 = \Omega_{nuc} - \Omega_{qgp}. \tag{4.23}$$

### 4.3.3 Entropy and equation of state

Generally, the thermodynamic systems are characterized by their equation of state and entropy. We will briefly discuss the entropy of the systems in different phases.

The pressure of the system can be obtained in a function of the baryon number density  $p(d, t)$  from

$$\frac{\partial\Omega}{\partial\mu} = -d, \tag{4.24}$$

and

$$\frac{\partial P}{\partial\mu} = d. \tag{4.25}$$

Using (4.21), we find that, at small baryon number density,

$$\begin{aligned}
\mu &= \int_{u_c}^{\infty} du \frac{d\sqrt{f(u)}}{\sqrt{f(u)(u^5 + d^2) - \frac{u_0^3}{u^3}f(u_0)(u_0^5 + d^2)}} + \frac{1}{3}u_c\sqrt{f(u_c)}, \\
&= \int_{u_c}^{\infty} du \frac{d\sqrt{f(u)}}{\sqrt{f(u)(u^5 + d^2) - \frac{u_0^3}{u^3}f(u_0)(u_0^5 + d^2)}} + \mu_{\text{onset}}, \\
\mu - \mu_{\text{onset}} &= \int_{u_c}^{\infty} du \frac{d\sqrt{f(u)}}{\sqrt{f(u)(u^5 + d^2) - \frac{u_0^3}{u^3}f(u_0)(u_0^5 + d^2)}}, \\
&= d \left[ \int_{u_c}^{\infty} du \frac{\sqrt{f(u)}}{\sqrt{f(u)(u^5) - \frac{u_0^3}{u^3}f(u_0)(u_0^5)}} + \mathcal{O}(d) \right], \\
&\approx d \left[ \int_{u_c}^{\infty} du \frac{\sqrt{f(u)}}{\sqrt{f(u)(u^5) - \frac{u_0^3}{u^3}f(u_0)(u_0^5)}} \right], \\
&\approx \epsilon d, \\
d &\approx \frac{(\mu - \mu_{\text{onset}})}{\epsilon}, \tag{4.26}
\end{aligned}$$

where  $\mu_{\text{onset}} \equiv \mu(d = 0) = \frac{1}{3}u_c\sqrt{f(u_c)}$ , the chemical potential at zero density. Consequently,

$$\begin{aligned}
\frac{\partial P}{\partial \mu} &= d \approx \frac{(\mu - \mu_{\text{onset}})}{\epsilon} \\
P(d) &\approx \frac{(\mu - \mu_{\text{onset}})^2}{2\epsilon} \approx \epsilon \frac{d^2}{2}, \\
p(d) &\approx \frac{(\mu - \mu_{\text{onset}})^2}{2\epsilon V_3} \approx \frac{\epsilon}{2V_3} d^2. \tag{4.27}
\end{aligned}$$

Therefore

$$p(d) \sim (\mu - \mu_{\text{onset}})^2 \sim d^2. \tag{4.28}$$

At large density,

$$\begin{aligned}
\mu &= \int_{u_c}^{\infty} du \frac{d\sqrt{f(u)}}{\sqrt{f(u)(u^5 + d^2) - \frac{u_0^3}{u^3}f(u_0)(u_0^5 + d^2)}} + \frac{1}{3}u_c\sqrt{f(u_c)}, \\
&= \int_{u_c}^{\infty} du \frac{\sqrt{f(u)}}{\sqrt{f(u)(\frac{u^5}{d^2} + 1) - \frac{u_0^3}{u^3}f(u_0)(\frac{u_0^5}{d^2} + 1)}} + \frac{1}{3}u_c\sqrt{f(u_c)}. \tag{4.29}
\end{aligned}$$

Using,

$$\begin{aligned}
\frac{u^5}{d^2} = v \rightarrow dv &= \frac{5u^4}{d^2} \rightarrow du = \frac{1}{5}d^2u^{-4}dv, \\
&= \frac{1}{5}d^{2/5}v^{-4/5}dv, \tag{4.30}
\end{aligned}$$

the chemical potential becomes

$$\begin{aligned}
\mu &= \frac{1}{5}d^{2/5} \int_{v_c}^{\infty} dv v^{-4/5} \frac{\sqrt{f(v)}}{\sqrt{f(v)(v+1) - \frac{v_0^3}{v^3}f(v_0)(v_0+1)}} + \frac{1}{3}u_c\sqrt{f(u_c)}, \\
&\approx \frac{1}{5}d^{2/5} \int_{v_c}^{\infty} dv v^{-4/5} \frac{\sqrt{f(v)}}{\sqrt{f(v) - \frac{v_0^3}{v^3}f(v_0)}}, \\
&\approx \xi d^{2/5}, \\
d &\approx \left(\frac{\mu}{\xi}\right)^{5/2}.
\end{aligned} \tag{4.31}$$

Therefore,  $d \sim \mu^{5/2}$  and thus

$$p(d) \sim \mu^{7/2} \sim d^{7/5}. \tag{4.32}$$

Interestingly, we have not specified which type of particle they are but the results for  $\mu(d)$  show that the behavior prefers to be fermionic. This is a consequence of the DBI action responses to the electric field.

The entropy is determined as a function of the temperature  $s(t)$  from the free-energy  $F(t, d)$ . The gripping phase is the deconfined phase since there is no temperature dependence in the confined phase. At low temperature, where the chiral symmetry is broken, we discover for both small and large densities that

$$s(t) \sim t^5, \tag{4.33}$$

and at the high temperature, where the chiral symmetry is restored, we find

$$s(t) \sim t^6. \tag{4.34}$$

ศูนย์วิทยทรัพยากร  
จุฬาลงกรณ์มหาวิทยาลัย

# Chapter V

## HOLOGRAPHIC MULTIQUARK AND ITS THERMODYNAMICS

In the deconfined phase, there are more various possible states than that of confined phase. Interestingly, a new kind of bound state consisting of quarks and anti-quarks without colorless condition can be formed. Generically, its construction consists of  $k_h$  strings hanging from the probe brane down to baryon vertex and some additional  $k_r$  strings stretching from the vertex to horizon. The configuration is called “multiquark”. In this chapter, we focus on the multiquark configuration in Sakai-Sugimoto model based on the Ref.[17, 73].

### 5.1 Balance conditions

According to the configuration of the “multiquark” state, the total action of the configuration is then

$$S = S_{D4} + \frac{k_h}{N_c} S_{F1} + \frac{k_r}{N_c} S'_{F1}, \quad (5.1)$$

where  $S_{D4} = \frac{1}{3} \mathcal{N} u_c \sqrt{f(u_c)} d$ , for baryon vertex in the deconfined phase (see (3.64)),  $S_{F1}$  and  $S'_{F1}$  are the hanging strings action and the radial string action which can be determined from the following procedure. For the hanging strings in deconfined background

$$\begin{aligned} \det(g_{MN}) &= \begin{vmatrix} -R^2 f(u) u^{3/2} & \\ & R^2 f^{-1}(u) u^{-3/2} [(u')^2 + f(u) u^3] \end{vmatrix}, \\ &= -R^4 [(u')^2 + f(u) u^3]. \end{aligned} \quad (5.2)$$

Therefore,

$$\begin{aligned} S_{F1} &= -\frac{n_s V_3}{2\pi\alpha'R} \int dt du [(u')^2 + f(u) u^3]^{1/2}, \\ &= -\mathcal{N} d \int du [(u')^2 + f(u) u^3]^{1/2}. \end{aligned} \quad (5.3)$$

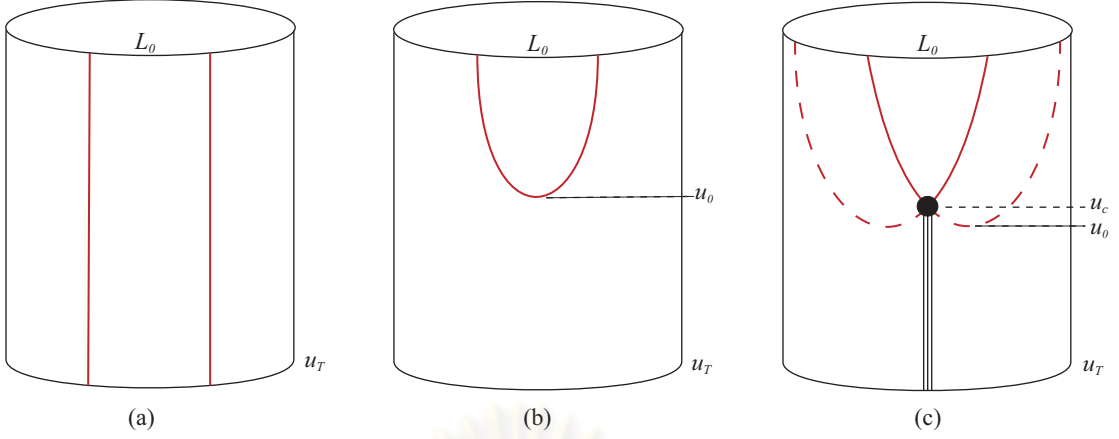


Figure 5.1: Different configurations of D8 and  $\overline{\text{D8}}$ -branes in the background field following the Sakai-Sugimoto model that are dual to the phases of (a)  $\chi_S$ -QGP, (b) vacuum and (c) multi-quark phase.

For the radial strings in deconfined background, the action takes the following form

$$\begin{aligned} S'_{F1} &= -\frac{n_s V_3}{2\pi\alpha'R} \int_{u_c}^{u_T} dt du, \\ &= \mathcal{N}d(u_c - u_T). \end{aligned} \quad (5.4)$$

The balance condition for a whole configuration can be determined from variation of the action with respect to  $u_c$  since the baryon vertex is assumed to be located at  $u = u_c$ . Consequently, the variation gives us the volume term and the surface term.

$$\begin{aligned} S &= \frac{1}{3}\mathcal{N}d u_c \sqrt{f(u_c)} - \frac{k_h}{N_c} \mathcal{N}d \int du [(u'_c)^2 + f(u_c)u_c^3]^{1/2} + \frac{k_r}{N_c} \mathcal{N}d(u_c - u_T), \\ &= \frac{\mathcal{N}}{N_c} d \left\{ \frac{N_c}{3} u_c \sqrt{f(u_c)} - k_h \int du [(u'_c)^2 + f(u_c)u_c^3]^{1/2} + k_r(u_c - u_T) \right\}. \end{aligned} \quad (5.5)$$

Based upon the assumption, the surface term provides us the additional balance condition.

$$\begin{aligned} \delta S_{\text{surface}} = 0 &= \frac{\mathcal{N}}{N_c} d \left\{ \frac{N_c}{3} \left[ \sqrt{f(u_c)} + \frac{3}{2\sqrt{f(u_c)}} \left( \frac{u_T}{u_c} \right)^3 \right] - k_h \frac{u'_c}{\sqrt{(u'_c)^2 + f(u_c)u_c^3}} \right. \\ &\quad \left. + k_r \right\} \delta u_c, \\ &= \frac{\mathcal{N}}{N_c} d \left\{ \frac{N_c}{3} \left[ \frac{1 + \frac{1}{2} \left( \frac{u_T}{u_c} \right)^3}{\sqrt{1 - \left( \frac{u_T}{u_c} \right)^3}} \right] - k_h \frac{u'_c}{\sqrt{(u'_c)^2 + f(u_c)u_c^3}} + k_r \right\} \delta u_c, \\ &= \frac{\mathcal{N}}{N_c} d \left\{ \frac{N_c}{3} \left[ \frac{1 + \frac{x^3}{2}}{\sqrt{1 - x^3}} \right] - k_h \frac{u'_c}{\sqrt{(u'_c)^2 + f(u_c)u_c^3}} + k_r \right\} \delta u_c. \end{aligned} \quad (5.6)$$



For simplicity, let's define  $G_0(x) \equiv \frac{1 + \frac{x^3}{2}}{\sqrt{1 - x^3}}$ , and  $A = \frac{u'_c}{\sqrt{(u'_c)^2 + f(u_c)u_c^3}}$ , then

$$\begin{aligned} \frac{N_c}{3}G_0(x) + k_r &= k_h A, \\ \frac{N_c}{3k_h}G_0(x) + \frac{k_r}{k_h} &= A \leq 1. \end{aligned} \quad (5.7)$$

The balance condition becomes

$$k_h \geq \frac{N_c}{3}G_0(x) + k_r. \quad (5.8)$$

## 5.2 Thermodynamics of holographic multiquark

In this section, we concentrate on the calculation of some important thermodynamical variables of the exotic multiquark states. The calculation will become much easier to evaluate when we use a proper reference point. From (3.74), the shape of holographic multiquark configuration can be determined from

$$(x'_4(u))^2 = \frac{1}{u^3 f(u)} \left[ \frac{f(u)(u^8 + u^3 d^2)}{F^2(u_c)} - 1 \right]^{-1} \quad (5.9)$$

where

$$F(u_c) = \frac{f(u_c)\sqrt{u_c^8 + u_c^3 d^2}}{\sqrt{f(u_c)(x'_4(u_c))^2 + u_c^{-3}}}(x'_4(u_c)). \quad (5.10)$$

According to balance condition for holographic multiquark configuration (see Appendix A. at (A.8) and (A.9)), we get

$$\begin{aligned} F(u_c) &= \frac{f(u_c)u_c^4 \sqrt{1 + \frac{d^2}{u_c^5}}}{3u_c f^{1/2}(u_c) \sqrt{1 + \frac{d^2}{u_c^5}}} d \left( 1 + \frac{1}{2} \left( \frac{u_T}{u_c} \right)^3 + 3n_s \sqrt{f(u_c)} \right) \\ &\quad \times \frac{1}{d} \sqrt{\frac{9u_c^2 \left[ 1 + \frac{d^2}{u_c^5} \right]}{\left( 1 + \frac{1}{2} \left( \frac{u_T}{u_c} \right)^3 + 3n_s \sqrt{f(u_c)} \right)^2} - \frac{d^2 u_c^{-3}}{f(u_c)}}, \\ &= \frac{u_c^3 \sqrt{f(u_c)}}{3} \left( 1 + \frac{1}{2} \left( \frac{u_T}{u_c} \right)^3 + 3n_s \sqrt{f(u_c)} \right) \\ &\quad \times \sqrt{\frac{9u_c^2 \left[ 1 + \frac{d^2}{u_c^5} \right]}{\left( 1 + \frac{1}{2} \left( \frac{u_T}{u_c} \right)^3 + 3n_s \sqrt{f(u_c)} \right)^2} - \frac{d^2 u_c^{-3}}{f(u_c)}}. \end{aligned} \quad (5.11)$$

$$\begin{aligned}
F(u_c) &= \frac{\sqrt{u_c^3 f(u_c)}}{3} \left( 1 + \frac{1}{2} \left( \frac{u_T}{u_c} \right)^3 + 3n_s \sqrt{f(u_c)} \right) \\
&\times \sqrt{\frac{9[u_c^5 + d^2]}{\left( 1 + \frac{1}{2} \left( \frac{u_T}{u_c} \right)^3 + 3n_s \sqrt{f(u_c)} \right)^2} - \frac{d^2}{f(u_c)}}.
\end{aligned} \tag{5.12}$$

$$\begin{aligned}
F^2(u_c) &= \frac{u_c^3 f(u_c)}{9} \left( 1 + \frac{1}{2} \left( \frac{u_T}{u_c} \right)^3 + 3n_s \sqrt{f(u_c)} \right)^2 \\
&\times \left[ \frac{9[u_c^5 + d^2]}{\left( 1 + \frac{1}{2} \left( \frac{u_T}{u_c} \right)^3 + 3n_s \sqrt{f(u_c)} \right)^2} - \frac{d^2}{f(u_c)} \right], \\
&= u_c^3 f(u_c) \left[ u_c^5 + d^2 - \frac{d^2}{9f(u_c)} \left( 1 + \frac{1}{2} \left( \frac{u_T}{u_c} \right)^3 + 3n_s \sqrt{f(u_c)} \right)^2 \right]. \\
F^2(u_c) &= u_c^3 f(u_c) \left[ u_c^5 + d^2 - \frac{d^2 \eta^2(u_c)}{9f(u_c)} \right],
\end{aligned} \tag{5.13}$$

where  $\eta(u_c) \equiv \left( 1 + \frac{1}{2} \left( \frac{u_T}{u_c} \right)^3 + 3n_s \sqrt{f(u_c)} \right)$ .

### 5.3 Calculation of the equation of state

In order to acquire the thermodynamics of multiquark, we will first investigate the relation between the pressure and the number density. According to the former section (see (4.21) and (4.1)), the grand potential density and the chemical potential of multiquark state are given by

$$\Omega = \int_{u_c}^{\infty} du \left[ 1 - \frac{F^2}{f(u)(u^8 + u^3 d^2)} \right]^{-1/2} \frac{u^5}{\sqrt{u^5 + d^2}}, \tag{5.14}$$

$$\mu = \int_{u_c}^{\infty} du \left[ 1 - \frac{F^2}{f(u)(u^8 + u^3 d^2)} \right]^{-1/2} \frac{d}{\sqrt{u^5 + d^2}} + \frac{1}{3} u_c \sqrt{f(u_c)} + n_s (u_c - u_T), \tag{5.15}$$

respectively where the reference is now turning to  $u_c$ . From  $\mu_{\text{onset}} \equiv \mu(d=0) = \frac{1}{3} u_c \sqrt{f(u_c)} + n_s (u_c - u_T)$ , the chemical potential is then

$$\begin{aligned}
\mu &= \int_{u_c}^{\infty} du \left[ 1 - \frac{F^2}{f(u)(u^8 + u^3 d^2)} \right]^{-1/2} \frac{d}{\sqrt{u^5 + d^2}} + \mu_{\text{onset}}, \\
&= \int_{u_c}^{\infty} du \left[ 1 - \frac{u_c^3 f(u_c) \left[ u_c^5 + d^2 - \frac{d^2 \eta^2(u_c)}{9f(u_c)} \right]}{f(u)(u^8 + u^3 d^2)} \right]^{-1/2} \frac{d}{\sqrt{u^5 + d^2}} + \mu_{\text{onset}}.
\end{aligned} \tag{5.16}$$

Originally, the differential relation of the grand potential  $G_\Omega$  can be written as

$$dG_\Omega = -PdV - SdT - Nd\mu, \tag{5.17}$$

where the parameters  $P$ ,  $V$ ,  $S$ ,  $T$ , and  $N$  are pressure, volume, entropy, temperature, and total number of particles in the system, respectively. Since the volume is not our interest, we define the volume density of  $G_\Omega$ ,  $S$ , and  $N$  to be  $\Omega$ ,  $s$ , and  $d$ , respectively. Accordingly, at a particular  $T$  and  $\mu$  we have

$$P = -G_\Omega/V \equiv -\Omega(T, \mu). \tag{5.18}$$

With assumption that the multiquark states distribute uniformly, we obtain

$$d = \frac{\partial P}{\partial \mu}(T, \mu). \tag{5.19}$$

Using the chain rule,

$$\left. \frac{\partial P}{\partial d} \right|_T = \left. \frac{\partial \mu}{\partial d} \right|_T d, \tag{5.20}$$

we get

$$P(d, T, n_s) = \mu(d, T, n_s) d - \int_0^d \mu(d', T, n_s) d(d'), \tag{5.21}$$

where we have assumed that the pressure is regulated to zero when there is no nuclear matter, i.e.  $d = 0$ .

### Small $d$ limit

In the very small  $d$  limit,  $u_c$  approaches  $u_0$ , and  $\eta(u_c)$  becomes  $\eta(u_0) + \mathcal{O}(d)$ . From (5.16), the baryon chemical potential can then be approximated to be

$$\begin{aligned}
\mu &\simeq d \left\{ \int_{u_c}^{\infty} du \left[ 1 - \frac{f(u_0)u_0^8}{f(u)u^8} - \frac{f(u_0)u_0^3 \left( 1 - \frac{\eta^2(u_0)}{9f(u_0)} \right) d^2}{f(u)u^8} \right]^{-1/2} u^{-5/2} \left( 1 - \frac{d^2}{2u^5} \right) \right\} \\
&\quad + \mu_{\text{source}},
\end{aligned} \tag{5.22}$$

where  $\mu_{source} = \frac{1}{3}u_c\sqrt{f(u_c)} + n_s(u_c - u_T)$ . After using the binomial expansion, the above equation can be approximated by keeping only the terms of order  $\mathcal{O}(d^2)$ . Consequently, the chemical potential becomes

$$\begin{aligned}
\mu - \mu_{source} &\simeq d \left\{ \int_{u_0}^{\infty} du \frac{u^{-5/2}}{\sqrt{1 - \frac{f(u_0)u_0^8}{f(u)u^8}}} \right. \\
&\quad \times \left( 1 - \frac{d^2}{2u^5} \right) \left( 1 - \frac{(f(u_0)u_0^3)/(f(u)u^8)}{\left[ 1 - \frac{f(u_0)u_0^8}{f(u)u^8} \right]} \left( 1 - \frac{\eta^2(u_0)}{9f(u_0)} \right) d^2 \right)^{-1/2} \left. \right\}, \\
&\simeq d \left\{ \int_{u_0}^{\infty} du \frac{u^{-5/2}}{\sqrt{1 - \frac{f(u_0)u_0^8}{f(u)u^8}}} \right. \\
&\quad \times \left( 1 - \frac{d^2}{2u^5} \right) \left( 1 + \frac{1}{2} \frac{(f(u_0)u_0^3)/(f(u)u^8)}{\left[ 1 - \frac{f(u_0)u_0^8}{f(u)u^8} \right]} \left( 1 - \frac{\eta^2(u_0)}{9f(u_0)} \right) d^2 \right) \left. \right\}, \\
&\simeq d \left\{ \int_{u_0}^{\infty} du \frac{u^{-5/2}}{\sqrt{1 - \frac{f(u_0)u_0^8}{f(u)u^8}}} \right. \\
&\quad \times \left( 1 + \frac{1}{2} \frac{(f(u_0)u_0^3)/(f(u)u^8)}{\left[ 1 - \frac{f(u_0)u_0^8}{f(u)u^8} \right]} \left( 1 - \frac{\eta^2(u_0)}{9f(u_0)} \right) d^2 - \frac{d^2}{2u^5} \right) \left. \right\}, \\
&\simeq d \left\{ \int_{u_0}^{\infty} du \frac{u^{-5/2}}{\sqrt{1 - \frac{f(u_0)u_0^8}{f(u)u^8}}} \right. \\
&\quad \times \left( 1 + \frac{1}{2} \frac{f(u_0)u_0^3}{f(u)u^8 - f(u_0)u_0^8} \left( 1 - \frac{\eta^2(u_0)}{9f(u_0)} \right) d^2 - \frac{d^2}{2u^5} \right) \left. \right\}, \\
&= d \left\{ \int_{u_0}^{\infty} du \frac{u^{-5/2}}{\sqrt{1 - \frac{f(u_0)u_0^8}{f(u)u^8}}} \right. \\
&\quad \times \left[ 1 + \left( \frac{f(u_0)u_0^3}{f(u)u^8 - f(u_0)u_0^8} \left( 1 - \frac{\eta^2(u_0)}{9f(u_0)} \right) - \frac{1}{u^5} \right) \frac{d^2}{2} \right] \left. \right\}, \\
&= \alpha_0 d - \beta_0(n_s) d^3, \tag{5.23}
\end{aligned}$$

where

$$\alpha_0 \equiv \int_{u_0}^{\infty} du \frac{u^{-5/2}}{\sqrt{1 - \frac{f(u_0)u_0^8}{f(u)u^8}}}, \tag{5.24}$$

$$\beta_0(n_s) \equiv \int_{u_0}^{\infty} du \frac{1}{2} \frac{u^{-5/2}}{\sqrt{1 - \frac{f(u_0)u_0^8}{f(u)u^8}}} \left( \frac{f(u_0)u_0^3}{f(u)u^8 - f(u_0)u_0^8} \left( 1 - \frac{\eta^2(u_0)}{9f(u_0)} \right) - \frac{1}{u^5} \right). \tag{5.25}$$

Using (5.19), the pressure as a function of baryon number density is then

$$\begin{aligned}
\frac{\partial P}{\partial(\mu - \mu_{\text{onset}})} &= \frac{\partial P}{\partial d} \frac{\partial d}{\partial(\mu - \mu_{\text{onset}})} = d, \\
\frac{\partial P}{\partial d} &= \frac{\partial(\mu - \mu_{\text{onset}})}{\partial d} d, \\
&\simeq (\alpha_0 - 3\beta_0(n_s)d^2) d, \\
\frac{\partial P}{\partial d} &\simeq \alpha_0 d - 3\beta_0(n_s)d^3, \\
P &\simeq \frac{\alpha_0}{2}d^2 - \frac{3}{4}\beta_0(n_s)d^4. \quad (5.26)
\end{aligned}$$

### Large $d$ limit

In the large  $d$  limit and relatively small  $T$ , using (5.16), the chemical potential becomes

$$\begin{aligned}
\mu &= \int_{u_c}^{\infty} du \left[ 1 - \frac{u_c^3 f(u_c) \left[ u_c^5 + d^2 - \frac{d^2 \eta^2(u_c)}{9f(u_c)} \right]}{u^3 f(u) (u^5 + d^2)} \right]^{-1/2} \frac{d}{\sqrt{u^5 + d^2}} + \mu_{\text{onset}}, \\
&\simeq \int_{u_c}^{\infty} du \left[ 1 - \frac{u_c^3 f(u_c) \left[ 1 - \frac{\eta^2(u_c)}{9f(u_c)} \right] d^2}{u^3 f(u) (u^5 + d^2)} \right]^{-1/2} \frac{d}{\sqrt{u^5 + d^2}} + \mu_{\text{onset}}, \\
&\simeq \int_{u_c}^{\infty} du \left[ 1 + \frac{1}{2} \frac{u_c^3 f(u_c) \left[ 1 - \frac{\eta^2(u_c)}{9f(u_c)} \right] d^2}{u^3 f(u) (u^5 + d^2)} \right] \frac{d}{\sqrt{u^5 + d^2}} + \mu_{\text{onset}}, \\
&\simeq \int_{u_c}^{\infty} du \frac{d}{\sqrt{u^5 + d^2}} + \frac{1}{2} u_c^3 f(u_c) \left[ 1 - \frac{\eta^2(u_c)}{9f(u_c)} \right] d^2 \int_{u_c}^{\infty} du \frac{d}{u^3 f(u) [u^5 + d^2]^{3/2}} \\
&\quad + \mu_{\text{onset}}, \\
&\simeq \int_{u_c}^{\infty} du \frac{1}{\sqrt{1 + \frac{u^5}{d^2}}} + \frac{1}{2} u_c^3 f(u_c) \left[ 1 - \frac{\eta^2(u_c)}{9f(u_c)} \right] \int_{u_c}^{\infty} du \frac{1}{u^3 f(u) \left[ 1 + \frac{u^5}{d^2} \right]^{3/2}} \\
&\quad + \mu_{\text{onset}}. \quad (5.27)
\end{aligned}$$

Using

$$\begin{aligned}
v = \frac{u^5}{d^2} \rightarrow dv &= \frac{5u^4}{d^2} du \rightarrow du = \frac{1}{5} \frac{d^2}{(vd^2)^{4/5}} dv, \\
&= \frac{1}{5} \frac{d^{2/5}}{v^{4/5}} dv,
\end{aligned}$$

the chemical potential becomes

$$\begin{aligned}
\mu &\simeq \frac{d^{2/5}}{5} \int_0^\infty dv \frac{v^{-4/5}}{\sqrt{1+v}} + \frac{1}{2} u_c^3 f(u_c) \left[ 1 - \frac{\eta^2(u_c)}{9f(u_c)} \right] \frac{d^{2/5}}{5} \\
&\quad \times \int_0^\infty dv \frac{1}{(vd^2)^{3/5} f(v) [1+v]^{3/2}} + \mu_{\text{onset}}, \\
&\simeq \frac{d^{2/5}}{5} \int_0^\infty dv \frac{v^{-4/5}}{\sqrt{1+v}} + \frac{1}{2} u_c^3 f(u_c) \left[ 1 - \frac{\eta^2(u_c)}{9f(u_c)} \right] \frac{d^{-4/5}}{5} \\
&\quad \times \int_0^\infty dv \frac{v^{-3/5}}{f(v) [1+v]^{3/2}} + \mu_{\text{onset}}.
\end{aligned}$$

The term containing  $d^{-4/5}$  goes to zero when  $d$  is large, therefore

$$\mu \simeq \frac{d^{2/5}}{5} \int_0^\infty dv \frac{v^{-4/5}}{\sqrt{1+v}} + \mu_{\text{onset}}. \quad (5.28)$$

Using beta function

$$\begin{aligned}
\beta(m+1, n+1) &= \int_0^\infty dx \frac{x^m}{[1+x]^{m+n+2}}, \\
&= \frac{\Gamma(m+1) \Gamma(n+1)}{\Gamma(m+n+2)},
\end{aligned} \quad (5.29)$$

we conclude that

$$\begin{aligned}
m = -\frac{4}{5} \rightarrow m+n+2 = \frac{1}{2} \rightarrow n &= \frac{1}{2} + \frac{4}{5} - 2, \\
&= -\frac{7}{10}.
\end{aligned}$$

Consequently, the chemical potential becomes

$$\begin{aligned}
\mu &\simeq \frac{d^{2/5}}{5} \frac{\Gamma(\frac{1}{5}) \Gamma(\frac{3}{10})}{\Gamma(\frac{1}{2})} + \mu_{\text{onset}}, \\
\mu - \mu_{\text{onset}} &\simeq \frac{d^{2/5}}{5} \frac{\Gamma(\frac{1}{5}) \Gamma(\frac{3}{10})}{\Gamma(\frac{1}{2})}.
\end{aligned} \quad (5.30)$$

Using (5.19) again, the pressure for large baryon number density is then

$$\begin{aligned}
\frac{\partial P}{\partial(\mu - \mu_{\text{onset}})} &= \frac{\partial P}{\partial d} \frac{\partial d}{\partial(\mu - \mu_{\text{onset}})} = d, \\
\frac{\partial P}{\partial d} &= \frac{\partial(\mu - \mu_{\text{onset}})}{\partial d} d, \\
&\simeq \left( \frac{2}{25} d^{-3/5} \frac{\Gamma(\frac{1}{5}) \Gamma(\frac{3}{10})}{\Gamma(\frac{1}{2})} \right) d, \\
&\simeq \frac{2}{25} \frac{\Gamma(\frac{1}{5}) \Gamma(\frac{3}{10})}{\Gamma(\frac{1}{2})} d^{2/5}, \\
P &\simeq \frac{2}{35} \frac{\Gamma(\frac{1}{5}) \Gamma(\frac{3}{10})}{\Gamma(\frac{1}{2})} d^{7/5}.
\end{aligned} \quad (5.31)$$



Furthermore, the energy density can be obtained via the relation  $d\rho = \mu d(d)$ .

Next, we consider the entropy of the multiquarks phase. From the differential of the free energy,

$$dF_E = -PdV - SdT + \mu dN, \quad (5.32)$$

the entropy is given by

$$S = -\frac{\partial F_E}{\partial T}. \quad (5.33)$$

The entropy density can then be written as

$$s = -\frac{\partial \mathcal{F}_E}{\partial T}, \quad (5.34)$$

where  $\mathcal{F}_E$  is the free energy density which relates to the grand potential density as  $\mathcal{F}_E = \Omega + \mu d$ . Since we have the pressure  $P = -\Omega$ , we can write

$$s = \frac{\partial P}{\partial T} - \left( \frac{\partial \mu}{\partial T} \right) d. \quad (5.35)$$

For both small  $d$  and large  $d$ , we can see from the formula of the pressure (see (5.26),(5.31), noting that  $\alpha_0, \beta_0$  is insensitive to temperature) and the chemical potential (see (5.23), (5.30)), that the dominant contribution comes from  $\mu_{source}$ , thus

$$s \simeq - \left( \frac{\partial \mu_{source}}{\partial T} \right) d. \quad (5.36)$$

The baryon chemical potential from the D8-branes is insensitive to the changes of temperature. This implies that the main contribution to the entropy density of the multiquark nuclear phase comes from the source term namely the vertex and strings.

Since

$$\frac{\partial \mu_{source}}{\partial T} = \frac{\partial}{\partial T} \left( \frac{1}{3} u_c \sqrt{f(u_c)} + n_s (u_c - u_T) \right), \quad (5.37)$$

$$\frac{\partial \mu_{source}}{\partial T} \approx \frac{\left( \frac{16\pi^2}{9} \right)^3 T^5}{u_0^2 \sqrt{1 - \left( \frac{u_T}{u_0} \right)^3}} - n_s \frac{32\pi^2 T}{9}, \quad (5.38)$$

where we have used the fact that  $u_c$  is approximately constant with respect to the temperature in the range between the gluon deconfinement and the chiral symmetry restoration (see Fig. 5.2). Therefore, we obtain

$$s \approx \frac{\left( \frac{16\pi^2}{9} \right)^3 T^5 d}{u_0^2 \sqrt{1 - \left( \frac{u_T}{u_0} \right)^3}} + n_s \frac{32\pi^2 T d}{9}. \quad (5.39)$$

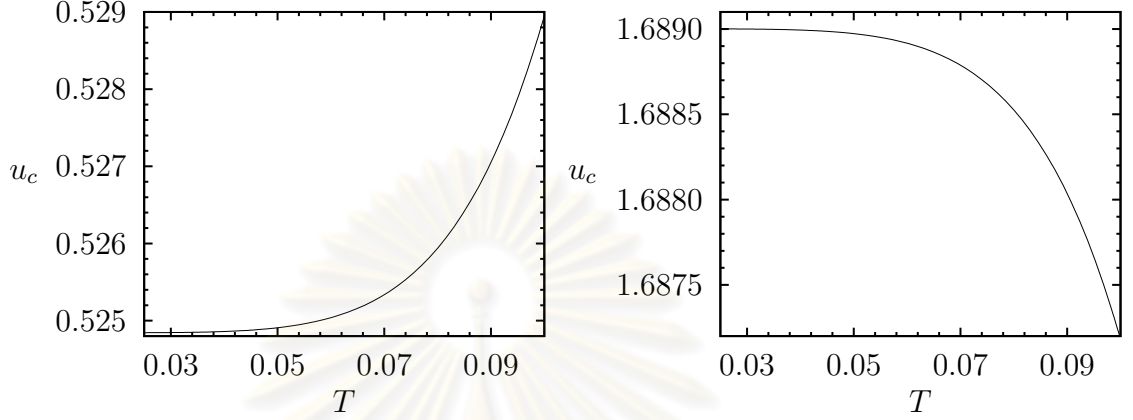


Figure 5.2: The graphs show the relations between  $u_c$  and  $T$  at small density (left) and at large density (right).

For small  $n_s$ , the entropy density is proportional to  $T^5$ . When  $n_s$  gets larger (carrying color charge), the entropy density becomes dominated by the color term  $s \propto n_s T$ . This is confirmed numerically in the next section. It has been found that the entropy density of the  $\chi_S$ -QGP scales as  $T^6$  [71] corresponding to the fluid of mostly free quarks and gluons. We can see that the effect of the color charge of the multiquarks as quasi-particles is to make them less like free particles with the temperature dependence  $\sim n_s T$ , i.e. much less sensitive to the temperature.

It is interesting to compare the dependence of pressure on the number density, (5.26) and (5.31), to the confined case at zero temperature studied in Ref. [74]. The power-law relations for both small and large density of the confined and deconfined multiquark phases are in the same form (for  $n_s = 0$ ). The reason is that the main contributions to the pressure for both phases are given by the D8-branes parts and they have similar dependence on the density for both phases. For the deconfined multiquark phase, the additional contributions from the source terms in (5.15),  $\mu_{source}$ , are mostly constant with respect to the density (this is because  $u_c$  becomes approximately independent of  $d$  for small and large  $d$  limits). Consequently, the constant contributions cancel out and affect nothing on the pressure.

On the contrary, the entropy density for the deconfined phase is dominated by the contributions from the sources namely the vertex and strings. The contri-

bution of the D8-branes is insensitive to the change of temperature and therefore does not affect the entropy density significantly. On the other hand, the additional source terms depend on the temperature and thus contribute dominantly to the entropy density. Once the temperature rises beyond the gluon-deconfined temperature, entropy density will increase abruptly (for sufficiently large density  $d$ ) and become sensitive to the temperature according to (5.39), due to the release of quarks from colorless confinement appearing as the sources. However, we will see later on using the numerical study in the section that for low densities and for small  $n_s$ , the numerical value of the entropy density is yet relatively small.

## 5.4 Numerical studies of the thermodynamic relations

From the analytic approximations in the previous section, we expect the pressure to appear as a straight line in the logarithmic scale for small and large  $d$  with the slope approximately 2 and  $7/5$  respectively. The relation between pressure and density of the multi-quarks from the full expressions can be plotted numerically as shown in Fig. 5.3-5.5. The pressure does not really depend on the temperature and we therefore present only the plots at  $T = 0.03$ . Remarkably, the transition from small to large  $d$  is clearly visible in the logarithmic-scale plots. The transition occurs around  $d_c \simeq 0.072$ . Interestingly, as shown in Fig. 5.5, the multi-quarks with larger  $n_s$  has less pressure than the ones with smaller  $n_s$  for  $d < d_c$  and *vice versa*. The dependence on  $n_s$  remains to be seen for small  $d$  as we can see from (5.26). For large  $d$ , the  $n_s$ -dependence is highly suppressed as predicted by (5.31).

The entropy density as a function of the temperature for various ranges of the density is shown in Fig. 5.6. The temperature dependence for both small and large  $d$  are in the same leading order of  $\simeq T^5$ . The baryon number density is linearly proportional to the pressure in the logarithmic-scale plot. For  $n_s > 0$ , we can see from (5.39) that the linear term in  $T$  should become more important. This is confirmed numerically as is shown in Fig. 5.6. The slope of the graph between the entropy density  $s$  and  $T$  in the double-log scale for  $n_s = 0$  (the left plot) and  $n_s = 0.3$  (the right plot) is approximately 5 and 1 respectively. Regardless of the temperature dependence, it should be emphasized that the numerical value of the entropy density for small densities and low  $n_s$  in Fig. 5.6 is quite small.

Finally, the relations between the baryon number density and chemical po-

tential are shown in Fig. 5.7. Temperature has a very small effect on these curves and is negligible for the range of temperature between the gluon deconfinement and the chiral-symmetry restoration. The baryon chemical potential depends linearly on the number density for small  $d$ . For large  $d$ , the relation between the chemical potential and number density becomes  $\mu \approx d^{2/5}$ . Interestingly, the multiquark quasi-particles behave like fermions as a result of being the electrical response to the DBI action [71].



ศูนย์วิทยทรัพยากร  
จุฬาลงกรณ์มหาวิทยาลัย

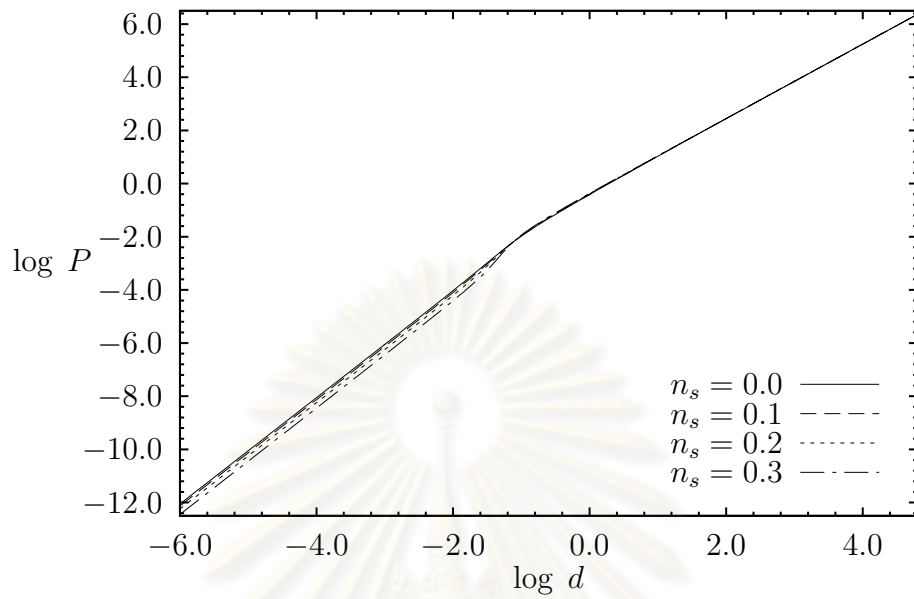


Figure 5.3: Pressure and density in logarithmic scale at  $T = 0.03$ .

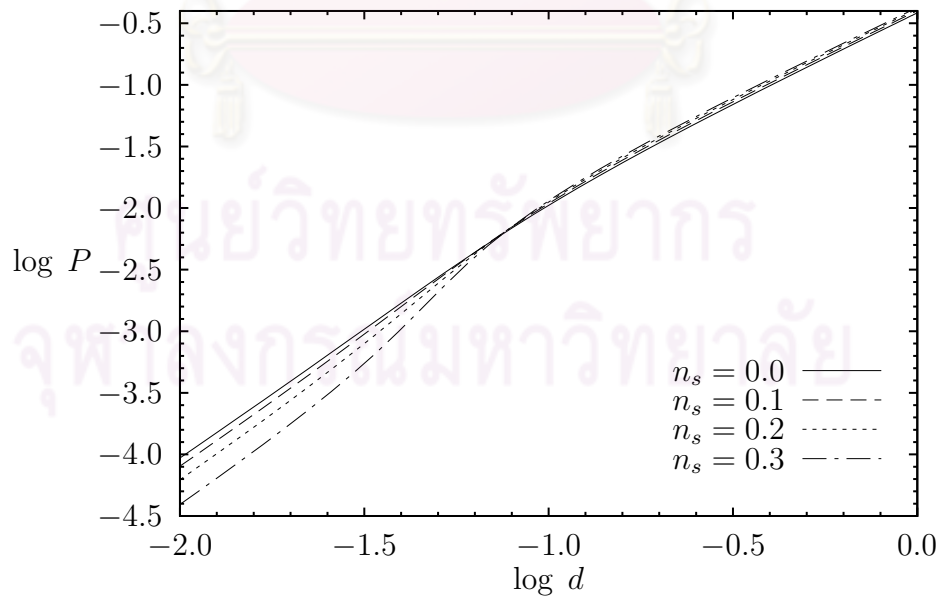


Figure 5.4: Pressure and density in logarithmic scale at  $T = 0.03$ , zoomed in around the transition region.

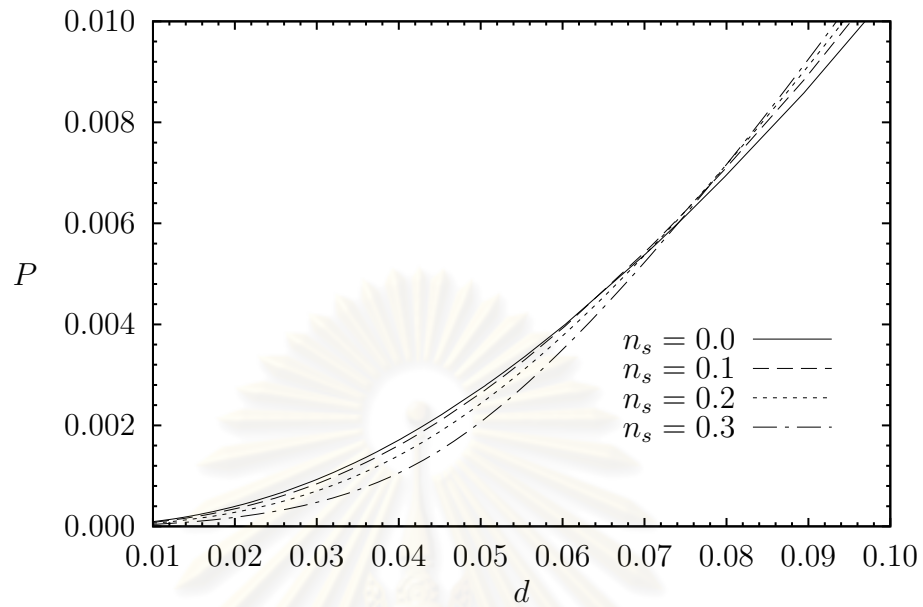


Figure 5.5: Pressure and density in linear scale.

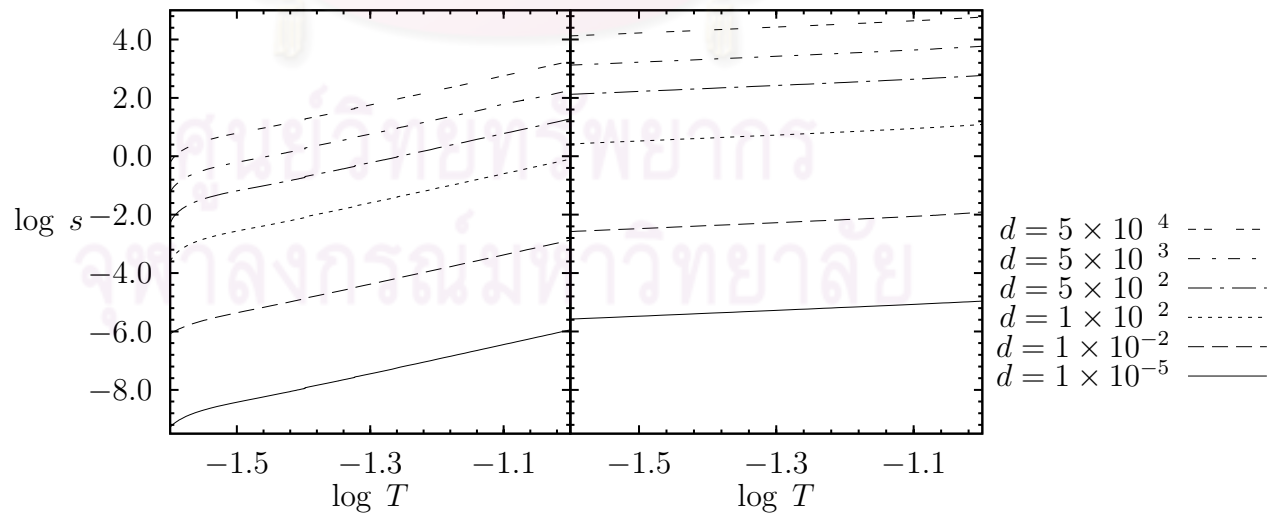


Figure 5.6: Relation between entropy and temperature in logarithmic scale for  $n_s = 0$  (left),  $0.3$  (right).



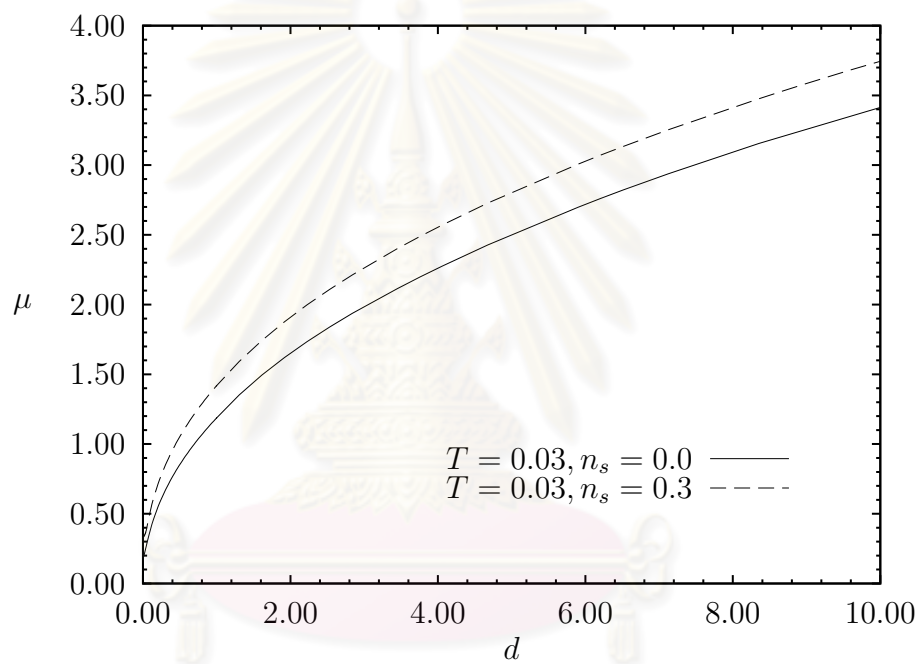


Figure 5.7: The baryon chemical potential and number density in logarithmic scale at  $T = 0.03$ .

# Chapter VI

## GRAVITATIONAL STABILITY OF THE DENSE WARM STAR IN THE DECONFINED PHASE

When a dying star collapses under its own gravity, it is generically believed that the degeneracy pressure of either electrons or neutrons would be able to stop the collapse to form a white dwarf or a neutron star. If the star is more massive than the upper mass limit of the neutron star, it would collapse into a black hole eventually. The mass limit of the neutron star is sensitive to the physics of warm dense nuclear matter but little is known about the equation of state of nuclear matter under high temperature and large density. Even though the original mass limit of the neutron star estimated by Oppenheimer, and Volkoff was only 0.7 solar mass [21, 22], the new limit when the nuclear interactions are included could be as large as 2.5 solar mass [75]. Under extreme pressure and density, the quarks within hadrons could be freed and wander around the interior of the star. In other words, quarks are effectively deconfined from the localized hadrons but confined by gravity within the star. Using the bag model to describe the state of being confined by gravity but possibly deconfined from the hadrons, it turns out that quark matter phase, e.g. strange star, is possible under extreme pressure and density.

However, physics of the deconfinement is largely unknown due to the non-perturbative nature of the strong interaction and the difficulty of lattice approach to deal with finite baryon density situation. The bag model are not always served as a reliable theoretical tool to explore the behaviour of quarks in the dense star when the deconfinement exists. It is therefore interesting to use the equation of state of the deconfined nuclear matter from the holographic model to investigate the behaviour of the dense star as a complementary tool to the bag model and other approaches.

In this chapter, we study a hypothetical multiquark star containing only the multiquark matter with uniform constant temperature [73]. The relations between pressure and density will be adopted directly from the holographic model as the equations of state of the quasi-particles. Since the pressure and density have very small temperature dependence for the range of temperatures under consideration, the results are valid generically.

A study into the gravitational stability of a spherically symmetric dense star can be performed using the Tolman-Oppenheimer-Volkoff equation [21, 22]. Generically, any spherical symmetric stars has a metric of the form

$$ds^2 = A(r)dt^2 - B(r)dr^2 - r^2d\Omega_2. \quad (6.1)$$

$$B(r) = \left(1 - \frac{A^*(r)}{r}\right)^{-1}, \quad (6.2)$$

$$\frac{dA^*(r)}{dr} = 8\pi\rho r^2, \quad (6.3)$$

and

$$\frac{dP(r)}{dr} = -\frac{(\rho + P)}{2} \frac{A'(r)}{A(r)} = -\frac{(\rho + P)}{2} \frac{8\pi Pr^3 + A^*(r)}{r(r - A^*(r))}. \quad (6.4)$$

The last equation is known as the Tolman-Oppenheimer-Volkoff (TOV) equation. The accumulated mass of the star,  $M(r)$ , can be determined by  $A^*(r) = 2M(r)$ . It has been proposed in Ref. [76] that the chemical potential defined in the term of background metric,  $\mu(r) = \frac{\epsilon_F}{\sqrt{A(r)}}$ , will automatically solve the TOV equation. Since

$$\frac{\mu'(r)}{\mu(r)} = -\frac{1}{2} \frac{A'(r)}{A(r)}. \quad (6.5)$$

Accordingly, the TOV takes the following form

$$\frac{dP(r)}{dr} = (\rho + P) \frac{\mu'(r)}{\mu(r)}, \quad (6.6)$$

In order to find equation of the state of the multiquark star, we need to consider the assisting relation from the first law of thermodynamics

$$dU = TdS - PdV + \mu dN. \quad (6.7)$$

In the case of compact dense warm star, it can be thought of an isolate system. After dividing out with infinitesimal in volume  $dV$ , the first law of thermodynamics becomes

$$\begin{aligned} \rho &= -P + \mu d, \\ \rho + P &= \mu d, \end{aligned} \quad (6.8)$$

where  $\rho = \frac{dU}{dV}$ , and  $d = \frac{dN}{dV}$ . Substituting (6.8) into (6.6) gives

$$P'(r) = d\mu'(r). \quad (6.9)$$

After differentiating the first law of thermodynamics (6.8) with the radius  $r$  (i.e.  $\frac{d\rho}{dr} = \rho'$ ), the law becomes

$$\rho' + P' = \mu'd + \mu d'. \quad (6.10)$$

Using chain rule,

$$\begin{aligned} \frac{\partial P}{\partial d} &= d \left( \frac{\partial \mu}{\partial d} \right), \\ d\mu &= \frac{1}{d} \left( \frac{\partial P}{\partial d} \right) d(d). \end{aligned} \quad (6.11)$$

Together with the first law of thermodynamics  $\rho + P = \mu d$ , the TOV equation then takes the following form,

$$d\mu = \frac{1}{d} \left( \frac{\partial P}{\partial d} \right) d(d). \quad (6.12)$$

Obviously, the chemical potential can be determined, as a function of the number density

$$\mu(d) = \int_0^d \frac{1}{\eta} \left( \frac{\partial P}{\partial \eta} \right) d\eta + \mu_{onset}, \quad (6.13)$$

where  $\mu_{onset} \equiv \mu(d=0)$ . Additionally, considering from the TOV equation (6.12) together with (6.10), the TOV equation becomes

$$\rho' = \mu d'. \quad (6.14)$$

The density  $d\rho = \mu d(d)$  can be integrated to

$$\rho(d) = \int_0^d \left[ \int_0^\eta \frac{1}{\eta'} \left( \frac{\partial P}{\partial \eta'} \right) d\eta' + \mu_{onset} \right] d\eta. \quad (6.15)$$

For a power-law equation of state,  $P = kd^\lambda$ , the chemical potential in Eq.(6.13), becomes

$$\begin{aligned} \mu(d) &= \int_0^d \frac{1}{d} \left( \frac{\partial P}{\partial \eta} \right) d\eta + \mu_{onset}, \\ &= \int_0^d \lambda k \eta^{\lambda-2} d\eta + \mu_{onset}, \\ &= \frac{\lambda k}{\lambda - 1} d^{\lambda-1} + \mu_{onset}. \end{aligned} \quad (6.16)$$

and eventually the equation of state is given by

$$\begin{aligned}\rho &= \int_0^d \left[ \frac{\lambda k}{\lambda - 1} \eta^{\lambda-1} + \mu_{onset} \right] d\eta, \\ &= \frac{1}{\lambda - 1} P + \mu_{onset} \left( \frac{P}{k} \right)^{1/\lambda}.\end{aligned}\quad (6.17)$$

For  $n_s = 0$ , at the transition point  $d = d_c$ , the energy density is given by Eq. (6.17),

$$\rho_c = \frac{k' d_c^{\lambda'}}{\lambda' - 1} + \mu_{onset} d_c, \quad (6.18)$$

where  $P = k' d^{\lambda'}$  (Eq. (5.26) suggests that  $\lambda' = 2$ ) is the equation of state of the small  $d$  region. We recalculate the relation Eq. (6.13), (6.15) for the large  $d$  region which match with this  $\rho_c$  to be

$$\mu = \mu_c + \lambda k \left( \frac{d^{\lambda-1}}{\lambda - 1} - \frac{d_c^{\lambda-1}}{\lambda - 1} \right), \quad (6.19)$$

$$\rho = \rho_c + \frac{1}{\lambda - 1} P + \mu_c \left[ \left( \frac{P}{k} \right)^{1/\lambda} - d_c \right] + k d_c^\lambda - \frac{\lambda k}{\lambda - 1} d_c^{\lambda-1} \left( \frac{P}{k} \right)^{1/\lambda}. \quad (6.20)$$

Numerical results and Eq. (5.31) suggest that  $\lambda = 7/5$  for the large  $d$  region.

For  $n_s > 0$ , assume the equation of state for small  $d$  is in the form of  $P = ad^{\lambda_1} + bd^{\lambda_2}$  (Eq. (5.26) suggests that  $\lambda_{1,2} = 2, 4$ ), the chemical potential and energy density for the small  $d$  region become

$$\mu = \mu_{onset} + \frac{\lambda_1 a d^{\lambda_1-1}}{\lambda_1 - 1} + \frac{\lambda_2 b d^{\lambda_2-1}}{\lambda_2 - 1}, \quad (6.21)$$

$$\rho = \mu_{onset} d + \frac{a d^{\lambda_1}}{\lambda_1 - 1} + \frac{b d^{\lambda_2}}{\lambda_2 - 1}. \quad (6.22)$$

We obtain the transition density in the similar fashion,

$$\rho_c = \mu_{onset} d_c + \frac{a d_c^{\lambda_1}}{\lambda_1 - 1} + \frac{b d_c^{\lambda_2}}{\lambda_2 - 1}. \quad (6.23)$$

For  $n_s = 0$ , numerical fittings suggest that  $k = 10^{-0.4}$ ,  $\lambda = 7/5$ ,  $d_c = 0.215443$ ,  $\mu_c = 0.564374$  (core) and  $k' = 1$ ,  $\lambda' = 2$ ,  $\mu_{onset} = 0.17495$  (crust). For  $n_s = 0.3$ , good fit parameters are  $k = 10^{-0.4}$ ,  $\lambda = 7/5$ ,  $d_c = 0.086666$ ,  $\mu_c = 0.490069$  (core) and  $a, b = 0.375, 180.0$ ;  $\lambda_{1,2} = 2, 4$ ;  $\mu_{onset} = 0.32767$  (crust). Varying the central density  $\rho_0$  of the star, we obtain the mass-density relation

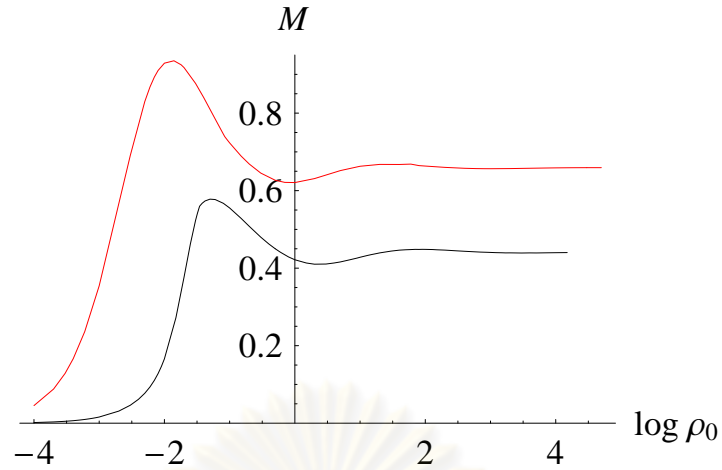


Figure 6.1: The relation between mass and central density of the multiquark star for multiquarks with  $n_s = 0$  (upper),  $0.3$  (lower).

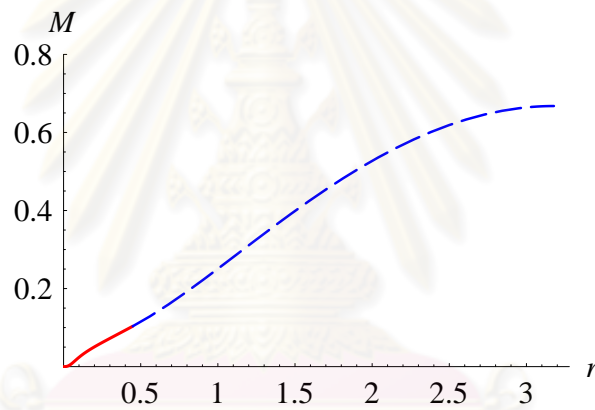


Figure 6.2: The accumulated mass distribution in the hypothetical multiquark star for the central density  $\rho_0 = 20$  and  $n_s = 0$ . The inner (outer) red (dashed-blue) line represents the core (crust) region.

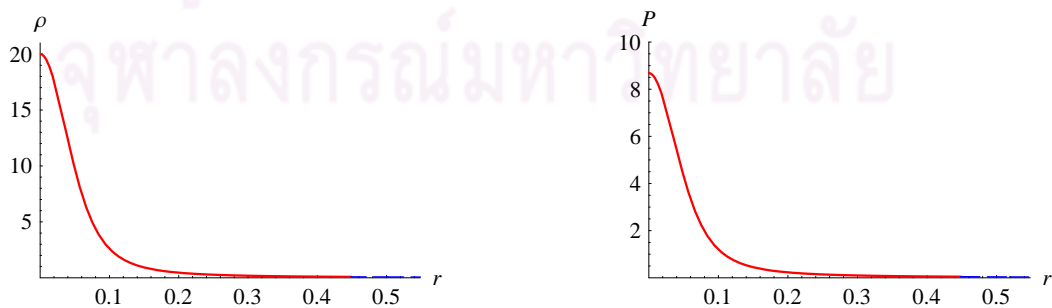


Figure 6.3: The density, and pressure distribution in the hypothetical multiquark star for the central density  $\rho_0 = 20$  and  $n_s = 0$ . The inner (outer) red (dashed-blue) line represents the core (crust) region.



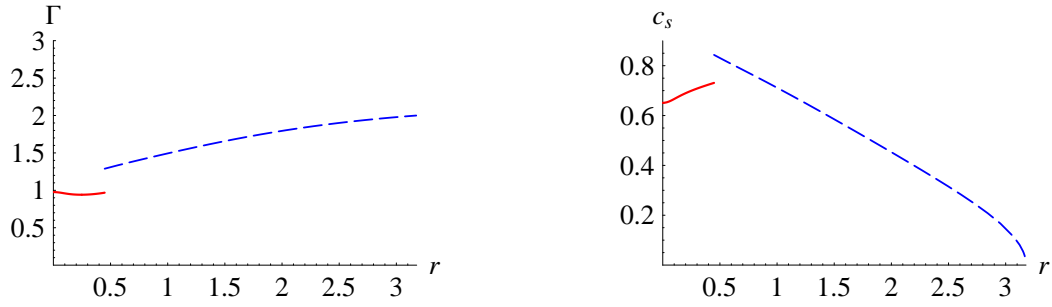


Figure 6.4: The adiabatic index at constant entropy ( $\Gamma$ ) and the sound speed ( $c_s$ ) distribution in the hypothetical multiquark star for the central density  $\rho_0 = 20$  and  $n_s = 0$ . The inner (outer) red (dashed-blue) line represents the core (crust) region.

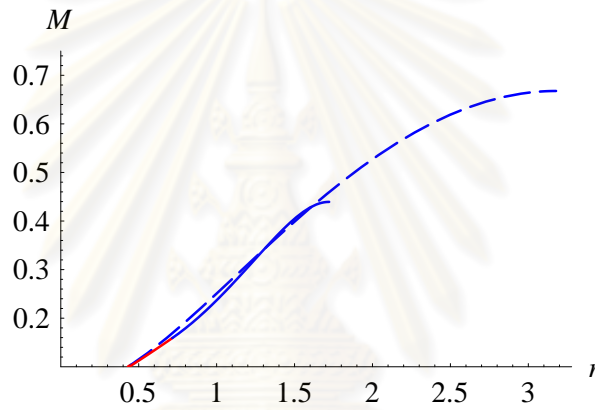


Figure 6.5: Comparison of the accumulated mass distribution in the hypothetical multiquark star for the central density  $\rho_0 = 20$  between  $n_s = 0$  and 0.3. The (dashed) blue line represents the crust region of multiquark star with  $n_s = 0.3$  (0). The red lines represent the core region of which both cases are almost the same.

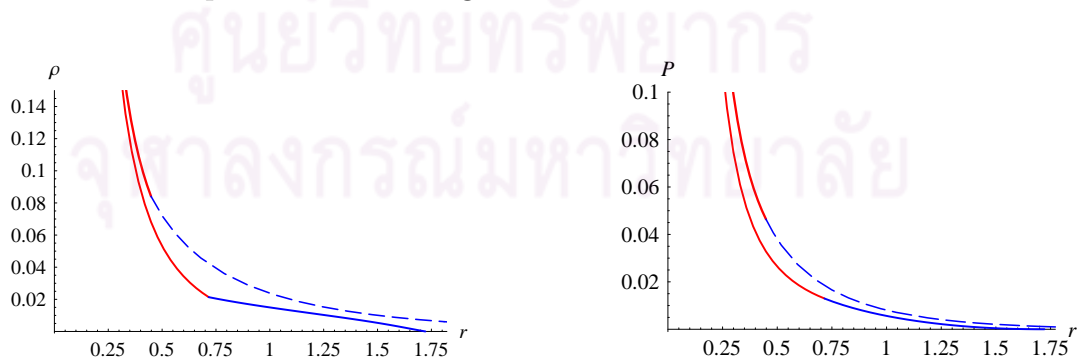


Figure 6.6: Comparison of the density, and pressure distribution in the hypothetical multiquark star for the central density  $\rho_0 = 20$  between  $n_s = 0$  and 0.3. The (dashed) blue line represents the crust region of multiquark star with  $n_s = 0.3$  (0). The red lines represent the core region of which both cases are almost the same.

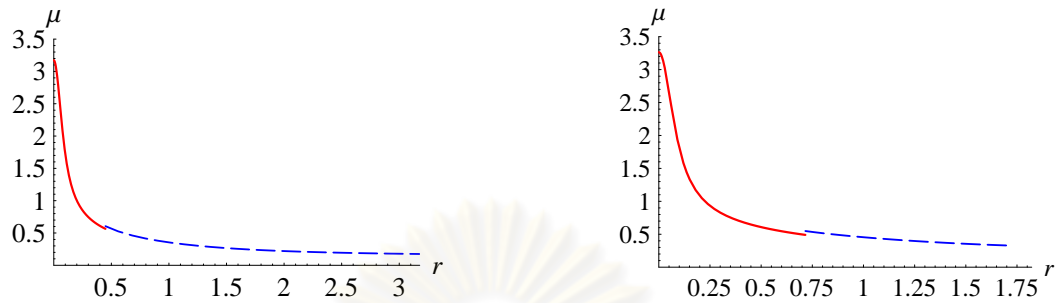


Figure 6.7: Comparison of the baryon chemical distributions in the hypothetical multiquark star for the central density  $\rho_0 = 20$  between  $n_s = 0$  (left) and 0.3 (right). The solid (dashed) red (blue) line represents the core (crust) region.

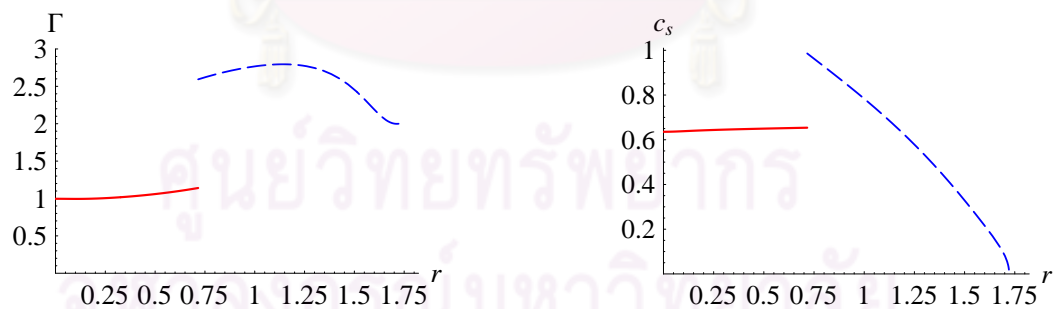


Figure 6.8: The adiabatic index at constant entropy ( $\Gamma$ ) and the sound speed ( $c_s$ ) distribution in the hypothetical multiquark star for the central density  $\rho_0 = 20$  and  $n_s = 0.3$ . The inner (outer) red (dashed-blue) line represents the core (crust) region.

in Fig. 6.1. Each curve has two maxima, a larger one in the small density region and a smaller one in the large density region. Each maximum corresponds to each power-law of the equation of state, the low density to the crust and the large density to the core. Interestingly, the contribution to the total mass of the multiquark star comes dominantly from the crust. This is shown in Fig. 6.2. Even though the density is much lower, the volume of the crust is proportional to the second power of the radius and thus makes the contribution of the crust to the total mass larger than the core's.

Figure 6.3 shows the pressure and density distribution within the multiquark star for the case of  $n_s = 0$  for the central density  $\rho_0 = 20$ . Even though the density and pressure decrease rapidly with respect to the radius of the star, they never quite reach zero. It turns out that when the density and pressure reach the critical values where the equation of state changes into the different power-law for small  $d$ , the crust region continues for a large fraction of the total radius of the star. This makes the crust mass contribution to the total mass of the star dominant as is shown in Fig. 6.2.

Some remarks should be made regarding the hydrodynamic properties of the multiquark phase (taken as nuclear liquid). At constant temperature and entropy, we can define the adiabatic index

$$\Gamma \equiv \frac{\rho}{P} \frac{\partial P}{\partial \rho}, \quad (6.24)$$

$$= \frac{\rho}{P} c_s^2, \quad (6.25)$$

where  $c_s$  is the sound speed in the multiquark liquid. They depend on the equation of state of the multiquark and their distributions within the multiquark star are shown in Fig. 6.4 for  $n_s = 0$ . The sound speed never exceeds the speed of light in vacuum. It is also found that the adiabatic index and the sound speed change within a small fraction as the central densities are varied for a given  $n_s$ .

The multiquark star with  $n_s = 0.3$  (having colour charges) converge to a smaller mass and radius at high central density (Fig. 6.5). Multiquarks with colour charges has lower pressure (and therefore smaller density) than the colourless ones for small density (Fig. 6.6). This smaller pressure makes the coloured multiquark star smaller and thus less massive than the colourless one. In more realistic situations, all of the possible multiquarks with varying  $n_s$  coexist in the multiquark phase. The mass limit and mass radius relation will vary between the two typical cases we consider here. Since the equations of state are found NOT to be sensitive to the temperature within the range between the gluon deconfinement

and the chiral symmetry restoration, our results should also be valid even when the temperature varies within the star (but not too high and too low, of course).

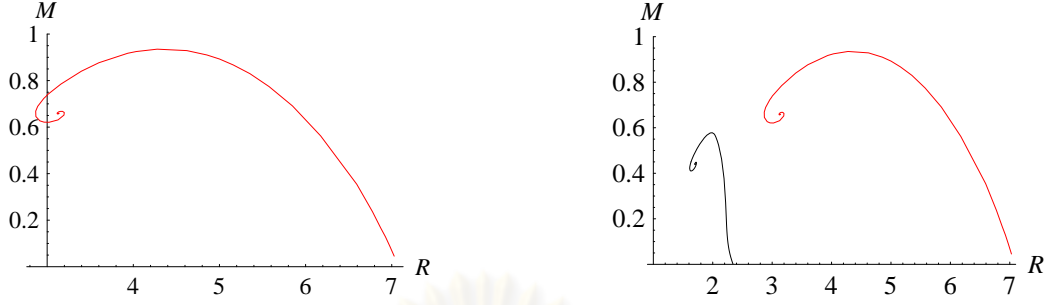


Figure 6.9: The relation between mass and radius of the multiquark star with (a)  $n_s = 0$ , (b)  $n_s = 0$  (red) and  $n_s = 0.3$  (black).

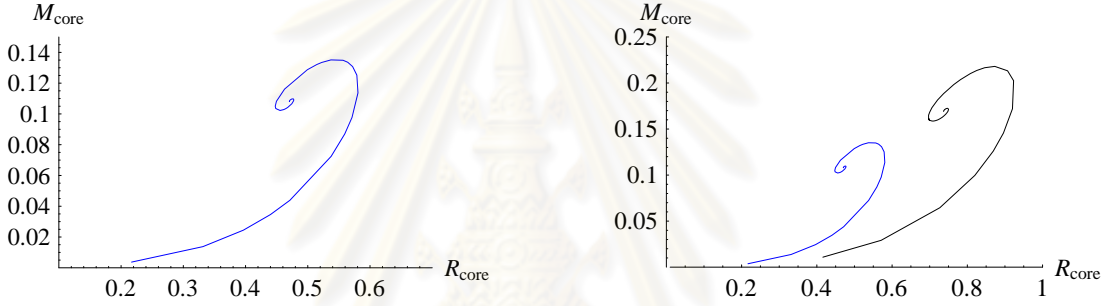


Figure 6.10: The relation between mass and radius of the core of the multiquark star with (a)  $n_s = 0$ , (b)  $n_s = 0$  (blue) and  $n_s = 0.3$  (black).

The baryon chemical potential distributions in the multiquark star for  $n_s = 0, 0.3$  are shown in Fig. 6.7. In the core region, the chemical potential distributions of both cases are similar due to the similarity of the equations of state for large density. A small jump of the chemical potential at the transition radius between core and crust region is the artifact from the power-law approximation. The value of the chemical potential at the transition radius from the full expression which we used in the numerical simulations is slightly different from the approximated value using the power-law.

The adiabatic index and sound speed of the multiquark phase for  $n_s = 0.3$  are shown in Fig. 6.8. The adiabatic index is higher than  $n_s = 0$  case but the sound speed in the low density region is distinctively higher. Around the transition density, the sound speed reaches the maximum value of about 0.986 of the speed of light in vacuum. For both  $n_s = 0, 0.3$  cases, it is obvious that the adiabatic index is closer to 1 in the core reflecting the fact that the density distribution is more condensed in the core region. The adiabatic index reaches  $\lambda' = 2$  at the star surface

since the the equation of state at zero density is  $P \propto \rho^{\lambda'}$  (i.e.  $\Gamma(\rho \rightarrow 0) = \lambda'$  for Eq. (6.17)).

The *spiral* relation between mass and radius of the multiquark star is shown in Fig. 6.9. As the central density is increasing, the mass and radius of the  $n_s = 0$  (0.3) multiquark star converge to the value of 0.659 (0.440) and 3.132 (1.704) respectively. For the core, the mass and radius of the core for  $n_s = 0$  (0.3) converge to the value of 0.108 (0.169) and 0.471 (0.737).

Finally, we would like to estimate these limits of mass and radius in the physical units. Since our dimensionless quantities are related to the physical quantities through conversion factors given in Table B.1 (Appendix B), both physical mass and radius vary with the energy density of the nuclear matter phase as  $\propto 1/\sqrt{\text{energy density scale}}$ . For a multiquark nuclear phase with energy density scale  $10 \text{ GeV}/\text{fm}^3$ , the conversion factor of the mass and radius are  $5.91 M_{\text{solar}}$  and 8.71 km respectively. This would correspond to the converging mass and radius (in the limit of very large central density) of  $3.89$  ( $2.60$ )  $M_{\text{solar}}$  and 27.29 (14.85) km for  $n_s = 0$  (0.3) multiquark star respectively.

In realistic situation, the nuclear phase in the outer region could lose heat out to the space in the form of radiation. The nuclear matter in the outer region of the crust will cool down and mostly become confined into neutrons and hadrons (e.g. hyperons, pions). This would make the multiquark crust to end at shorter radius than the estimated value and render the multiquark star to be smaller and less massive than the estimated values in the hypothetical prototype. For example, for the energy density scale  $10 \text{ GeV}/\text{fm}^3$ , the critical density is  $\rho_c \approx 1.5 \times 10^{18} \text{ kg}/\text{m}^3$  ( $n_s = 0$ ). This is still a sufficiently large density for the neutron layer to be formed. If the temperature of the nuclear matter in the crust region falls below the deconfinement temperature, the multiquarks will be confined into extremely dense neutrons and hadrons instead. For a typical neutron star, the distance of the neutron layer out to the star surface is roughly 5-6 km [77]. If we add this number to the radius of the multiquark core,  $0.471 \times 8.71 \simeq 4.10$  km, we end up with a more realistic estimation for the multiquark star with radius  $\sim 10$  km. Regardless of the name, only the core region is in the deconfined multiquark phase and the content of the outer layers are the confined nucleons.

# Chapter VII

## DISCUSSION AND SUMMARY

In this work, we have reviewed many holographic models ranging from AdS/CFT (Chapter 2) to Sakai-Sugimoto model(Chapter 3). The confined and deconfined nuclear matter have been studied in Sakai-Sugimoto model. Their thermodynamics and many important parameters have been calculated in Chapter 4. Interestingly, deconfinement at the moderate temperature below chiral restoration temperature in the high density limit exhibits various phase structures. A particular state of the deconfined nuclear matter consisting of fundamental nuclear matter called multiquark has been studied in Sakai-Sugimoto model. Additionally, the holographic multiquark model and its thermodynamics at the range of temperature between deconfinement to chiral symmetry restoration temperature have been explored in Chapter 5.

In the gluon-deconfined phase of the general Sakai-Sugimoto model, multi-quark states can exist in the intermediate range of temperatures between the deconfinement and the chiral symmetry restoration temperature at the sufficiently high density (Chapter 6). They are thermodynamically more stable than the other phases and therefore they can play important role in the physics of compact warm stars. By analytical and numerical methods, the equation of state of the multi-quark nuclear matter can be approximated by two power-laws in the small and large density region. Roughly speaking, the pressure is proportional to  $d^2$  and  $d^{7/5}$  for the small and large number density ( $d$ ) regions respectively.

It is also found that the effect of the colour charges of the multiquark is to reduce the pressure of the multiquarks when the density is small. At higher densities, multiquarks with color charges exert slightly larger pressure than the colorless ones. The temperature dependence of the entropy density shows an  $s \propto T^5$  relation and the color charge dependence  $s_{colour} \propto n_s T$  (see Fig. 5.6 and Eq. (5.39)). This implies that the multiquarks with color charges have larger entropy but their number of degrees of freedom depend less sensitively on the temperature. Multiquarks in the deconfined phase behave like quasi-particles with



the entropy density being less sensitive to the temperature than the gas of mostly free gluons and quarks in the  $\chi_S$ -QGP phase.

Using the power-law equations of state for both small and large density regions, a spherically symmetric Einstein field equation was solved to obtain the Tolman-Oppenheimer-Volkoff equation. By solving this equation numerically, we establish the mass, density and pressure distribution of the hypothetical multi-quark star. It turns out that the multi-quark star is separated into two layers, a core with higher density and a crust with lower density. Mass limit curve is also obtained as well as the mass sequence plot between the mass and radius of the multi-quark star. They show typical spiral behavior of the star sequence plots. The mass limit curve shows two peaks corresponding to the equation of state of the small and the large density. Analyses show that the most contribution to the total mass is mainly from the crust. The adiabatic index at constant entropy,  $\Gamma$ , and the sound speed,  $c_s$ , of the multi-quark nuclear phase within the star are calculated numerically. For large density,  $\Gamma$  is approximately close to 1 and  $c_s$  is roughly within range 0.6 – 0.7 of the speed of light. For small density,  $\Gamma$  is in the range 1.3 – 2.0 (2.0 – 3.0) and  $c_s$  is roughly 0 – 0.85 (0 – 0.99) for multi-quark with  $n_s = 0$  (0.3).

ศูนย์วิทยทรัพยากร  
จุฬาลงกรณ์มหาวิทยาลัย

## REFERENCES

- [1] F. Karsch. Lattice QCD at finite temperature, AIP Conf. Proc. 631 (2003) 112.
- [2] E. Shuryak and I. Zahed. Towards a theory of binary bound states in the quark gluon plasma. Phys. Rev. D70 (2004): 054507[hep-ph/0403127].
- [3] E. Shuryak and I. Zahed. Rethinking the properties of the quark gluon plasma at  $T \sim T_c$ . Phys. Rev. C70 (2004): 021901, [hep-ph/0307267].
- [4] J. Liao and E. Shuryak. Polymer chains and baryons in a strongly coupled quark-gluon plasma. Nuc. Phys. A775 (2006): 224[hep-th/0508035].
- [5] E. Squires. The bag model of hadrons. Rep. Prog. Phys. 42 (1979): 1187.
- [6] R. Gupta. Introduction to Lattice QCD. (1998):[hep-lat/9807028v1].
- [7] O. Philipsen. Lattice QCD at finite temperature and density. Eur.Phys.J.ST 152 (2007):29-60.
- [8] J. Maldacena. The large N limit of superconformal field theories and supergravity, Adv. Theor. Math. Phys. **2**, 231 (1998) [Int. J. Theor. Phys. 38 1113 (1999)][hep-th/9711200].
- [9] J. Maldacena. Wilson loops in large N field theories. Phys. Rev. Lett. 80 (1998): 4859-4862[hep-th/9803002].
- [10] S. Rey and J. Yee. Macroscopic strings as heavy quarks in large N gauge theory and anti-de Sitter supergravity. Eur. Phys. J. C22 (2001): 379-394[hep-th/9803001].
- [11] S. Rey, S. Theisen, and J. Yee. Wilson-Polyakov loop at finite temperature in large N gauge theory and anti-de Sitter supergravity. Nucl. Phys. B 527 (1998): 171-186[hep-th/9803135].
- [12] A. Brandhuber, N. Itzhaki, J. Sonnenschein, and S. Yankielowicz. Baryon from supergravity. JHEP 07 (1998): 046[hep-th/9806158].

- [13] K. Ghoroku, M. Ishihara, A. Nakamura and F. Toyoda. Multi-Quark Baryons and Color Screening at Finite Temperature. Phys. Rev. D79 (2009): 066009 [0806.0195 [hep-th]].
- [14] K. Ghoroku and M. Ishihara. Baryons with D5 Brane Vertex and  $k$ -Quarks States. Phys. Rev. D77 (2008): 086003[0801.4216 [hep-th]].
- [15] M. Carlucci, F. Giannuzzi, G. Nardulli, M. Pellicoro and S. Stramaglia. AdS-QCD quark-antiquark potential, meson spectrum and tetraquarks. Eur. Phys. J. C57 (2008): 569[0711.2014 [hep-ph]].
- [16] W. Wen. Multi-quark potential from AdS/QCD. Int. J. Mod. Phys. A23 (2008): 4533 [0708.2123 [hep-th]].
- [17] P. Burikham, A. Chatrabhuti and E. Hirunsirisawat. Exotic multi-quark states in the deconfined phase from gravity dual models. JHEP 05 (2009): 006[0811.0243v2 [hep-ph]].
- [18] T. Sakai and S. Sugimoto. Low energy hadron physics in holographic QCD. Prog. Theor. Phys. 113 (2005): 843-882[hep-th/0412141].
- [19] T. Sakai and S. Sugimoto. More on a holographic dual of QCD. Prog. Theor. Phys. 114 (2005): 1083-1118[hep-th/0507073].
- [20] O. Aharony. The non-AdS/non-CFT correspondence, or three different paths to QCD. hep-th/0212193.
- [21] J. Oppenheimer and G. Volkoff. On Massive Neutron Cores. Phys. Rev. 55 (1939): 374.
- [22] R. Tolman. Static solutions of Einstein's field equations for spheres of fluid. Phys. Rev. 55 (1939): 364.
- [23] S. Gubser and A. Karch. From Gauge-String Duality to Strong Interactions: A Pedestrians Guide. Annu. Rev. Nucl. Part. Sci. 59 (2009): 14568.
- [24] O. Aharony, S. Gubser, J. Maldacena, H. Ooguri and Y. Oz. Large N Field Theories, String Theory and Gravity. Phys.Rept. 323 (2000) :183-386[hep-th/9905111]
- [25] G. Gibbons and K. Maeda. Black Holes and Membranes in Higher Dimensional Theories with Dilaton Fields. Nucl. Phys. B298 (1988): 741.

- [26] D. Garfinkle, G. Horowitz and A. Strominger. Charged black holes in string theory. Phys. Rev. D43 (1991): 31403143.
- [27] G. Horowitz and A. Strominger. Black strings and P-branes. Nucl. Phys. B360 (1991):197209.
- [28] J. Polchinski. Dirichlet Branes and Ramond-Ramond Charges. Phys. Rev. Lett. 75 (1995): 4724-4727
- [29] S. Gubser, I. Klebanov, and A. Peet. Entropy and temperature of black 3-branes. Phys. Rev. D54 (1996): 39153919[hep-th/9602135v3].
- [30] E. Witten. Anti-de Sitter space, thermal phase transition, and confinement in gauge theories. Adv. Theor. Math. Phys. 2 505 (1998): [hep-th/9803131].
- [31] I. Klebanov and L. Thorlacius. The Size of p-Branes. Phys. Lett. B371 (1996): 51-56[hep-th/9510200v4].
- [32] S. Das and S. Mathur. Comparing decay rates for black holes and D-branes. Nucl.Phys. B478 (1996): 561-576[hep-th/9606185v2].
- [33] C. Callan and J. Maldacena. D-Brane Approach to Black Hole Quantum Mechanics. Nucl. Phys. B472 (1996): 591[hep-th/9602043v2].
- [34] S. Das, G. Gibbons and S. Mathur. Universality of Low Energy Absorption Cross Sections for Black Holes. Phys. Rev. Lett. 78 (1997): 417419.
- [35] I. Klebanov. World Volume Approach to Absorption by Non-dilatonic Branes. Nucl.Phys. B496 (1997): 231-242[hep-th/9702076v2].
- [36] S. Gubser and I. Klebanov. Absorption by Branes and Schwinger Terms in the World Volume Theory. Phys. Lett. B413 (1997): 41-48[hep-th/9708005v3].
- [37] A. Karch and A. Katz. Adding flavor to AdS/CFT. JHEP 0206 (2002): 043[hep-th/0205236].
- [38] A. Karch, E. Katz and N. Weiner. Hadron masses and screening from AdS Wilson loops, Phys. Rev. Lett. 90 (2003): 091601[hep-th/0211107].
- [39] M. Kruczenski, D. Mateos, R. Myers and D. Winters. Towards a holographic dual of large- $N(c)$  QCD. JHEP 0405 (2004): 041[hep-th/0311270].
- [40] M. Kruczenski, D. Mateos, R. Myers and D. Winters, Meson spectroscopy in AdS/CFT with flavour. JHEP 0307 (2003): 049[hep-th/0304032].

- [41] T. Sakai and J. Sonnenschein. Probing flavored mesons of confining gauge theories by supergravity. JHEP 0309 (2003): 047[hep-th/0305049].
- [42] H. Nastase. On Dp-Dp+4 systems. QCD dual and phenomenology:[hep-th/0305069].
- [43] J. Babington, J. Erdmenger, N. Evans, Z. Guralnik and I. Kirsch. Chiral symmetry breaking and pions in non-supersymmetric gauge / gravity duals. Phys. Rev. D69 (2004): 066007[hep-th/0306018].
- [44] X. Wang and S. Hu, Intersecting branes and adding flavors to the Maldacena-Nunez background, JHEP 0309 (2003): 017[hep-th/0307218].
- [45] P. Ouyang. Holomorphic D7-branes and flavored  $N = 1$  gauge theories. Nucl. Phys. B699 (2004): 207[hep-th/0311084].
- [46] C. Nunez, A. Paredes and A. Ramallo. Flavoring the gravity dual of  $N = 1$  Yang-Mills with probes. JHEP 0312 (2003): 024[hep-th/0311201].
- [47] S. Hong, S. Yoon and M. Strassler. Quarkonium from the fifth dimension. JHEP 0404 (2004): 046[hep-th/0312071].
- [48] N. Evans and J. Shock. Chiral dynamics from AdS space. Phys. Rev. D70 (2004): 046002[hep-th/0403279].
- [49] J. Barbon, C. Hoyos, D. Mateos and R. Myers. The holographic life of the eta'. JHEP 0410 (2004): 029[hep-th/0404260].
- [50] M. Bando, T. Kugo, A. Sugamoto and S. Terunuma. Pentaquark baryons in string theory. Prog. Theor. Phys. 112 (2004): 325[hep-ph/0405259].
- [51] B. Burrington, J. Liu, L. A. Zayas and D. Vaman. Holographic duals of flavored  $N = 1$  super Yang-Mills: Beyond the probe approximation. JHEP 0502 (2005): 022[hep-th/0406207].
- [52] J. Pons, J. Russo and P. Talavera. Semiclassical string spectrum in a string model dual to large  $N$  QCD. Nucl. Phys. B 700 (2004): 71-88[hep-th/0406266]
- [53] K. Ghoroku and M. Yahiro. Chiral symmetry breaking driven by dilaton. Phys. Lett. B 604 (2004): 235[hep-th/0408040].
- [54] J. Erdmenger and I. Kirsch. Mesons in gauge / gravity dual with large number of fundamental fields. JHEP 0412 (2004): 025[hep-th/0408113].



- [55] D. Arean, D. Crooks and A. Ramallo. Supersymmetric probes on the conifold. JHEP 0411 (2004): 035[hep-th/0408210].
- [56] G. de Teramond and S. Brodsky. Baryonic States in QCD From Gauge/String Duality at Large  $N_c$ . [ hep-th/0409074.]
- [57] I. Klebanov and J. Maldacena. Superconformal Gauge Theories and Non-Critical Superstrings. Int.J.Mod.Phys. A19 (2004): 5003-5016 [hep-th/0409133].
- [58] M. Kruczenski, L. Zayas, J. Sonnenschein and D. Vaman. Regge trajectories for mesons in the holographic dual of large- $N(c)$  QCD. JHEP 0506 (2005): 046[hep-th/0410035].
- [59] Y. Imamura. On String Junctions in Supersymmetric Gauge Theories. Prog.Theor.Phys. 112 (2004): 1061-1086 [hep-th/0410138].
- [60] S. Kuperstein. Meson spectroscopy from holomorphic probes on the warped deformed conifold. JHEP 0503 (2005): 014[hep-th/0411097].
- [61] P. Benincasa and A. Buchel. Hydrodynamics of Sakai-Sugimoto model in the quenched approximation. Phys. Lett. B 640 (2006):108 [hep-th/0605076].
- [62] K. Peeters, J. Sonnenschein and M. Zamaklar. Holographic decays of largespin mesons. JHEP 0602 (2006): 009[hep-th/0511044].
- [63] K. Peeters, J. Sonnenschein and M. Zamaklar. Holographic melting and related properties of mesons in a quark gluon plasma. Phys. Rev. D 74 (2006): 106008[hep-th/0606195].
- [64] Y. Gao, W. Xu and D. Zeng. Jet quenching parameters of Sakai-Sugimoto Model. [hep-th/0611217].
- [65] O. Bergman and G. Lifschytz. Holographic  $U(1)_A$  and String Creation. JHEP 0704 (2007): 043[hep-th/0612289].
- [66] K. Nawa, H. Suganuma and T. Kojo. Baryons in Holographic QCD. Phys. Rev. D75 (2007): 086003[hep-th/0612187].
- [67] K. Nawa, H. Suganuma and T. Kojo. Brane-induced Skyrmions: Baryons in Holographic QCD. Prog.Theor.Phys.Suppl. 168 (2007): 231-236[hep-th/0701007v2].



- [68] K. Hashimoto, T. Hirayama and A. Miwa. Holographic QCD and Pion Mass. JHEP 0706 (2007): 020[hep-th/0703024v2].
- [69] D. Hong, M. Rho, H. Yee and P. Yi. Chiral Dynamics of Baryons from String Theory. Phys. Rev. D 76 (2007): 061901[hep-th/0701276v2].
- [70] D. Hong, M. Rho, H. Yee and P. Yi. Dynamics of Baryons from String Theory and Vector Dominance. JHEP 0709 (2007): 063[arXiv:0705.2632 [hep-th]].
- [71] O. Bergman, G. Lifschytz and M. Lippert. Holographic Nuclear Physics. JHEP 11 (2007): 056[hep-th/0708.0326].
- [72] O. Aharony, J. Sonnenschein and S Yankielowicz. A holographic model of deconfinement and chiral symmetry restoration. Annals Phys. 322 (2007): 1420-1443[arXiv:hep-th/0604161v2]
- [73] P. Burikham, E. Hirunsirisawat and S. Pinkanjanarod. Thermodynamic Properties of Holographic Multiquark and the Multiquark Star. JHEP 06 (2010): 040[1003.5470v2 [hep-ph]].
- [74] K. Kim, S. Sin and I. Zahed. The Chiral Model of Sakai-Sugimoto at Finite Baryon Density. JHEP 01 (2008): 002[arXiv:0708.1469[hep-th]].
- [75] A. Akmal, V. Pandharipande and D. Ravenhall. The equation of state of nucleon matter and neutron star structure. Phys. Rev. C58 (1998): 1804[nucl-th/9804027].
- [76] J. de Boer, K. Papadodimas and E. Verlinde. Holographic Neutron Stars.[arXiv:0907.2695[hep-th]].
- [77] F. Weber. "Strange Quark Matter and Compact Stars", Prog.Part. Nucl. Phys. 54 (2005): 193[astro-ph/0407155].



# APPENDICES

ศูนย์วิทยทรัพยากร  
จุฬาลงกรณ์มหาวิทยาลัย

# Appendix A

## BALANCE CONDITION FROM VARIATIONAL PRINCIPLE

Another way to find the balance condition can be obtained from variation of the total action with respect to the cusp position  $u_c$ .

$$\begin{aligned}
 \tilde{S} &= \tilde{S}_{D8} + S_{\text{source}} = \int_{u_c}^{\infty} du \tilde{L}(x'_4(u), d, t) + S_{\text{source}} \\
 \left. \frac{\partial \tilde{S}}{\partial u_c} \right|_{d,t,l} &= \int_{u_c}^{\infty} du \frac{\delta \tilde{S}_{D8}}{\delta u} \frac{\partial u}{\partial u_c} + \int_{u_c}^{\infty} du \frac{\delta \tilde{S}_{D8}}{\delta x'_4} \frac{\partial x'_4}{\partial u_c} \Big|_{d,t,l} + \left. \frac{\partial S_{\text{source}}}{\partial u_c} \right|_{d,t,l} \\
 0 &= -\tilde{L}(u_c) + \int_{u_c}^{\infty} du \frac{\delta \tilde{S}_{D8}}{\delta x'_4} \frac{\partial x'_4}{\partial u_c} \Big|_{d,t,l} + \left. \frac{\partial S_{\text{source}}}{\partial u_c} \right|_{d,t,l} \quad (\text{A.1})
 \end{aligned}$$

Since we use a proper coordinate with a proper length

$$l = 2 \int_{u_c}^{\infty} du x'_4(u), \quad (\text{A.2})$$

we get

$$\begin{aligned}
 \frac{1}{2} \frac{\partial l}{\partial u_c} &= \int_{u_c}^{\infty} du \frac{\delta l}{\delta u} \frac{\partial u}{\partial u_c} \Big|_{d,t,l} + \int_{u_c}^{\infty} du \frac{\partial x'_4}{\partial u_c} \Big|_{d,t,l} \\
 0 &= \int_{u_c}^{\infty} du x'_4(u) \frac{\partial u}{\partial u_c} \Big|_{d,t,l} + \int_{u_c}^{\infty} du \frac{\partial x'_4}{\partial u_c} \Big|_{d,t,l} \\
 &= -x'_4(u_c) + \int_{u_c}^{\infty} du \frac{\partial x'_4}{\partial u_c} \Big|_{d,t,l} \\
 x'_4(u_c) &= \int_{u_c}^{\infty} du \frac{\partial x'_4}{\partial u_c} \Big|_{d,t,l} \quad (\text{A.3})
 \end{aligned}$$

After substituting (A.3) into (A.1) and requiring the total action to be stationary with respect to variation of  $u_c$ , we obtain

$$\tilde{L}(u_c) - x'_4(u_c) \frac{\delta \tilde{S}_{D8}}{\delta x'_4} \Big|_{u_c} = \left. \frac{\partial S_{\text{source}}}{\partial u_c} \right|_{d,t,l} \quad (\text{A.4})$$

$$x'_4(u_c) = \left[ \tilde{L}(u_c) - \left. \frac{\partial S_{\text{source}}}{\partial u_c} \right|_{d,t,l} \right] / \left. \frac{\delta \tilde{S}_{D8}}{\delta x'_4} \right|_{u_c} \quad (\text{A.5})$$

For multiquark phase,

$$\begin{aligned}\tilde{S}_{D8} &= \int_{u_c}^{\infty} du \tilde{L}(u) \text{ (from Eq. 3.56)} \\ &= \mathcal{N} \int_{u_c}^{\infty} du u^4 \sqrt{f(u)(x'_4(u))^2 + u^{-3}} \sqrt{1 + \frac{d^2}{u^5}}\end{aligned}\quad (\text{A.6})$$

$$S_{\text{source}} = \mathcal{N}d \left[ \frac{1}{3}u_c \sqrt{f(u_c)} + n_s(u_c - u_T) \right] \quad (\text{A.7})$$

Using (3.56),(3.74), and (A.7)

$$\begin{aligned}x'_4(u_c) &= \frac{[f(u_c)(x'_4(u_c))^2 + u_c^{-3}]^{1/2}}{u_c^4 f(u_c) x'_4(u_c) \left[1 + \frac{d^2}{u_c^5}\right]^{1/2}} \left\{ \right. \\ &\quad u_c^4 [f(u_c)(x'_4(u_c))^2 + u_c^{-3}]^{1/2} \left[1 + \frac{d^2}{u_c^5}\right]^{1/2} \\ &\quad \left. - \frac{d f^{1/2}(u_c)}{3} \left(1 + \frac{3}{2f(u_c)} \left(\frac{u_T}{u_c}\right)^3 + \frac{3}{f^{1/2}(u_c)} n_s\right) \right\} \\ f(u_c)(x'_4(u_c))^2 &= f(u_c)(x'_4(u_c))^2 + u_c^{-3} \\ &\quad - \frac{d f^{1/2}(u_c) [f(u_c)(x'_4(u_c))^2 + u_c^{-3}]^{1/2}}{3 u_c^4 \left[1 + \frac{d^2}{u_c^5}\right]^{1/2}} \\ &\quad \times \left(1 + \frac{3}{2f(u_c)} \left(\frac{u_T}{u_c}\right)^3 + \frac{3}{f^{1/2}(u_c)} n_s\right) \\ f(u_c)(x'_4(u_c))^2 + u_c^{-3} &= \frac{(3u_c)^2 f(u_c) \left[1 + \frac{d^2}{u_c^5}\right]}{d^2 \left(f(u_c) + \frac{3}{2} \left(\frac{u_T}{u_c}\right)^3 + 3f^{1/2}(u_c) n_s\right)^2} \quad (\text{A.8}) \\ (x'_4(u_c))^2 &= \frac{(3u_c)^2 \left[1 + \frac{d^2}{u_c^5}\right]}{d^2 \left(f(u_c) + \frac{3}{2} \left(\frac{u_T}{u_c}\right)^3 + 3f^{1/2}(u_c) n_s\right)^2} - \frac{u_c^{-3}}{f(u_c)} \\ x'_4(u_c) &= \frac{1}{d} \sqrt{\frac{9u_c^2 \left[1 + \frac{d^2}{u_c^5}\right]}{\left(1 + \frac{1}{2} \left(\frac{u_T}{u_c}\right)^3 + 3n_s \sqrt{f(u_c)}\right)^2} - \frac{d^2 u_c^{-3}}{f(u_c)}} \quad (\text{A.9})\end{aligned}$$

# Appendix B

## DIMENSIONAL TRANSLATION TABLE

| quantity | dimensionless variable | physical variable         |
|----------|------------------------|---------------------------|
| pressure | $P$                    | $\frac{c^4}{Gr_0^2} P$    |
| density  | $\rho$                 | $\frac{c^2}{Gr_0^2} \rho$ |
| mass     | $M$                    | $\frac{r_0 c^2}{G} M$     |
| radius   | $r$                    | $r_0 r$                   |

Table B.1: Dimensional translation table of relevant physical quantities,  $r_0 \equiv \left(\frac{GN}{c^4 \tau V_3}\right)^{-1/2} = \left(\frac{G}{c^4}(\text{energy density scale})\right)^{-1/2}$ .

ศูนย์วิทยทรัพยากร  
จุฬาลงกรณ์มหาวิทยาลัย

# VITAE

Mr. Sitthichai Pinkanjanarod was born in 13 March 1980 and received his Bachelor's degree in physics with honor from Kasetsart University in 2001. He has studied particle physics and quantum field theory for his Master's degree. His research interests are in theoretical elementary particle physics, especially in the area of Superstrings phenomenology and Astrophysics

## Employment

1. 2003-present Lecturer at Department of Physics, Kasetsart University

## Presentations

1. Holographic Description On Mass Limit Of A Multiquark Star: The Siam Physics Congress 2010, River Kwai Village Hotel, Kanchanaburi, Thailand (25-27 March 2010).
2. Holographic Model of A Multiquark Star: The 17<sup>th</sup> National Graduate Research Conference, Rajabhat Buriram University, Buriram, Thailand (25 June 2010).

ศูนย์วิทยทรัพยากร  
จุฬาลงกรณ์มหาวิทยาลัย